

GEOMETRIZATION OF N -EXTENDED 1-DIMENSIONAL SUPERSYMMETRY ALGEBRAS

CHARLES DORAN, KEVIN IGA, GREG LANDWEBER, AND STEFAN MÉNDEZ-DIEZ

ABSTRACT. The problem of classifying off-shell representations of the N -extended one-dimensional super Poincaré algebra is closely related to the study of a class of decorated graphs known as *Adinkras*. We show that these combinatorial objects possess a form of emergent supergeometry: Adinkras are equivalent to very special super Riemann surfaces with divisors. The method of proof critically involves Grothendieck’s theory of “dessins d’enfants”, work of Cimasoni-Reshetikhin expressing spin structures on Riemann surfaces via dimer models, and an observation of Donagi-Witten on parabolic structure from ramified coverings of super Riemann surfaces.

CONTENTS

1. Introduction	2
Acknowledgements	4
2. Review of Adinkras	5
2.1. The $(1 N)$ Superalgebra	5
2.2. Adinkras	6
3. From Chromotologies to Riemann Surfaces	9
3.1. The N -cube	14
3.2. General Adinkra Chromotologies	24
3.3. The Exterior Tensor Product	31
4. From Odd Dashings to Spin Structures	39
4.1. From Odd Dashings to Kasteleyn Orientations	39
4.2. From Kasteleyn Orientation to Spin Curve	43
4.3. Description as a Super Riemann Surface	46
5. From Engineering Dimension to Morse Divisor	51
5.1. From Engineering Dimension to Discrete Morse Function	52
5.2. Description as a Divisor	61
Appendix A. Completion of Proof of Theorem 1	62
References	67

1. INTRODUCTION

In mathematics, the term “supersymmetry” is used to describe algebraic structures which possess a \mathbb{Z}_2 -grading and obey standard sign conventions related to that grading. These algebraic structures can be attached to other mathematical objects which are, say, topological or geometric in nature. As a result, many standard mathematical objects have well-studied “super” variants, e.g., manifolds \rightarrow super manifolds or Riemann surfaces \rightarrow super Riemann surfaces.

In physics, the term “supersymmetry” is much more specific, referring to structures which are equivariant with respect to extensions of the super Poincaré algebra. The Lorentz group is the Lie group of isometries of Minkowski space, or more precisely its double cover, replacing $\mathrm{SO}(1, d-1)$ with $\mathrm{Spin}(1, d-1)$. The Poincaré group is the Lorentz group together with translations, $\mathrm{Spin}(1, d) \times \mathbb{R}^{1, d-1}$. The super Poincaré group is the Lie supergroup obtained by extending the Poincaré group by infinitesimal odd elements, called supersymmetry generators, which square to spacetime derivatives, the infinitesimal generators of translations. At the Lie algebra level, the supersymmetry generators span the odd component of the super Poincaré algebra. While supersymmetry algebras can refer to extensions of the super Poincaré algebra, here we will be dealing with only the super Poincaré algebra.

The physical representations of the super Poincaré group and super Poincaré algebra come in two forms. Both are representations on spaces of fields, i.e., maps from Minkowski space to a finite-dimensional \mathbb{Z}_2 -graded representation of $\mathrm{Spin}(1, d-1)$. The \mathbb{Z}_2 -grading decomposes the fields into *bosons* and *fermions*, and the Lorentz action decomposes the fields into irreducible components, each corresponding to a different type of particle. The assembly of several such particles into a representation of supersymmetry is called a *supermultiplet*. The Poincaré group acts naturally on such spaces of fields, and the question which remains is how the supersymmetry generators in the super Poincaré algebra will act.

In off-shell representations, the super Poincaré algebra acts on dynamically unconstrained spaces of fields, while on-shell representations restrict the action to fields which satisfy the equations of motion, usually coming from a Lagrangian via the Euler-Lagrange equations. Although on-shell representations are more complicated physically, they are more natural from the point of view of representation theory. On the other hand, in off-shell representations the supersymmetry is manifest from the description of the particles in the supermultiplet, allowing us to separate the representation theory from the physics, i.e., the Lagrangian, and facilitating quantization.

Graphs known as Adinkras were proposed by Faux and Gates in [17] as a fruitful way to investigate off-shell representations of the super-Poincaré algebra. These combinatorial objects were rigorously defined, and their connections to Clifford algebras and coding theory explored, in a long series of works by the DFGHILM collaboration [12, 14, 15, 23, 11]. Adinkras are graphs with vertices representing

the particles in a supermultiplet and edges corresponding to the supersymmetry generators. In combinatorial terms, Adinkras are N -regular, edge N -colored bipartite graphs with signs assigned to the edges and heights assigned to the vertices, subject to certain conditions. Details can be found in Section 2 below.

It is useful to think of an Adinkra as consisting of a *chromotopology*, which captures the underlying bipartite graph with its N -coloring, together with two more compatible structures: an *odd dashing*, which marks the edges with signs, and a *height assignment*, which labels each of the vertices with an integer. A complete characterization of chromotopologies was achieved in [15]. For each N , there is a natural chromotopology on the Hamming cube I^N , with vertices labeled by elements of \mathbb{F}_2^N . The one-skeleton of the Hamming cube serves as a “universal cover” for arbitrary chromotopologies, the covering map being realized by taking cosets with respect to doubly even binary linear error correcting codes $C \subset \mathbb{F}_2^N$.

In Section 3 we show how to canonically associate to a given chromotopology a Riemann surface. The N -regular, edge N -coloring gives us a cyclic ordering of the edges at each vertex of the graph based on their color. We call such an ordering a *rainbow*. This provides the structure of a Ribbon graph, and, following Grothendieck, we are led through the Belyi curve construction to a presentation of the associated Riemann surface as a covering space over \mathbb{CP}^1 , branched over $\{0, 1, \infty\}$, with the graph embedded as the inverse image of the line segment $[0, 1]$. One consequence of coming from a chromotopology is that the 2-faces of this surface are precisely those bounded by 4-edge cycles with edges colored by two adjacent colors from the rainbow (opposite edges having the same color). Although changing the ordering of colors in our rainbow will a priori yield a different Riemann surface, we show that in fact it results in a global conjugation of the monodromy group of the covering space, and hence isomorphic Riemann surfaces. This fits well with the expectation from physics, as equivalence under permutation of the colors is a consequence of R -symmetry. We also reinterpret a purely combinatorial operation of exterior tensor product of Adinkras in geometric terms as a multi-point connected sum of the associated Riemann surfaces.

The odd dashing condition was completely characterized by [11]. Up to a notion of equivalence under a series of *vertex switches*, each of which flips the parity of the markings on all the edges adjacent to a given vertex, the difference between two odd dashings on the same Adinkra was shown to correspond to a class in the first cohomology of I^N/C viewed as a cubical complex. This is remarkably similar to the situation with spin structures on manifolds: the existence of a spin structure on an orientable manifold M is determined by the second Stiefel-Whitney class of the tangent bundle $w_2(TX) \in H^2(M; \mathbb{Z}_2)$. A necessary and sufficient condition for spin structures to exist is $w_2(TX) = 0$, and the difference of two such spin structures is characterized by an element in $H^1(M; \mathbb{Z}_2)$, so that the set of spin structures is in bijection with $H^1(M; \mathbb{Z}_2)$.

In Section 4 we show that this connection with spin structures is by no means coincidental. Firstly, in the context of dimer models on surface graphs, Cimasoni and Reshetikhin have demonstrated that a certain kind of edge marking, known as a Kastelyn orientation, is (up to equivalence) in one-to-one correspondence with spin structures on the surface. Given a bipartition of the vertices of the surface graph, a Kastelyn orientation is equivalent to an odd dashing. The correspondence between equivalence classes of Kastelyn orientations and spin structures is as affine spaces, and requires a base dimer configuration to be an isomorphism. A base dimer configuration is provided by the union of all edges of (any given) color, making the interpretation of an odd dashing as a spin structure canonical.

As observed by Donagi and Witten in [10], a Riemann surface with spin structure that is also a branched cover of $\mathbb{C}\mathbb{P}^{(1|1)}$ is endowed with a super Riemann surface structure, with Ramond punctures. In our case, this introduces Ramond punctures at the center of each quadrilateral 2-face, and leaves us with a canonical super Riemann surface structure.

What remains of the last ingredient of an Adinkra, the height assignment on vertices? As the name suggests, the height assignment can, on the one hand, be viewed as a discretization of a height function on the Riemann surface. This “discretized Morse function” interpretation is quite natural, and the saddle points all lie at the positions of Ramond punctures and the maximums and minimums occur at vertices of the embedded Adinkra. The height assignment simultaneously, and equally naturally, admits an interpretation as a divisor on the (super) Riemann surface. Operations such as raising and lowering of nodes [22], which play a key role in the physical application of Adinkras, are now geometrically meaningful operations on these “Morse divisors”.

Geometrized chromotopologies are very special as Riemann surfaces, and they remain so even when viewed as Belyi curves. Spin structures that correspond to odd-dashings on an Adinkra are likewise distinguished. The same is true for the Morse-divisors coming from height assignments. The fact that Adinkras correspond to very special points in a moduli space of well-studied geometric objects may provide a key new tool for understanding supersymmetric representation theory. It is our hope that the category of spin curves with Morse-divisor which has emerged through geometrizing Adinkrizable supermultiplets may also be naturally broadened to include geometric incarnations of both non-Adinkrizable supermultiplets [26, 13], and worldline reductions (“shadows”) of on-shell supermultiplets of physical interest.

ACKNOWLEDGEMENTS

We would like to thank S.J. Gates, Jr. and T. Hübsch for extended discussions and useful suggestions while writing this paper. We would also like to thank J. Iverson for computing the generators of the monodromy groups for some of the examples in Sage. CD and SMD acknowledge the support from the Natural

Sciences and Engineering Resource Council of Canada, the Pacific Institute for the Mathematical Sciences, and the McCalla Professorship at the University of Alberta. GL acknowledges the support by a grant from the Simons Foundation (Award Number 245784).

2. REVIEW OF ADINKRAS

As noted in the introduction, the first step in describing irreducible off-shell representations of the N -extended 1-dimensional super Poincaré algebra is to present them as graphs called Adinkras. We are interested in the elementary N -extended Poincaré superalgebra in 1-dimensional Minkowski space, the $(1|N)$ superalgebra for short. Here elementary means a classical Lie algebra with no central extensions and no other additional internal bosonic symmetries. We begin this section by reviewing the $(1|N)$ superalgebra. We will then review what an Adinkra is, as well as the main features that will be needed later.

2.1. The $(1|N)$ Superalgebra. In 1-dimensional Minkowski space there is a single time-like direction τ . Translations in this direction are generated by ∂_τ . Therefore $(1|N)$ superalgebras are generated by ∂_τ and N real supersymmetry generators Q_I . The supersymmetry generators commute with ∂_τ and satisfy the following anti-commutation relations

$$(1) \quad \{Q_I, Q_J\} = 2i\delta_{IJ}\partial_\tau,$$

where δ_{IJ} is the Kroenecker delta.

In the physics literature this is often written in terms of parameter dependent operators

$$(2) \quad \delta_Q(\epsilon) \equiv -i\epsilon^I Q_I,$$

where ϵ^I is a set of N Grassmann variables and Einstein's summation convention is being used. With this identification, equation 1 takes the equivalent form

$$(3) \quad [\delta_Q(\epsilon_1), \delta_Q(\epsilon_2)] = 2i\epsilon_1^I \epsilon_2^I \partial_\tau.$$

Every representation of the $(1|N)$ superalgebra decomposes as a collection of irreducible representations of the $(1|1)$ superalgebra. The $(1|1)$ superalgebra has 2 irreducible representations, the scalar and spinor multiplets. The scalar multiplet consists of a real commuting bosonic field, ϕ , and a real anticommuting fermionic field ψ with supersymmetry transformations

$$(4) \quad \begin{aligned} Q\phi &= \pm\psi \\ Q\psi &= \pm i\dot{\phi}. \end{aligned}$$

The spinor representation also consists of a real commuting field B and a real anticommuting field η , but the with different transformation rules

$$(5) \quad \begin{aligned} Q\eta &= \pm iB \\ QB &= \pm \dot{\eta}. \end{aligned}$$

Real, finite-dimensional, linear representations of the $(1|N)$ superalgebra are spanned by a basis of real bosonic component fields $\phi_1(\tau), \dots, \phi_m(\tau)$ and real fermionic component fields $\psi_1(\tau), \dots, \psi_l(\tau)$. The super supersymmetry generators Q_1, \dots, Q_N act linearly on the representation and satisfy equation 1. Such representations are called real supermultiplets, hence why we referred to the scalar and spinor representations of the $(1|1)$ superalgebra as the real and spinor multiplets earlier. We will be interested in off-shell supermultiplets. This means that the component fields do not satisfy any differential equations other than equation 1. We will assume all supermultiplets are off-shell unless otherwise stated. Off-shell supermultiplets have the same number of bosonic and fermionic component fields.

For off-shell supermultiplets, the supersymmetry transformation rules are

$$(6) \quad \begin{aligned} Q_I \phi_A(\tau) &= c \partial_\tau^\lambda \psi_B(\tau) \\ Q_I \psi_B(\tau) &= \frac{i}{c} \partial_\tau^{1-\lambda} \phi_A(\tau), \end{aligned}$$

where $c = \pm 1$ and $\lambda = 0$ or 1 .

Note that the time derivative has engineering dimension $[\partial_\tau] = 1$. It can be seen from equation 1 that $[Q_I] = \frac{1}{2}$. c , λ , and B occurring in equation 6 generally depend on A and I . For example, c clearly differentiates between the \pm options occurring in equations 4 and 5. On the other hand, λ differentiates between the scalar and spinor multiplet transformations. In order for the component fields to have definite engineering weight

$$(7) \quad \lambda = [\phi_A] - [\psi_B] + \frac{1}{2},$$

assuming the coefficients of equation 6 are dimensionless.

2.2. Adinkras. An Adinkra is a graphical representation of a supermultiplet and its supersymmetry transformations originally proposed in [17]. As noted in the introduction, there is a wealth of literature further studying Adinkras and establishing their precise mathematical formulation such as [12, 14, 15, 23, 11]. A good overview of their mathematical aspects can be found in [37]. An Adinkra is a bipartite N -regular colored graph where the edges have an orientation and a dashing.

Consider a $(1|N)$ supermultiplet \mathcal{M} spanned by component fields $\phi_1, \dots, \phi_m, \psi_1, \dots, \psi_m$. \mathcal{M} can be represented as an Adinkra if all of the supersymmetry generators send each component field to a single component field. The corresponding Adinkra has a white vertex for each bosonic field ϕ_A and a black vertex for each

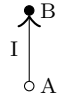

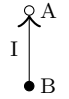

Action of Q_I	Adinkra	Action of Q_I	Adinkra
$Q_I \begin{bmatrix} \psi_B \\ \phi_A \end{bmatrix} = \begin{bmatrix} i\dot{\phi}_A \\ \psi_B \end{bmatrix}$		$Q_I \begin{bmatrix} \psi_B \\ \phi_A \end{bmatrix} = \begin{bmatrix} -i\dot{\phi}_A \\ -\psi_B \end{bmatrix}$	
$Q_I \begin{bmatrix} \phi_A \\ \psi_B \end{bmatrix} = \begin{bmatrix} i\dot{\psi}_B \\ \phi_A \end{bmatrix}$		$Q_I \begin{bmatrix} \phi_A \\ \psi_B \end{bmatrix} = \begin{bmatrix} -i\dot{\psi}_B \\ -\phi_A \end{bmatrix}$	

TABLE 1. The correspondence between Adinkras and the action of the supersymmetry generators on the component fields. Each white vertex of an Adinkra corresponds to a bosonic component field and its time derivatives. Similarly, each black vertex corresponds to a fermionic component field and its time derivatives. The edges will be colored by color I corresponding to the index of the supersymmetry generator.

fermionic field ψ_A , $1 \leq A \leq m$. The white vertex corresponding to ϕ_A is connected to the black vertex corresponding to ψ_B by an edge of color I if Q_I sends ϕ_A to ψ_B (or its time derivative) by equation 6. The edge is oriented from the white vertex to the black vertex if $\lambda = 0$ and the other way if $\lambda = 1$. It is dashed if $c = -1$ and solid if $c = 1$. This correspondence is pictured in Table 1. We will now review some important features of Adinkras that we will need later.

First note that every vertex has exactly one edge of each color adjacent to it. This is because each supercharge acts on each component field taking it to exactly one other component field (or its time derivative). For any component field $f(\tau)$, $\pm f(\tau)$ and all of its time derivatives are represented by the same vertex in the corresponding Adinkra. By equation 1, $Q_I Q_J = -Q_J Q_I$ for $I \neq J$, so $Q_I Q_J f$ and $-Q_J Q_I f$ are represented by the same vertex in an Adinkra. This means that if you start at any vertex and then go along an edge of any color I , then go along the edge of any other color J , it is the same as going color J then color I . Another way to say this is that starting at any vertex and then going color I , then color J , then color I and then color J again returns you to the same vertex[17]. We refer to this closed loop as a *2-colored loop*.

Furthermore, as we go around each 2-colored loop, there must be an odd number of dashed edges [17]. $Q_I f$ is given by equation 6. The edge representing $Q_I f$ is dashed if and only if the term c is -1 . $Q_J Q_I f$ will pick up a factor of a different “ c ” that can be \pm and determines if the edge correspond to $Q_J(Q_I f)$ is dashed or not. By equation 1, $Q_I Q_J f(\tau)$ and $Q_J Q_I f(\tau)$ must have opposite sign. These means that of the 4 different factors of c (2 appearing in $Q_I Q_J f$ and 2 appearing in $Q_J Q_I f$) an odd number of them must be odd. Therefore the total number of dashed edges as we go around the I/J 2-colored loop must be odd.

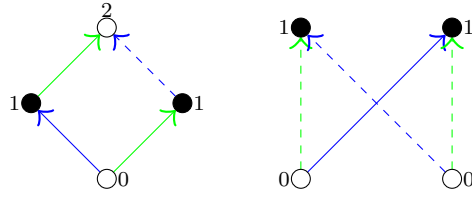


FIGURE 1. An example of 2 different $N = 2$ Adinkras with the heights of their vertices labeled.

Also as you go around a 2-colored loop you will traverse an even number of edges with their orientation and even number against their orientation. As you traverse edge color I and then edge color J starting at any vertex, whether you go with or against the orientation of the edges determines how many factors of ∂_τ are picked up. Since you must get the same number of time derivatives if you instead go color J and then color I for the engineering dimension to match, you must go with or against the orientations of the same number of edges. Therefore the number of edges you go with the orientation of, and against the orientation of as you go around the entire 2-colored loop must both be even.

The orientation of the edges defines a height function on the vertices of the Adinkra that corresponds to the engineering dimension of the component fields[12]. If V is the set of vertices of an Adinkra, a height function is a function $h : V \rightarrow \mathbb{Z}$ such that $h(b) = h(a) + 1$ if there is an edge going from a to b . Adding a constant to any height function gives another height function. This allows us to choose a height function so that the heights of the bosons are even and the heights of the fermions are odd, which can be normalized so that the height of the vertex is twice the engineering dimension of the corresponding component field. The height should be viewed as a minimum engineering dimension of the objects represented by the vertex, since the vertices of an Adinkra represent not only the component fields, but their time derivatives as well and every application of ∂_τ increases the engineering dimension by 1. See Figure 1 for an example of 2 different $N = 2$ Adinkras with their height functions shown.

Forgetting the dashing, orientation and coloring of all of the edges in an Adinkra leaves what is called the *topology* of the Adinkra. The topology of an Adinkra together with its edge coloring is called its *chromotopology*. One of the most important Adinkra topologies is the topology of the N -cube. This is the the topology consisting of the vertices and edges of the N -cube, $[0, 1]^N$. The topologies of both Adinkras pictured in Figure 1 are those of the 2-cube. In fact they have have the same chromotopologies. All N -cubes have a unique chromotopology[15]. Even though the Adinkras in Figure 1 have the same chromotopologies they are not the same, since they have different orientations (hence height assignments) and dashings.

The colored N -cube, $I^N = [0, 1]^N$, has 2^N vertices and $N2^{N-1}$ edges. We can embed I^N in \mathbb{R}^N so that the vertices are located at all 2^N possible points (x_1, \dots, x_N) with $x_i = 0$, or 1 . This associates the vertices of the colored N -cube with the elements of \mathbb{F}_2^N , where \mathbb{F}_2 is the field of order 2. The weight of a vertex is the number of nonzero entries in (x_1, \dots, x_N) . The vertices with even weight are white while the vertices with odd weight are black. Two vertices (x_1, \dots, x_N) and (y_1, \dots, y_N) are connected by an edge of color I if they only differ in the I th component. That is, if $x_i = y_i$ for $i \neq I$ and $x_I = 1 - y_I$.

It was shown in [15] that the set of Adinkra chromotopologies is equivalent to the set of colored N -cubes mod doubly even codes. A *code* is a linear subspace of \mathbb{F}_2^N . A code C is doubly even if every codeword (element of the code) has weight divisible by 4. Every code has a basis since it is a linear subspace of \mathbb{F}_2^N . The basis, c_1, c_2, \dots, c_k is called the *generating set*. The dimension of the code is k , and it is the same for any generating set of a given code. For a doubly-even code C , I^N/C means that we identify vertices of I^N if they differ by codewords as elements of \mathbb{F}_2^N . Furthermore, if vertices v and w are identified then the edge of color I incident to v is identified with the edge of color I incident to w for all I . That is, the vertices of an Adinkra can be viewed as cosets of a doubly even code in \mathbb{F}_2^N . In this way, the colored N -cube can be thought of as a universal cover for general Adinkra chromotopologies. It is in general quite difficult to find doubly-even codes for a given N , see [32] for an extensive list.

R -symmetry is a symmetry that transforms the supercharges Q_I . For real N -extended supersymmetry, the group of R -symmetries is $O(N)$. The matrix subgroup of $O(N)$ consisting of permutation matrices corresponds to permuting the Q_I . The action of the permutation subgroup can easily be seen on an Adinkra by permuting the colors corresponding to the Q_I . As noted in [15], it is not clear that for physical significance it is enough to only consider permutation equivalence. In the following section we will show that Adinkra chromotopologies describe Riemann surfaces and that these surfaces are invariant under the action of the permutation subgroup. The same issues of extending to the entire R -symmetry group still exist, but working in a higher dimensional space may provide new methods for approaching the problem.

3. FROM CHROMOTOPOLOGIES TO RIEMANN SURFACES

In the previous section we reviewed how irreducible off-shell representations of $(1|N)$ superalgebras can be presented as graphs called Adinkras. In this section we will see how an Adinkra chromotopology canonically defines a Riemann surface as a covering space of $\mathbb{C}\mathbb{P}^1$. This is done by first showing that an Adinkra chromotopology has the structure of a ribbon graph and then using the Grothendieck correspondence to associate a Riemann surface to the ribbon graph.

A *ribbon graph* (also known as a *fat graph*) is a connected graph that assigns to each vertex of the graph a cyclic permutation of the half edges adjacent to the

vertex. As we saw in the previous section the chromotopology of an Adinkra is a connected, colored N -regular bipartite graph.

Definition 1. A *rainbow* is a choice of a cyclic ordering of the colors of a colored graph.

An Adinkra naturally determines a rainbow given by the order of the supersymmetry generators the colors represent. A chromotopology together with a rainbow defines a ribbon graph, since an Adinkra is N -regular and N -colored. The ribbon structure is defined by assigning to each white vertex the cyclic permutation of the half-edges adjacent to it given by the rainbow (since there is exactly one half-edge of each color adjacent to the vertex) and to each black vertex assign the cyclic permutation of half-edges adjacent to it in the opposite order of the rainbow¹.

Definition 2. A *Belyi pair*, (X, β) is a closed Riemann surface X equipped a Belyi map, $\beta : X \rightarrow \mathbb{CP}^1$ that is ramified at most over $\{0, 1, \infty\}$.

A bipartite ribbon graph is equivalent to a Belyi pair by the Grothendieck correspondence. This can also be shown to be equivalent to a monodromy map $\alpha : F_2 \rightarrow S_d$ where F_2 is the free group on 2 generators and S_d is the symmetry group on d elements, the total number of edges. There are many references for the Grothendieck correspondence. Good references for our current applications are [25] and [29].

This shows that every chromotopology with a rainbow up to equivalence (in the sense of ribbon graphs) determines a unique Belyi pair up to equivalence. The Belyi map, $\beta : X \rightarrow \mathbb{CP}^1$ maps all of the white vertices to 0, all of the black vertices to 1, all of the edges to the real line segment $(0, 1)$ and the center of all the 2-faces (described below) of the surface X to ∞ .

As described in [29], the Riemann surface X is constructed by attaching 2-cells to certain closed loops in the graph. Which loops we attach 2-cells to is determined by the ribbon structure. Since we chose the order of the colors at the white vertices to be opposite the order at the black vertices the faces will be 4-gons². Recall that any 2 colors in an Adinkra form a closed loop starting at any vertex by following color I , color J , color I and then color J again. The Riemann surface associated to a chromotopology is obtained by “filling in” (attaching 2-cells to) some of these 2-colored loops, determined by the rainbow. If the rainbow sends color I to color J then the boundaries of the faces are determined as follows: if an edge of color I comes into a white vertex we then leave the white vertex along the unique edge of color J that is incident to it³. Since the the order of the colors at the black

¹We could have let the elements of S_{2d} at each black vertex have the same order as the rainbow instead, as discussed in [25, 29], but this would not take into account the bipartite structure.

²If we chose the order of the colors at the white and black vertices to be the same then the faces would be $2N$ -gons[29].

³What is meant by enters and leaves is determined by the orientation of the surface which is inherited by the orientation the Belyi base \mathbb{CP}^1 and will be discussed in more detail later.

vertices is opposite the rainbow and we entered the black vertex along color J , we will leave along the edge of color I . The other half of this edge of color I is incident to a new white vertex, since Adinkras do not contain double edges. Repeating, we leave the new white vertex along color J , which takes us to a new black vertex (again it must be new since there are no double edges). Finally, leaving that black vertex along color I takes us back to the original white vertex since we have completed a 2-colored loop. This 2-colored loop defines the boundary of a 2-face. This shows that the 2-colored loops of adjacent colors in the rainbow are “filled in”. More precisely, if the rainbow is given by (C_1, C_2, \dots, C_N) where C_i represent the N colors. Then 2-cells are attached to all of the C_1/C_2 2-colored loops, C_2/C_3 2-colored loops, $\dots, C_{N-1}/C_N$ 2-colored loops, and C_N/C_1 2-colored loops.

Using the classification of Adinkra chromotopologies in terms of error correcting codes from [15] discussed in section 2, we refer to an Adinkra chromotopology obtained from quotienting the colored N -cube by k -dimensional doubly even code as an (N, k) Adinkra chromotopology, $A_{(N,k)}$. Note that for a given N and k there may be more than one distinct chromotopology. That is, two (N, k) Adinkra chromotopologies, $A_{(N,k)}$ and $\tilde{A}_{(N,k)}$, may not be equivalent as chromotopologies, but they will have equivalent topologies. $A_{(N,k)}$ has 2^{N-k} vertices, 2^{N-k-1} white vertices and 2^{N-k-1} black vertices. There are $d = N2^{N-k-1}$ edges since there is a unique edge of a given color coming out of every white vertex and N total colors. Let $X_{(N,k)}$ be the Riemann surface in the Belyi pair associated to $A_{(N,k)}$.

Proposition 1. $X_{(N,k)}$ has genus $g = 1 + 2^{N-k-3}(N-4)$, for $N \geq 2$. Furthermore, for $1 \leq N \leq 3$ there are no doubly even codes and $X_{(N,0)}$ has genus 0.

Proof. By the Grothendieck correspondence a Belyi pair is equivalent to a Dessins d’enfants. Therefore the graph $A_{(N,k)}$ together with the 2-faces gives a cellular decomposition of $X_{(N,k)}$. We already know the number of vertices and edges in $A_{(N,k)}$, which gives us the number of 0-cells and 1-cells of the cellular decomposition of $X_{(N,k)}$. We now just need to determine the number of 2-cells, and then we can compute the Euler characteristic and compare to the genus.

There are 2^{N-k-1} edges of color C_i in $A_{(N,k)}$, one coming out of each white vertex. For $N \geq 2$ there exists another color, and any other color C_j partitions the edges of color C_i into pairs. In other words, if the white vertex of one of the edges of color C_i , call it e_A is connected to the black vertex of another edge of color C_i , call it e_B , by color C_j then the black vertex of edge e_A is connected to the white vertex of e_B by C_j . This is just completing the C_i/C_j 2-color loops. Therefore there are half as many C_i/C_j 2-color loops as number of edges of a given color (there are the same number of edges of any color), so there are 2^{N-k-2} 2-color loops for a given 2 colors. Since there are N different types of 2-colored loops that we attach 2-cells to, given by the N adjacencies in the rainbow, we

It *does not* correspond the orientation of the edges in the Adinkra which is forgotten in the chromotopology.

attach $N2^{N-k-2}$ 2-cells to $A_{(N,k)}$ to obtain the associated Riemann surface $X_{(N,k)}$ in the the Belyi pair.

Therefore by the relationship between genus and Euler characteristic we see

$$\begin{aligned} 2 - 2g &= 2^{N-k} - N2^{N-k-1} - N2^{N-k-2} \\ &= 2^{N-k-2}(4 - N). \end{aligned}$$

Isolating g gives the desired formula.

The maximum weight of an element of \mathbb{F}_2^N is N . Therefore for $N \leq 3$ the weight of all code words cannot be divisible by 4 and there are no doubly even code. For $N = 2, 3$ the formula for the genus with $k = 0$ shows the genus is 0. For $N = 1$, the associated surface is the Belyi base, hence is genus 0. \square

Recall that $\beta(A_{(N,k)})$ is the graph in \mathbb{CP}^1 consisting of one white vertex at 0, one black vertex at 1 and a single edge connecting them, call it Σ_0 . Since $\beta^{-1}(0)$ and $\beta^{-1}(1)$ both have order 2^{N-k-1} but $\beta^{-1}((0,1))$ has order $N2^{N-k-1}$ with N edges coming together at each vertex, β has order N ramification over 0 and 1. The only other place there can be any ramification is over ∞ since β is a Belyi map. $\beta^{-1}(\infty)$ consists of the center of the 2-faces which there are $N2^{N-k-2}$ of. Therefore there is order 2 ramification over ∞ .

As noted, we can represent a Belyi pair as a monodromy given by a subgroup of S_d generated by 2 elements. Following [29], number all of the half edges incident to a white vertex from 1 to d and label the other half of the half edge i (the half that is incident to a black vertex) $i + d$. We choose to label the monodromies by the edges since $X_{(N,k)}$ is unramified over $(0,1)$. Define an N -cycle in S_d at each white vertex by listing the half edges incident to the vertex ordered by their colors in the order of the rainbow. The N -cycles associated to different white vertices are disjoint since a half edge can only be incident to one white vertex. $A_{(N,k)}$ has 2^{N-k-1} white vertices. Define π_w to be the product of the 2^{N-k-1} disjoint N -cycles associated to all of the white vertices in S_d . At each of the black vertices list the half-edges incident to the vertex in the opposite order of the rainbow to define an element of S_{2d} . Define π_b to be the product in S_{2d} of the 2^{N-k-1} disjoint N -cycles associated to the black vertices. Let λ be the product of transpositions in S_{2d} that exchange the half-edges making up an edge. In particular, given our labeling,

$$(8) \quad \lambda = \prod_{i=1}^d (i, i + d).$$

The generators of the monodromy group for the Belyi map $\beta : X \rightarrow \mathbb{CP}^1$ are

$$(9) \quad \sigma_0 = \pi_w \quad \text{and} \quad \sigma_1 = \lambda\pi_b\lambda.$$

These describe the monodromies over 0 and 1 respectively. To see how σ_0 encodes the data of the monodromy over 0. Let us move in a small loop $\ell(t)$ around $0 \in \mathbb{CP}^1$ in the counter-clockwise direction relative to the orientation of \mathbb{CP}^1 , i.e. using the right-hand rule. This loop will intersect the single edge Σ_0 once, so let's consider

this point as the base point of the loop. The loop will lift by β to 2^{N-k-1} loops $\tilde{\ell}_i$ around each of the white vertices. Each $\tilde{\ell}_i$ will now intersect the N edges (one of each color) of $A_{(N,k)}$ that are incident to the white vertex $\tilde{\ell}_i$ encloses. Therefore we see that the base point of ℓ is lifted to N copies for each $\tilde{\ell}_i$. The monodromy is described by listing the edges that are intersected by each $\tilde{\ell}_i$ in order as you move counter-clockwise relative to the orientation inherited by \mathbb{CP}^1 by β . By construction the edges will be intersected in the same order as the rainbow, since the 2-cells are filled in between consecutive colors. This is exactly the data encoded by σ_0 . A similar argument applies for σ_1 as well. Note that the order of the map β is d . This can be determined directly from $\sigma_i \in S_d$, $i \in \{0, 1\}$. Since σ_i contains 2^{N-k-1} disjoint N -cycles, we see that the order of β is the number of disjoint cycles in σ_i times the length of the *cycles* themselves. The fact that σ_i is the product of disjoint N -cycles corresponds to $X_{(N,k)}$ having order N ramification over the Belyi base.

The monodromy over ∞ is given by

$$(10) \quad \sigma_\infty = (\sigma_0 \sigma_1)^{-1}.$$

$\beta^{-1}(\infty)$ consists of the centers of the 2-cells, each of which has order 2 ramification. From this we see that σ_∞ will consist of $N2^{N-k-2}$ disjoint 2-cycles. The transpositions will consist of 2 of the edges of the same color that make up the 2-color face (this uniquely determines the other 2 edges bounding the face). We can think of this encoding the data of the map as follows. Consider a loop ℓ that goes clockwise around $\infty \in \mathbb{CP}^1$ relative to the orientation of \mathbb{CP}^1 . We can choose it so that it is based at a point in $(0, 1)$. ℓ lifts to $N2^{N-k-2}$ loops $\tilde{\ell}_i$ around the centers of the 2-cells of $X_{N,k}$. As we saw earlier the ramification over ∞ is order 2, so $\tilde{\ell}_i$ now passes through 2 copies of the base point. If one base point is on an edge of color C_l that bounds the 2-cell containing $\tilde{\ell}_i$ then the other base point is on the other edge of color C_l that bounds that 2-cell. σ_∞ encodes this information. We could also view it as listing the 2 edges that are incoming to the 2 white vertices that make up the face (or the 2 edges that are outgoing from the 2 black vertices in the face). Here incoming and outgoing is as we go along $\tilde{\ell}_i$ in the clockwise direction relative to the orientation inherited from \mathbb{CP}^1 by β . We have chosen clockwise here so that the notion of incoming and outgoing matches the rainbow at the white vertices. If we instead went counter-clockwise, we would just need to exchange outgoing and incoming. This is a result of choosing counter-clockwise as the orientation of the rainbow at the white vertices.

While σ_∞ completely determines the 2 cells of the Belyi pair, it is not always as convenient since you cannot just look at it and immediately read off all 4 edges that make up each face. It is often more convenient to look at

$$(11) \quad \pi_\infty = \lambda \pi_w \pi_b \in S_{2d}.$$

π_∞ consists of $N2^{N-k-2}$ disjoint 4-cycles [25]. The elements of the 4-cycles list the incoming half-edge at each vertex as we move around the face clockwise relative to the orientation. Each 4-cycle has 2 half edges of the same color incoming at the black vertices and 2 half edges of the same color incoming at the white vertices. σ_∞ can be obtained from π_∞ by dropping the 2 half edges incoming at the black vertices, i.e. the ones with labels greater than d , creating 2-cycles from the 4-cycles.

We will show that the Belyi map for the N -cube A_N with the choice of a rainbow factors through the Belyi map for $A_{(N,k)}$ with the same rainbow. That is, that there exists a map of Riemann surfaces $\varphi : X_N \rightarrow X_{(N,k)}$ such that $\beta_N = \beta_{(N,k)} \circ \varphi$. Furthermore, we will show that they both factor through a map to the space B_N which is \mathbb{CP}^1 with one white vertex at 0, one black vertex at ∞ and N edges connecting them, one of each color. The edges are the lines with $\arg = e^{\frac{2\pi i}{N}}$ and the inverse image of ∞ from the Belyi base are the N -th roots of -1 .

Let us first look at the N -cube, A_N , in some detail since all other chromotopologies can be obtained from projections of A_N .

3.1. The N -cube. Let us first describe the monodromies for the the Belyi pair (X_N, β) obtained from the N -cube. To do this we need to label the half edges.

Proposition 2. *A_N has $m = 2^{N-1}$ black vertices and m white vertices. We can label the black vertices as $1_b, 2_b, \dots, m_b$ and the white vertices as $1_w, 2_w, \dots, m_w$ so that i_w is connected to i_b by color 1, and for $k \geq 2$ i_w is connected by color k to $(i + 2^{k-2})_b$ if $1 \leq i \pmod{2^{k-1}} \leq 2^{k-2}$ and $(i - 2^{k-2})_b$ otherwise. Any white vertex can be chosen to be 1_w .*

Proof. We will prove this by induction on the size of the cube. For the 1-cube this is trivial since there is only one white vertex and 1 black vertex. We label them 1_w and 1_b respectively. They are connected by edge color 1. Since this does not illustrate connections by colors other than 1 let us look at the next case; the 2-cube. Pick any white vertex in A_2 and label it 1_w . Label the point connected to it by the first color 1_b . Label the point connect to 1_w by the second color 2_b . This point must be distinct from 1_b or else there would be a double edge. Finally label the point connected to 2_b by color 1 as 2_w . Note that if you start at 2_w and follow colors 1, then 2 and then 1 again, then you end at 1_b . This shows that color 2 must connect 1_b and 2_w . This labeling of the points satisfies the conditions of the proposition. We could have picked the other white vertex to be 1_w by starting there instead.

Now assume we can come up with such a labeling for k -cubes A_k with $k \leq N-1$. If we remove color N , A_N decomposes to 2 disjoint copies of A_{N-1} by Corollary 4.8 and Proposition 4.9 of [37]. In the language of [14] we would say the N -cube is 1-color decomposable. Now pick any white vertex and call the disjoint copy of A_{N-1} obtained by removing color N that contains it $A_{N-1}^{(1)}$. Call the other copy $A_{N-1}^{(2)}$. Label the point chosen $1_w^{(1)}$. By the inductive assumption we can label the

rest of the points in $A_{N-1}^{(1)}$ by $i_q^{(1)}$, where $1 \leq i \leq 2^{N-2}$ and $q = b, w$, such that the labeling meets the conditions of the proposition. Since color N decomposed A_N into $A_{N-1}^{(1)}$ and $A_{N-1}^{(2)}$, color N must connect points in $A_{N-1}^{(1)}$ to points in $A_{N-1}^{(2)}$. Label the point in $A_{N-1}^{(2)}$ connected to $1_b^{(1)}$ by color N , $1_w^{(2)}$. Now label the rest of the points of $A_{N-1}^{(2)}$ as $i_q^{(2)}$ according to the inductive hypothesis. Finally, we define a labeling i_q on the entire A_N to be such that for vertices $x \in A_{N-1}^{(1)}$ they are labeled by $i(x)_q = i^{(1)}(x)_q$ and vertices $x \in A_{N-1}^{(2)}$ are labeled by $i(x)_q = (i^{(2)}(x) + 2^{N-2})_q$.

For any white vertex $x \in A_N$, either $x \in A_{N-1}^{(1)}$ or $x \in A_{N-1}^{(2)}$. If $x \in A_{N-1}^{(j)}$ and y_k is connected to x by color $k \leq N-1$, then $y \in A_{N-1}^{(j)}$, by definition of $A_{N-1}^{(j)}$. For $x \in A_{N-1}^{(1)}$, it is labeled by $i_w = i_w^{(1)}$. Let y_1 be labeled by $j_b = j_b^{(1)}$. By construction of the labeling on $A_{N-1}^{(1)}$, $j_b^{(1)} = i_b^{(1)}$ and we see that y_1 is labeled by i_b . Let y_k be labeled by $l_b = l_b^{(1)}$. By construction, if $1 \leq i^{(1)} \pmod{2^{k-1}} (= i \pmod{2^{k-1}}) \leq 2^{k-2}$, then $l_b^{(1)} = (i^{(1)} + 2^{k-2})_b = (i + 2^{k-2})_b$, and $l_b^{(1)} = (i^{(1)} - 2^{k-2})_b = (i - 2^{k-2})_b$ otherwise. When $x \in A_{N-1}^{(2)}$, then it is labeled by $i_w = (i^{(1)} + 2^{N-2})_w$. y_1 is labeled by $j_b = (j^{(2)} + 2^{N-2})_b = (i^{(2)} + 2^{N-2})_b = i_b$. Now for $k \leq N-1$ let y_k be labeled by l_b . If $i \pmod{2^{k-1}} = (i^{(2)} + 2^{N-2}) \pmod{2^{k-1}} = i^{(2)} \pmod{2^{k-1}}$ is between 1 and 2^{k-2} , then $l_b = (l^{(2)} + 2^{N-2})_b = (i^{(2)} + 2^{k-2} + 2^{N-2})_b = (i + 2^{k-2})_b$. Otherwise, $l_b = (l^{(2)} + 2^{N-2})_b = (i^{(2)} - 2^{k-2} + 2^{N-2})_b = (i - 2^{k-2})_b$.

It remains only to show that the conditions of the proposition are met by points connected by color N . We will do this by induction on the white vertices, but first we need the following result.

Claim 1. If i_w is connected to j_b by color k , then color k must connect i_b and j_w .

Proof. j_w is connected to j_b by color 1, which is connected to i_w by color k . Following color 1 again gets us to i_b . Therefore to complete the 2-colored loop, i_b and j_w must be connected by color k . \square

By construction, 1_w is connected to $(1 + 2^{N-2})_b$ by color N . Now assume i_w is connected to $(i + 2^{N-2})_b$ for all $i \leq l-1$ for some $l \leq 2^{N-2}$. For $l \geq 2$ there exists $k \leq N-1$ such that $2^{k-2} + 1 \leq l \leq 2^{k-1}$. Color k connects l_w to $(l - 2^{k-2})_b$. By the inductive assumption $(l - 2^{k-2})_w$ is connected to $(l - 2^{k-2} + 2^{N-2})_b$ by color N . Therefore, by the claim $(l - 2^{k-2})_b$ is connected to $(l - 2^{k-2} + 2^{N-2})_w$ by color N . $l - 2^{k-2} \in [1, 2^{k-2}]$, since k was chosen so that $l \in [2^{k-2} + 1, 2^{k-1}]$. This shows that $(l - 2^{k-2} + 2^{N-2})_w$ is connected to $(l + 2^{N-2})_b$ by color N . Therefore, to complete the k/N 2-colored loop starting at l_w , l_w and $(l + 2^{N-2})_b$ must be connected by color N . This only deals with the first 2^{N-2} white vertices. Let $2^{N-2} + 1 \leq i \leq 2^{N-1}$. As just shown i_b is connected to $(i - 2^{N-2})_w$ by color N . Therefore by the claim, i_w is connected to $(i - 2^{N-2})_b$ by color N . And as shown, this labeling meets all of the conditions of the proposition. Furthermore we could have started with any white vertex as 1_w . \square

Corollary 1. *The edges of the N -cube A_N can be labeled so that the monodromy group corresponding to the Belyi map is generated by*

$$\sigma_0 = (1\ 2\ \cdots\ N)(N+1\ N+2\ \cdots\ 2N)\ \cdots\ ((m-1)N+1\ (m-1)N+2\ \cdots\ mN)$$

and

$$\sigma_1 = (a_N^{(1)}\ a_{N-1}^{(1)}\ \cdots\ a_1^{(1)})\ \cdots\ (a_N^{(m)}\ a_{N-1}^{(m)}\ \cdots\ a_1^{(m)}),$$

where $a_1^{(i)} = (i-1)N+1$ and for $k \neq 1$

$$(12) \quad a_k^{(i)} = \begin{cases} (2^{k-2} + i - 1)N + k, & \text{if } i \pmod{2^{k-1}} \in [1, 2^{k-2}], \\ (i - 1 - 2^{k-2})N + k, & \text{otherwise.} \end{cases}$$

Proof. Label the vertices of A_N as in Proposition 2. Label the edge of color k in the rainbow at i_w to be $(i-1)N+k$. For now let us think of the rainbow as being $(1, 2, 3, \dots, N)$, so that the k th color in the rainbow is color k . We will see later that changing the rainbow (performing an R -symmetry) will give equivalent Belyi pairs. σ_0 is obtained by taking the edge colors in order at each white vertex giving

$$\sigma_0 = (1\ 2\ \cdots\ N)(N+1\ N+2\ \cdots\ 2N)\ \cdots\ ((m-1)N+1\ (m-1)N+2\ \cdots\ mN).$$

σ_1 is obtained by taking the edge colors in reverse order at each black vertex. Therefore $a_k^{(i)}$ is given by the label of the edge of color k incident with i_b . i_b is connected to i_w by color 1, and the edge with color 1 incident to 1_w is labeled $(i-1)N+1$. Therefore, $a_1^{(i)} = (i-1)N+1$. For $k \neq 1$, i_b is connected to $(i+2^{k-2})_w$ by color k if $i \pmod{2^{k-1}} \in [1, 2^{k-2}]$. The edge of color k incident to $(i+2^{k-2})_w$ is $(i+2^{k-2}-1)+k$. If $i \pmod{2^{k-1}} \notin [1, 2^{k-2}]$, then color k connects i_b to $(i-2^{k-2})_w$. The color k edge incident to $(i-2^{k-2})_w$ is labeled by $(i-2^{k-2}-1)N+k$. Therefore, $a_k^{(i)}$ is as required. \square

Note that relabeling the edges will give equivalent Belyi coverings. Relabeling the edges changes the label everywhere it appears in σ_q , $q = 0, 1$. If we exchange the labels of edges i and j , then σ_q is conjugated by (i, j) . Since all possible relabelings can be generated by the transpositions, we see that all relabelings will give rise to monodromy generators $\tilde{\sigma}_q = g^{-1}\sigma_q g$ for some $g \in S_{N2^{N-1}}$, giving an equivalent Belyi covering.

The colors represent the generators of the supersymmetry algebra Q_i . Color i represents Q_i . We have numbered the Q_i 1 through N and used that ordering to define the rainbow which determines which 2-colored loops of A_N we attach 2-cells to in order to create X_N . The mathematics of the algebra and the physics it represents does not depend on the arbitrary order we chose for the generators of the algebra. Therefore we would like for the geometrization of the algebra to not depend on the ordering of the supersymmetry generators. Changing the order of the Q_i changes the rainbow which changes where we attach the 2-cells. We show now that changing the rainbow gives an equivalent Belyi pair.

Theorem 1. *If A_N and \tilde{A}_N are N -cubes with different rainbows then they give rise to equivalent Belyi pairs.*

Proof. We assume $N \geq 3$ since the result is trivial for small N . Give A_N the edge labeling from Corollary 1 with rainbow $(1, 2, \dots, N)$. \tilde{A}_N has the the same underlying graph, the only thing that is different is the rainbow, i.e. the cyclic order of the N colors. The difference between A_N and \tilde{A}_N is completely encoded in a permutation of the order of the N colors, i.e. an element of S_N . This means that for any 2 N -cubes A_N and \tilde{A}_N with rainbows $r \in S_N$ and $\tilde{r} \in S_N$ respectively there exists $g \in S_N$ such that $\tilde{r} = grg^{-1}$. $(1, 2)$ and $(1, 2, \dots, N)$ generate all of S_N . Therefore, it is enough to show that the belyi pair for A_N with rainbow $r = (1, 2, \dots, N)$ is equivalent to the Belyi pair for \tilde{A}_N with rainbow $\tilde{r} = grg^{-1}$ for just $g = (1, 2)$ and $(1, 2, \dots, N)$.

Let us first consider the case where \tilde{A}_N is obtained from A_N by exchanging the order of colors 1 and 2 in the rainbow. Since we have labeled the edges A_N as in Corollary 1, $\sigma_0 = \sigma_0^{(1)}\sigma_0^{(2)} \dots \sigma_0^{(2^{N-1})}$, where $\sigma_0^{(i)} = ((i-1)N+1 \ (i-1)N+2 \dots \ iN)$, and $\sigma_1 = \sigma_1^{(1)}\sigma_1^{(2)} \dots \sigma_1^{(2^{N-1})}$, where $\sigma_1^{(i)} = (a_N^{(i)} \ a_{N-1}^{(i)} \dots \ a_1^{(i)})$ with $a_k^{(i)}$ as in Corollary 1. We can give \tilde{A}_N the same labeling as A_N since they have the same underlying graphs, but the rainbow is now $\tilde{r} = (2, 1, 3, 4, \dots, N)$. Therefore the difference between σ_q and $\tilde{\sigma}_q$ will be the order of the colors. Changing the rainbow will keep the numbers appearing in each disjoint N -cycle (the edges incident to the vertex), $\sigma_0^{(i)} = ((i-1)N+1 \ (i-1)N+2 \dots \ iN)$, the same but the order of each one mod N will change from $(1 \ 2 \dots \ N-1 \ 0)$ in the same way. Therefore,

$$(13) \quad \tilde{\sigma}_0^{(i)} = ((i-1)N+2 \ (i-1)N+1 \ (i-1)N+3 \dots \ iN),$$

and

$$(14) \quad \tilde{\sigma}_1^{(i)} = (a_N^{(i)} \ a_{N-1}^{(i)} \dots \ a_3^{(i)} \ a_1^{(i)} \ a_2^{(i)}).$$

Every natural number i can be written as the sum of distinct powers of 2. The sum contains 2^0 if and only if i is odd. This allows us to partition the odd numbers based on whether there are even or odd number powers of 2 left in the sum after we remove the copy of 2^0 . Let S_o to be the set of all odd i such that $i-1$ can be written as the sum of an odd number of distinct powers of 2 with powers between 1 and $N-2$. Similarly, let S_e be the set of all odd i such that $i-1$ can be written as the sum of an even number of distinct powers of 2 with powers between 1 and $N-2$. Note that $S_o \cup S_e$ contains all odd numbers between 1 and 2^{N-1} . 1 is in S_e . Now define

$$(15) \quad \alpha = \prod_{\substack{i=1 \\ \text{odd}}}^{2^{N-1}} (a_1^{(i)}, a_2^{(i+1)})(a_1^{(i+1)}, a_2^{(i)}),$$

$$(16) \quad \beta_o = \prod_{i \in S_o} (a_1^{(i)}, a_1^{(i+1)})(a_2^{(i)}, a_2^{(i+1)}),$$

and

$$(17) \quad \beta_e = \prod_{i \in S_e} \prod_{k=3}^N (a_k^{(i)}, a_k^{(i+1)}).$$

Finally, let

$$(18) \quad \gamma = \alpha\beta_o\beta_e.$$

In Appendix A we prove

Claim 2. $\tilde{\sigma}_q$ can be obtained from σ_q by conjugation by γ .

Since the generators of the monodromy groups for A_N and \tilde{A}_N are related by a global conjugacy, i.e. the generating sets are mapped to each other by conjugation by a single element, the corresponding Belyi pairs are equivalent.

Now let us consider the case of $g = (1, 2, \dots, N)$. Conjugation by this g in S_N leaves the rainbow r invariant. This is just a cyclic permutation of the rainbow and therefore leaves σ_0 and σ_1 invariant as elements of S_d . The Belyi pairs are therefore trivially equivalent.

All possible permutations of the rainbow are generated by these 2, since $(1\ 2)$ and $(1\ 2 \cdots N)$ generate S_N . Therefore all possible rainbows will give equivalent Belyi pairs. \square

Note that we can view the action of the permutation subgroup of the R -symmetry group on an Adinkra chromotopology with a rainbow as a permutation of the rainbow. As discussed in section 2, the permutation subgroup of the full R -symmetry group $O(N)$ is the largest subgroup whose action on an Adinkra is well defined. Therefore, as an abuse of notation, we will refer to the permutation subgroup as an R -symmetry. Recall that R -symmetry exchanges the action of different Q_i . As a concrete example, consider X_N with rainbow $(1, 2, \dots, N)$ and the R -symmetry that exchanges the action of Q_1 and Q_3 . If $Q_1\phi_0 = \psi_1$ and $Q_3\phi_0 = \psi_3$ this is represented in the graph A_N that is embedded in X_N by the white vertex representing ϕ_0 being connected to the black vertex representing ψ_1 by color 1 and to the black vertex representing ψ_3 by color 3. In our labeling scheme we can identify ϕ_0 with the vertex 1_w and ψ_i with the vertices i_b .

Under the normal view of R -symmetry, we would represent the R -symmetry that exchanges the action of Q_1 and Q_3 by exchanging the colors of the edges of colors 1 and 3. This makes sense, since after the R -symmetry $Q_1\phi_0 = \psi_3$ and $Q_3\phi_0 = \psi_1$. Under this viewpoint of R -symmetry the Q_i remain represented by color i and therefore 1_w should now be connected to 3_b by color 1 and to 1_b by color 3. Call this chromotopology \tilde{A}_N . Note that with this viewpoint, the rainbow is unchanged by R -symmetry. Under the R -symmetry we just changed the action of a couple of Q_i , not their ordering.

In fact we should really view the rainbow as labeling which Q_i each color represents. Since the rainbow determines which 2-colored loops we attach 2-cells to in order to create \tilde{X}_N , we are still attaching 2-cells based on the same adjacent colors. The 2-cells that are attached to loops containing only colors that aren't adjacent to 1 or 3 will remain unchanged. Let us look at the $1/N$ 2-colored faces as an example. The $1/N$ 2-colored loops in \tilde{A}_N are equivalent to $3/N$ 2-colored loops in A_N , by construction. This shows that the Riemann surface \tilde{X}_N is isomorphic to leaving the chromotopology A_N unchanged but using the rainbow $(3, 2, 1, 4, \dots, N)$. In this viewpoint we are changing which Q_i the different colors represent. We are able to do this because we have the extra information of the rainbow that encodes this data. In this way we fix the chromotopology and transfer the information we would have had by changing the coloring to changing the rainbow.

To explicitly show that the equivalent descriptions of R -symmetric surfaces described above is compatible with the Belyi map, consider \tilde{A}_N with the same labeling as A_N so that the edges labeled $kN + 1$ in A_N are now color 3 in \tilde{A}_N (as opposed to color 1 in A_N) and the edges labeled $kN + 3$ in A_N are now color 1 in \tilde{A}_N . Therefore the monodromy at each white vertex i_w in \tilde{A}_N , which is given by the edges incident to i_w in the order of the rainbow $(1, 2, 3, \dots, N)$, is $((i - 1)N + 3, (i - 1)N + 2, (i - 1)N + 1, (i - 1)N + 4, \dots, iN)$. This is the same as the monodromy at each white vertex for A_N with rainbow $(3, 2, 1, 4, \dots, N)$. A similar argument holds for the monodromies at the black vertices giving equivalent Belyi pairs.

Corollary 2. *The Belyi pair (X_N, β) associated to the A_N is invariant under the action of the permutation subgroup of the R -symmetry group.*

Proof. Since we can view R -symmetries as permuting the rainbow the corollary follows immediately from Theorem 1. \square

Theorem 2 (Jones [29]). *The Belyi pair (X_N, β) for the N cube with rainbow $(1, 2, \dots, N)$ factors through the Belyi pair $(B_N, \tilde{\beta})$. Here B_N is \mathbb{CP}^1 with a single white vertex at 0, a single black vertex at ∞ and one edge of each color connecting the vertices. Edge color j is given by the line with $\arg = \frac{2\pi j}{N}$. The Belyi map for B_N is⁴*

$$(19) \quad \tilde{\beta}(x) = \frac{x^N}{x^N + 1}.$$

First note that this is indeed a Belyi pair. $\tilde{\beta}$ is a degree N covering that has order N ramification over 0 and 1 (at 0 and ∞ in B_N), and is unramified everywhere else. Jones shows that the Belyi pair for A_N factors through $(B_N, \tilde{\beta})$ by noting that the automorphism group of the N -cube contains a normal subgroup isomorphic to the

⁴There is a typo in [29] that incorrectly states $\tilde{\beta} = \left(\frac{x}{x-1}\right)^n$. This error is carried through to the computation of $\tilde{\beta}^{-1}$.

direct sum of 2^{N-1} copies of \mathbb{Z}_2 generated by half turns of faces. Notice that the generating set equates the white vertices that make up a face and the two black vertices that are incident to the face.

In the language of [15] the quotient $f : X_N \rightarrow B_N$ is the quotient of the cube (where the vertices are labeled by element of \mathbb{F}_2^N) by the maximally even subcode of \mathbb{F}_2^N . Note that the maximally even subcode of \mathbb{F}_2^N , C_N , is generated by $(c_1, c_2, \dots, c_{N-1})$, where c_i is the code word that has 1's in the i th and $(i+1)$ th position and 0's everywhere else. Let us also define $c_N = [1, 0, 0, \dots, 0, 1] = c_1 c_2 \cdots c_{N-1}$. Modding A_N by C_N clearly gives the embedded graph of B_N , let us call it Σ_N . All of the white vertices represent even code words and all of the black vertices represent odd code words. Therefore all of the white vertices are in C_N and the black vertices are not. Following [15], edges of the same color incident to equivalent points are equated. Therefore all of the edges of a given color are equated, showing that $f(A_N) = \Sigma_N$. Note that the generators of C_N connect the 2 white vertices incident to the 2-colored faces (the ones with adjacent colors). So the generators of the doubly even code are equivalent to the generators of the subgroup of $\text{Aut}(A_n)$.

Attach each disjoint N -cycles in σ_q , $q = 1, 2$, to the vertex whose monodromy the cycle represents. Using the labeling in corollary 1, $\sigma_0^{(i)}$ is attached to vertex i_w and $\sigma_1^{(i)}$ is attached to i_b . Modding out by the code C_N divides \mathbb{F}_2 into 2 cosets of size 2^{N-1} , thus it divides the N -cycles attached to each cycle into 2 cosets. Under the action of an even code, $\sigma_0^{(i)}$ cannot be in the same coset as the $\sigma_1^{(i)}$ since even codes preserve the bipartite structure. In our current case of modding out by C_N , one coset consists of all the $\sigma_0^{(i)}$ while the other contains all of the $\sigma_1^{(i)}$. The vertices of $\Sigma_N \subset B_N$ represent the cosets of the cube under the action of C_N . So the monodromy over the white and black vertex can be represented by one element of the corresponding coset of N -cycles. Note that we should use the same set of numbers in the N -cycles at the black vertices as we do at the white vertices. This makes sense since the projection on the $\sigma_1^{(i)}$'s is compatible with the projection on the $\sigma_0^{(i)}$'s. If i_w is identified with j_w by the code and i_w is connected to k_b and j_w is connected to l_b by color t then the code must identify k_b and l_b , so when we say that the projection is compatible with the monodromy, we mean that identifying $\sigma_0^{(i)}$ and $\sigma_0^{(j)}$ forces identifying $\sigma_1^{(l)}$ and $\sigma_1^{(k)}$. Recall that $\sigma_0^{(i)} = ((i-1)N+1, (i-1)N+2, \dots, iN)$, so equating $\sigma_0^{(i)}$ and $\sigma_0^{(j)}$ corresponds to equating $(i-1)N+m$ and $(j-1)N+m$ for $1 \leq m \leq N$. $\sigma_1^{(l)} = (a_N^{(l)}, a_{N-1}^{(l)}, \dots, a_1^{(l)})$, where $a_m^{(l)}$ represents the edge of color m incident to l_b (the formula is given in corollary 1). $a_t^{(k)} = (i-1)N+t$, since k_b is connected to i_w by color t . Similarly, $a_t^{(l)} = (j-1)N+t$, so we see that after equating $\sigma_0^{(i)}$ and $\sigma_0^{(j)}$, $a_t^{(k)}$ and $a_t^{(l)}$ are already equated. By following the same argument for each color, we see that performing the projection on the $\sigma_0^{(i)}$'s forces the compatible

projection on the $\sigma_1^{(i)}$'s. The Belyi map factors through the projection f , since the projection is compatible with the generators of the monodromy group of the Belyi map. In our current case, we can pick the monodromy at $1_w, (1, 2, \dots, N)$, as the representative of the single coset of white dots in Σ_N . This is equivalent to taking all of the elements of the $\sigma_q^{(i)}$'s mod N (where we represent $0 \pmod{N}$ by N). Therefore this forces the representative of the single coset of black dots to be $(N, N - 1, \dots, 1)$. This is exactly the monodromy of B_N .

It would be nice to explicitly see the action of f on the faces of X_N . As we saw previously, the monodromy over infinity, σ_∞ , describes the faces. However, under the projection f , all of the disjoint 2-cycles in σ_∞ get sent to the identity, since edges of the same color are identified. Despite the first appearance of losing the information about the faces, this is actually an important statement. We have shown that $\beta = \tilde{\beta} \circ f$. As shown β has order N ramification over 0 and 1 and order 2 ramification over infinity, while $\tilde{\beta}$ has order N ramification over 0 and 1 and is unramified elsewhere. The fact that $\tilde{\beta}$ is unramified over ∞ is seen by the fact that σ_∞ projects to the identity under f . Furthermore we see that all of the ramification of X_N over the Belyi base is split so that all of the order N ramification (the ramification over 0 and 1) is contained in $\tilde{\beta} : B_N \rightarrow \mathbb{CP}^1$ and all of the order 2 ramification occurs in $f : X_N \rightarrow B_N$ at the centers of the 2-cells.

The data of the faces of B_N is still contained in σ_0 and σ_1 , but is harder to see since their product σ_∞ is the identity for B_N . In this case it is better to look at π_∞ (equation 11). For B_N with rainbow given by $(1, 2, \dots, N)$, if we label the half edge of color i incident to the white vertex in Σ_N i and the half edge incident to the black vertex $i + N$ then

$$\pi_\infty = \pi_\infty^{(1)} \pi_\infty^{(2)} \cdots \pi_\infty^{(N)},$$

where $\pi_\infty^{(i)} = (i, i + N + 1)$ if we identify $2N + 1$ with $N + 1$. All of the faces of B_N are 2-gons. Each transposition in π_∞ lists the incoming half-edge at the 2 vertices as we go clockwise around the N -faces of B_N . π_∞ for A_N consists of disjoint 4-cycles, listing the incoming half-edges at each of the 4-vertices that make up a face. f equates the edges of the same color in π_∞ for X_N to give π_∞ for B_N . Therefore we can view the action of f on the faces in 2 parts. Each 2-colored 4-gon face in X_N is first mapped to a face with 2 sides by identifying the points diagonal to each other (accounting for the order 2 ramification) and then all of the 2-gons with the same 2-color boundary are identified. Note that from this we see that the information of the rainbow is completely contained in B_N . The rainbow is what determines which 2-colored loops of A_N are filled in to create X_N , but the faces can be viewed as the pullback of the faces of B_N . Once the rainbow is decided for B_N , determining which 2-colored 2-gons of Σ_N to attach 2-cells to, the rainbow for A_N and which faces are filled in is fixed. Furthermore, B_N is the first possible place the rainbow can be seen, as it is where the edge in the Belyi base is split into N colored edges.

Before going over an example, let us describe the monodromy of f , as it will be needed later.

Theorem 3. *The monodromy group of (X_N, f) is generated by $\rho_i \in S_{2^{N-1}}$, $1 \leq i \leq N - 1$ with*

$$(20) \quad \rho_1 = (1, 2)(3, 4) \cdots (2^{N-1} - 1, 2^{N-1})$$

$$(21) \quad \rho_i = \prod_{\substack{j=1 \\ 1 \leq j \bmod 2^{i-1} \leq 2^{i-2}}}^{2^{N-1}} (j, j + 2^{i-2} + 2^{i-1}), \text{ for } i \neq 1.$$

Proof. As noted, $f : X_N \rightarrow B_N$ is an order 2^{N-1} covering map with order 2 ramification at the centers of the 2-faces. Note that the ramification is over the roots of -1 in B_N which are the inverse images of ∞ in the Belyi base under $\tilde{\beta}$. Therefore we can describe the monodromy group of f by the monodromies over the centers of the N faces of B_N , the N th roots of -1 . Label the center of the $i/(i+1)$ 2-colored face i_f and consider a small loop around i_f that is based at the white vertex. It lifts by f to 2^{N-2} loops around the centers of the $i/(i+1)$ 2-colored faces in X_N . Each lift now has 2 base points given by the 2 white vertices incident to the face the loop is in. We can encode the monodromy at the center of each face to be the transposition that exchanges these 2 vertices. Note that we are labeling the monodromy of f by the vertices instead of by the edges as we did for the Belyi map.

We could not define the monodromy of the Belyi map by the vertices because the Belyi map is ramified over the vertices. f is unramified at the vertices and we can associate the 2^{N-1} sheets of $f^{-1}(B_N)$ with the 2^{N-1} white vertices of X_N . Also note that as previously shown it is enough to describe the action on the white vertices since the action on the black vertices is then fixed.

Define ρ_i to be the product of the transpositions associated to the center of each $i/(i+1)$ 2-colored face. Then ρ_i , $1 \leq i \leq N - 1$ generate the monodromy group for f and $\rho_N^{-1} = \rho_1 \rho_2 \cdots \rho_{N-1}$. For the cube, using the labeling of vertices from proposition 2, color 1 connects j_w to j_b which is connected to $(j + (-1)^{j+1})_w$ by color 2. Therefore,

$$(22) \quad \rho_1 = (1, 2)(3, 4) \cdots (2^{N-1} - 1, 2^{N-1}).$$

For $1 < i < N$ and $1 \leq j \pmod{2^{i-1}} \leq 2^{i-2}$, j_w is connected to $(j + 2^{i-2})_b$ by color i . $1 \leq j + 2^{i-2} \pmod{2^i} \leq 2^{i-1}$ because of the bounds of j . Therefore, $(j + 2^{i-2})_b$ is connected to $(j + 2^{i-2} + 2^{i-1})_w$ by color $i + 1$. This shows that for fixed color $i \neq 1, N$, if j_w is a white vertex of the $i/(i+1)$ 2-colored face with $1 \leq j \pmod{2^{i-2}} \leq 2^{i-1}$ then $(j + 2^{i-2} + 2^{i-1})_w$ is the other white vertex incident to the face. Note that this describes all of the white vertices since by construction

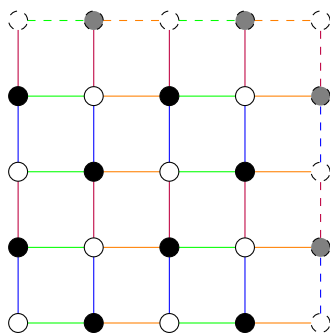


FIGURE 2. The $(4, 0)$ Adinkra with rainbow (green, blue, orange, purple) embedded in a torus. The top row is identified with the bottom row and the right column is identified with the left column. The $(4, 1)$ Adinkra embedding is obtained by taking only the left half of the $(4, 0)$ embedding.

$(j + 2^{i-2} + 2^{i-1}) \pmod{2^{i-2}} > 2^{i-1}$, or it's 0. Therefore for $i \neq 1, N$,

$$(23) \quad \rho_i = \prod_{\substack{j=1 \\ 1 \leq j \pmod{2^{i-1}} \leq 2^{i-2}}}^{2^{N-1}} (j, j + 2^{i-2} + 2^{i-1}).$$

□

For later convenience we note here that the $N/1$ 2-colored faces are described by ρ_N which is the inverse of the product of the other $N - 1$ ρ_i and is given by

$$(24) \quad \rho_N = \prod_{j=1}^{2^{N-2}} (j, j + 2^{N-2}).$$

Example 1 (The 4-Cube). Consider A_4 with rainbow $(1, 2, 3, 4)$ with corresponding Belyi pair (X_4, β) . X_4 has genus 1 by proposition 1, so is an elliptic curve (its complex structure is pulled back from $\mathbb{C}\mathbb{P}^1$ by β), see Figure 2. The monodromy group of β is generated by

$$(25) \quad \sigma_0 = (1, 2, 3, 4)(5, 6, 7, 8)(9, 10, 11, 12)(13, 14, 15, 16) \cdots$$

$$(26) \quad \cdots (17, 18, 19, 20)(21, 22, 23, 24)(25, 26, 27, 28)(29, 30, 31, 32)$$

and

$$(27) \quad \sigma_1 = (20, 11, 6, 1)(24, 15, 2, 5)(28, 3, 14, 9)(32, 7, 10, 13) \cdots$$

$$\cdots (4, 27, 22, 17)(8, 31, 18, 21)(12, 19, 30, 25)(16, 23, 26, 29).$$

The faces are described by

$$(28) \quad \begin{aligned} \pi_\infty = & (1, 34, 5, 38)(2, 35, 14, 47)(3, 36, 27, 60)(4, 33, 20, 49) \cdots \\ & \cdots (6, 39, 10, 43)(7, 40, 31, 64)(8, 37, 24, 53)(9, 42, 13, 46) \cdots \\ & \cdots (11, 44, 19, 52)(12, 41, 28, 57)(15, 48, 23, 56)(16, 45, 32, 61) \cdots \\ & \cdots (17, 50, 21, 54)(18, 51, 30, 63)(22, 55, 26, 59)(25, 58, 29, 62) \end{aligned}$$

Now label the half-edge of color i incident to the white vertex in B_4 i and the half-edge incident to the black vertex $i + 32$. For $\tilde{\beta} : B_4 \rightarrow \mathbb{CP}^1$

$$\tilde{\pi}_\infty = (1, 34)(2, 35)(3, 36)(4, 33).$$

As always $f : X_4 \rightarrow B_4$ projects σ_0 onto $(1, 2, 3, 4)$ and σ_1 onto $(4, 3, 2, 1)$. More interesting is how we can see the action on the faces by looking at the action of f on π_∞ . f projects all of the 1/2-colored faces in X_N ; $(1, 34, 5, 38)$, $(9, 42, 13, 46)$, $(25, 58, 29, 62)$, and $(17, 50, 21, 54)$ onto the 1/2 colored face in B_N $(1, 34)$. Similarly the 4 $i/(i + 1)$ faces in X_N map onto the 1 $i/(i + 1)$ face in B_N , which can be realized as the map that sends each number j appearing in each 4-cycle to $j \pmod{4}$ if $j \leq 32$ and $j \pmod{4} + 32$ otherwise. Here we represent 0 $\pmod{4}$ by 4.

Finally we consider the generators of the monodromy of f :

$$(29) \quad \rho_1 = (1, 2)(3, 4)(5, 6)(7, 8)$$

$$(30) \quad \rho_2 = (1, 4)(2, 3)(5, 8)(6, 7)$$

$$(31) \quad \rho_3 = (1, 7)(2, 8)(3, 5)(4, 6)$$

$$(32) \quad \rho_4 = (1, 5)(2, 6)(3, 7)(4, 8).$$

The numbers appearing in the ρ_i represent the 8 white vertices in X_4 . Each 2 cycle represents a single face that the 2 vertices listed are incident to. ρ_i represents the 4 $i/(i + 1)$ faces that get equated by f . Note that ρ_4 which represents the 4/1 faces is given by $\rho_1\rho_2\rho_3$.

3.2. General Adinkra Chromotopologies. As described in [15], all Adinkra chromotopologies $A_{(N,k)}$ can be obtained by quotienting the cube A_N by a k -dimensional doubly even code $C_{(N,k)}$. Let us start by considering the case where A_N has the rainbow $(1, 2, \dots, N)$. $A_{(N,k)}$ inherits the same rainbow. We will first show that, like the N -cube, the Belyi pair $(X_{(N,k)}, \beta_k)$ factors through $(B_N, \tilde{\beta})$.

Proposition 3. *The Belyi pair $(X_{(N,k)}, \beta_k)$ with rainbow $(1, 2, \dots, N)$ associated to any Adinkra chromotopology $A_{(N,k)}$ factors through the Belyi pair $(B_N, \tilde{\beta})$.*

Proof. Label the white vertices in $X_{(N,k)}$ 1_w to $(2^{N-k-1})_w$ and the black vertices 1_b to $(2^{N-k-1})_b$. Label the edge of color i incident to j_w $(j - 1)N + i$. Therefore

the monodromy for $\beta_{(N,k)}$ over 0 is given by

$$\sigma_0 = \prod_{j=1}^{2^{N-k-1}} ((j-1)N+1, (j-1)N+2, \dots, jN).$$

Therefore following the prescription for σ_1 and letting $m = 2^{N-k-1}$, we find

$$\sigma_1 = (a_N^{(m)}, a_{N-1}^{(m)}, \dots, a_1^{(m)})(a_N^{(m-1)}, a_{N-1}^{(m-1)}, \dots, a_1^{(m-1)}) \dots (a_N^{(1)}, \dots, a_1^{(1)}).$$

Here $a_i^{(j)}$ is the color i edge adjacent to j_b , so in particular $a_i^{(j)} \pmod{N} \equiv i \pmod{N}$.

Every doubly even code $C_{(N,k)}$ is a subcode of the maximally even code C_N . Therefore modding $A_{(N,k)} \cong A_N/C_{(N,k)}$ out by C_N is well defined, and moreover $A_{(N,k)}/C_N \cong A_N/C_N$. $\Sigma_N \subset B_N$ is obtained from $A_{(N,k)}$ by identifying all of the white vertices and identifying all of the black vertices. Therefore under the action of C_N all of the N -cycles associated to the 2^{N-k-1} white vertices are identified, all of the N -cycles associated to the black vertices are identified. Following the same argument as for the N -cube, we can choose the representative the coset of the 2^{N-k-1} N -cycles associated to the white vertices of $A_{(N,k)}$ (the representative of the white vertex in B_N) to be $(1, 2, \dots, N)$. This is equivalent to equating the $\sigma_0^{(i)} \pmod{N}$ where we represent $0 \pmod{N}$ by N . This forces σ_1 to be $(N, N-1, \dots, 1)$, giving the monodromy of B_N . Therefore the projection $X_{(N,k)} \rightarrow B_N$ is compatible with the monodromy groups of β_k and $\tilde{\beta}$, so the Belyi pair $(X_{(N,k)}, \beta_k)$ factors through the Belyi pair $(B_N, \tilde{\beta})$. \square

We would now like to show that (X_N, β) factors through $(X_{(N,k)}, \beta_k)$. Before discussing the general case, let us look at a specific example.

Example 2 (The $[4, 1]$ Adinkra). Let $A_{(4,1)}$ be an Adinkra chromotopology obtained by modding the 4-cube, A_4 out by the code $[1, 1, 1, 1]$. Pick the white vertex in $A_{(4,1)}$ that corresponds to the equivalence class of $1_w \in A_4$ and label it $\tilde{1}_w$. Label the vertex connected to $\tilde{1}_w$ by color 1 $\tilde{1}_b$, and for $2 \leq i \leq 4$ label the vertex connected to $\tilde{1}_w$ by color i , \tilde{i}_b . Finally label the vertex connected to \tilde{i}_b by color 1, i_w . This labels all 8 vertices (4 white and 4 black) of $A_{(4,1)}$. As usual label the edge of color i incident to vertex \tilde{j}_w $(j-1)4+i$. Using this labeling we find

$$(33) \quad \sigma_0^{(4,1)} = (1, 2, 3, 4)(5, 6, 7, 8)(9, 10, 11, 12)(13, 14, 15, 16)$$

and

$$(34) \quad \sigma_1^{(4,1)} = (1, 16, 11, 6)(2, 5, 12, 15)(3, 14, 9, 8)(4, 7, 10, 13).$$

The code generated by $[1, 1, 1, 1]$ has 2 elements, so it divides the white vertices of A_4 into 4 cosets each containing 2 elements. Using the labeling of A_4 from proposition 2 and associating 1_w with the code word $[0, 0, 0, 0]$, $[1, 1, 1, 1]$ connects i_w to $(9-i)_w$. This divides the 8 N -cycles attached to each of the 8 white vertices

in A_4 , into 4 cosets containing 2 elements each. The 4-cycles appearing in $\sigma_0^{(4,1)}$ are the representatives of those cosets. Similarly, i_b is connected to $(9-i)_b$ by $[1, 1, 1, 1]$, splitting the 4-cycles attached to each of the black vertices into 4 cosets containing 2 elements. Each of the 4-cycles appearing in $\sigma_1^{(4,1)}$ is a representative of one of these cosets. Picking a representative for each coset corresponding to a white vertex in $A_{(4,1)}$ determines the representative for each coset corresponding to a black vertex.

Each coset corresponds to the white vertices consists of 2 4-cycles, $((i-1)4+1, (i-1)4+2, (i-1)4+3, i4)$ and $((8-i)4+1, (8-i)4+2, (8-i)4+3, (9-i)4)$. The representatives we have chosen is equivalent to equating $(i-1)4+j$ and $(8-i)4+j$ and then using the smaller number as the representative. The choice of a representative is equivalent to a labeling; we have chosen a label for the edges in $A_{(4,1)}$ which can be viewed as an equivalence class of 2 edges in A_4 . Now consider for example the 4-cycle $(1, 16, 11, 6)$ appearing in $\sigma_1^{(4,1)}$. It is the representative of the coset consisting of the 2 elements $(1, 20, 11, 6)$ and $(29, 16, 23, 26)$ (see equation 27). The identification of $(i-1)4+j$ in one cycle and $(9-i)4+j$ in the other cycle is already forced and we have already labeled the edges by the smaller number in the identification, forcing the representative to be given by $(1, 16, 11, 6)$. This shows that the projection from A_4 to $A_{(4,1)}$ extends to a projection of the associated Riemann surfaces $p : X_N \rightarrow X_{(4,1)}$ such that $\beta = \beta_{(4,1)} \circ p$.

Let us look at the action on the faces. The face of $X_{(4,1)}$ are described by

$$(35) \quad \pi_\infty = (1, 34, 5, 38)(2, 35, 14, 47)(3, 36, 7, 40)(4, 33, 16, 45) \cdots \\ \cdots (6, 39, 10, 43)(8, 37, 12, 41)(9, 42, 13, 46)(11, 44, 15, 48).$$

Each face of $X_{(4,1)}$ is the image of 2 faces in X_N under p . Again we can view each 4-cycle as a representative of 2 4-cycles appearing in π_∞ for A_4 (equation 28). For example $(1, 34, 5, 38)$ is the representative of the equivalence class consisting of $(1, 34, 5, 38)$ and $(29, 62, 25, 58)$. Note that the representative of the equivalence class is forced by our choice of the representatives at the white vertices. Recall that the black half-edges are the white half plus 32.

$X_{(4,1)}$ has genus 1 by proposition 1, so is also a torus. We can see that if we give X_4 as pictured in Figure 2 standard (x, y) coordinates, $p : X_4 \rightarrow X_{(4,1)}$ is given by $p(x, y) = (2x, x+y)$. That is, it is the map from the torus to the torus that wraps around the diagonal twice. The left half of Figure 2 can be taken as a fundamental domain for $X_{(4,1)}$.

The general case works similarly. Already with such a simple example it was difficult to follow the representatives of the edges through to the different types of 4-cycles. This is because modding out by a code divides \mathbb{F}_2^N , hence the vertices, into cosets, not the edges. It is difficult to convert the cosets consisting of vertices into the edges incident to those vertices. It would be better if we could describe the monodromy groups in terms of vertices. We cannot describe the Belyi maps

β and β_k in terms of the vertices because they are ramified there. Luckily we have seen that both (X_N, β) and $(X_{(N,k)}, \beta_k)$ factor through $(B_N, \tilde{\beta})$, see Figure 3. Therefore, letting $f : X_N \rightarrow B_N$ be such that $\beta = \tilde{\beta} \circ f$ and $g : X_{(N,k)} \rightarrow B_N$ be

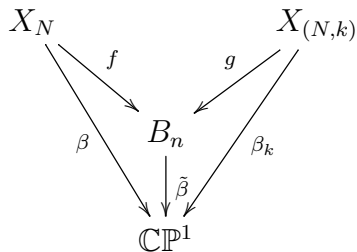


FIGURE 3. Factorization of (X_N, β) and $(X_{(N,k)}, \beta_k)$ through $(B_N, \tilde{\beta})$.

such that $\beta_k = \beta_k \circ g$, it is enough to show that (X_N, f) factors through $(X_{(N,k)}, g)$, and we can label the monodromies of f and g by the vertices of X_N and $X_{(N,k)}$ since they are both unramified there.

Recall that the monodromy of f is described by ρ_i , $1 \leq i \leq N$, which are given by equations 22 through 24. ρ_i is the product of 2^{N-2} disjoint 2-cycles. The 2-cycles represents the 2 white vertices incident to each of the 2^{N-2} $i/(i+1)$ 2-colored faces. We can describe the monodromy of g in the same way, where $\rho_i(g)$ is 2^{N-k-2} disjoint 2-cycles, each representing the 2 white vertices incident to each $i/(i+1)$ 2-colored face. The same argument used to define ρ_i by lifting loops from B_N applies here to obtain the result.

Theorem 4. (X_N, f) factors through $(X_{(N,k)}, g)$.

Proof. Let $p : X_N \rightarrow X_{(N,k)}$ be the projection induced by the map $A_N \rightarrow A_{(N,k)} = A_N/C$, for some k -dimensional doubly even code. Since the code C is k -dimensional and even it divides the even elements of \mathbb{F}_2^N , and hence the white vertices of X_N , into 2^{N-k-1} cosets with 2^k elements. Each white vertex in $X_{(N,k)}$ represents one of these cosets. To show that (X_N, f) factors through $(X_{(N,k)}, g)$ we need to show that if 2 white vertices of X_N are in the same coset when we mod out by C then every 2-cycle in $\rho_i(f)$ containing those 2 vertices are identified by p in $\rho_i(g)$ for each i .

Consider 2 white vertices in X_N that are in the same coset in A_N/C . Label them A and B . First note that the 2-cycle (A, B) does not appear in ρ_i for all i . Suppose (v_1, v_2) appears in ρ_i , that means going color i then color $i+1$ (or vice versa) will take you from v_1 to v_2 . This means that the elements of \mathbb{F}_2^N that v_1 and v_2 represent are connected by an element with only 2 non-zero entries, one for color i and the other for color $i+1$. Therefore v_1 and v_2 cannot be connected by a word in C because it is doubly even. (A, B) cannot be in ρ_i since A and B are connected by a word in C by assumption.

Now suppose (A, D) and (B, E) appear in ρ_i where as before A and B are connected by some word $c \in C$. Then by construction from [15], D and E are also connected by c . Therefore the projection from $A_N \rightarrow A_{(N,k)}$ respects the monodromies of f and g , completing the proof. \square

Note that in the above proof we see a new reason for why we must mod the N -cube out by a double even code to get an Adinkra. The code has to be even to preserve the bipartite structure. However, an even code would identify white vertices incident to the same face, i.e. equate vertices that appear in the same transposition in some representative of the ρ_i . Therefore we can view the evenness condition to preserve the bipartite structure and double evenness condition to ensure the proper action on the faces of the induced Riemann surfaces. X_N must be unramified over $X_{(N,k)}$ since f contains all of the order 2 ramification for β and $\tilde{\beta}$ contains all of the order N ramification. Therefore p must map faces to distinct faces as is ensured by the code being doubly even.

Example 3 (The Adinkra [4, 1] Revisited). The generators of f for the 4-cube are given by equations 29 through 32. As noted in Example 2, the projection $p_A : A_4 \rightarrow A_{(4,1)} = A_4 / \langle [1, 1, 1, 1] \rangle$ sends white vertex i to white vertex $9 - i$ using the labeling of proposition 2 (which was used for equations 29 through 32). $\rho_i(X_{(4,1)})$ can be obtained from $\rho_i(X_4)$ by identifying the 2-cycles according to the action of p_A . For example consider $\rho_1(X_4) = (1, 2)(3, 4)(5, 6)(7, 8)$ (equation 29). The cosets in $A_{(4,1)}$ are

$$(36) \quad \{\{1, 8\}, \{2, 7\}, \{3, 6\}, \{4, 5\}\}.$$

From this we see that $(1, 2)$ and $(7, 8)$ should be equated, and $(3, 4)$ and $(5, 6)$ should be equated. If we choose the smaller number in each coset as the representative we find

$$(37) \quad \rho_1(X_{(4,1)}) = (1, 2)(3, 4).$$

Now consider equation 30, $\rho_2(X_4) = (1, 4)(2, 3)(5, 8)(6, 7)$. From equation 36 we see that $(1, 4)$ and $(5, 8)$ should be equated, and $(2, 3)$ and $(6, 7)$ should be equated. Furthermore, since we already chose the representatives of the cosets we find

$$(38) \quad \rho_2(X_{(4,1)}) = (1, 4)(2, 3).$$

Similarly we find

$$(39) \quad \rho_3(X_{(4,1)}) = (1, 2)(3, 4),$$

$$(40) \quad \rho_4(X_{(4,1)}) = (1, 4)(2, 3).$$

This is the same as one would find if they wrote down $\rho_i(X_{(4,1)})$ directly using the labeling of $A_{(4,1)}$ from Example 2.

Recall that for the 4-cube, the monodromy of f is generated by $\rho_1(X_4)$, $\rho_2(X_4)$, and $\rho_3(X_4)$ with $\rho_4(X_4) = (\rho_1(X_4)\rho_2(X_4)\rho_3(X_4))^{-1}$. From the above example

we see that the monodromy group of $(X_{(4,1)}, g)$ has only 2 generators. $\rho_1(X_{(4,1)})$ exchanges white vertices that are connected by $[1, 1, 0, 0]$, while $\rho_3(X_{(4,1)})$ connects white vertices connected by $[0, 0, 1, 1]$. Therefore, since $[1, 1, 0, 0] + [0, 0, 1, 1] = [1, 1, 1, 1]$, the generator of the code, we see that $\rho_1(X_{(4,1)}) = (\rho_3(X_{(4,1)}))^{-1}$, as was found in the above example. For the general case

Proposition 4. *The monodromy group of $X_{(N,k)}$ has $N - k - 1$ generators.*

Proof. Let $X_{(N,k)}$ be the Riemann surface associated to the chromotopology $A_{(N,k)} = A_N/C$ for some k -dimensional doubly even code C . Each of the generators of C determines a relation on the $N - 1$ generators for the monodromy of (X_N, f) . \square

Corollary 3 (Corollary to Theorem 4). *The Belyi pair (X_N, β) factors through $(X_{(N,k)}, \beta_k)$*

We now have a sequence of covering spaces with any composition that ends at the base being a Belyi map, see Figure 4.

$$\begin{array}{c} X_N \\ \downarrow p \\ X_{(N,k)} \\ \downarrow g \\ B_n \\ \downarrow \tilde{\beta} \\ \mathbb{CP}^1 \end{array}$$

FIGURE 4.

To go from the monodromy of g (or $g \circ p$) to the monodromy of β all we need is $\rho_i(X_{(N,k)})$ and the rainbow. $\sigma_0(X_{(N,k)})$ can be obtained from only the rainbow. Pick any white vertex and label the edge of color l incident to it l . The monodromy at this point is now given by the rainbow. Now pick any other white vertex and label the edge of color l incident to it $N + l$. The rainbow with N added to every entry. Continuing in this way we can always write σ_0 as

$$(41) \quad \sigma_0(X_{(N,k)}) = \sigma_0^{(1)} \sigma_0^{(2)} \cdots \sigma_0^{(2^{n-k-1})},$$

where $\sigma_0^{(j)}$ is given by the rainbow with $(j - 1)N$ added to each entry. Now σ_∞ is completely determined by the $\rho_i(X_{(N,k)})$. Recall that σ_∞ is given by the incoming edges at the white vertices. The ρ_i list all of the white vertex pairs bounding a face. Therefore, for each 2-cycle appearing in a ρ_i change the element from the white vertex it labels to the incoming edge at that vertex as you go around the

corresponding face clockwise using the edge labeling we've already determined. σ_∞ is the product of all of these new 2-cycles.

Now let us consider R -symmetry for a general Adinkra⁵. As noted in our discussion of R -symmetry for the N -cube, we can view an R -symmetry as leaving the chromotopology alone and changing the rainbow. There was nothing specific to the N -cube in that argument, so we see the same is true for general Adinkras. Recall that from this viewpoint we consider the extra data of the rainbow as encoding which supersymmetry generator each color represents rather than considering each supersymmetry generator fixed to the same color as is usually the case. Since the rainbow is entirely determined by B_N , we can view the relationship between R -symmetric Adinkras as the pullback of the relationship between R -symmetric B_N 's.

Proposition 5. *If Σ_N is related to $\tilde{\Sigma}_N$ by an R -symmetry then the corresponding Belyi pairs $(B_N, \tilde{\beta})$ and $(\tilde{B}_N, \tilde{\beta})$ are equivalent.*

Proof. We can consider the case where B_N has the rainbow $(1, 2, \dots, N)$. We just need to show that changing the rainbow by $(1, 2)$ and $(1, 2, \dots, N)$ gives equivalent Belyi curves since $(1, 2)$ and $(1, 2, \dots, N)$ generate all of S_N . As with the case of the N -cube, changing the rainbow by $(1, 2, \dots, N)$ is trivial since the rainbow is invariant under conjugation by $(1, 2, \dots, N)$. The monodromy of $(B_N, \tilde{\beta})$ is

$$\begin{aligned}\sigma_0 &= (1, 2, \dots, N) \\ &\text{and} \\ \sigma_1 &= (N, N-1, \dots, 1).\end{aligned}$$

\tilde{B}_N has rainbow $(1, 2)(1, 2, \dots, N)(1, 2) = (2, 1, 3, \dots, N)$. Therefore the monodromy of $(\tilde{B}_N, \tilde{\beta})$ is generated by

$$\begin{aligned}\tilde{\sigma}_0 &= (2, 1, 3, \dots, N) \\ &\text{and} \\ \tilde{\sigma}_1 &= (N, N-1, \dots, 3, 1, 2).\end{aligned}$$

We see that $\tilde{\sigma}_q = (1, 2)\sigma_q(1, 2)$ for $q = 0, 1$. Therefore by the Grothendieck correspondence $(B_N, \tilde{\beta})$ and $(\tilde{B}_N, \tilde{\beta})$ are equivalent Belyi pairs. \square

⁵Again, when we refer to an R -symmetry we really mean the permutation subgroup of the full R -symmetry group $O(N)$.

By Theorems 1 and 4 and proposition 5 we have a commutative diagram

$$(42) \quad \begin{array}{ccc} X_N & \xrightarrow{\cong} & \tilde{X}_N \\ p \downarrow & & \downarrow \tilde{p} \\ X_{(N,k)} & & \tilde{X}_{(N,k)} \\ g \downarrow & & \downarrow \tilde{g} \\ B_n & \xrightarrow{\cong} & \tilde{B}_N. \end{array}$$

Proposition 6. *If $A_{(N,k)}$ and $\tilde{A}_{(N,k)}$ are related by an R -symmetry then the corresponding Belyi pairs $(X_{(N,k)}, \beta_k)$ and $(\tilde{X}_{(N,k)}, \tilde{\beta}_k)$ are equivalent.*

Proof. As usual it is enough to consider the R -symmetry that exchanges the action of Q_1 and Q_2 . $X_{(N,k)}$ and $\tilde{X}_{(N,k)}$ have the same chromotopology, the only difference is their rainbows. Therefore we can label their vertices so that $\rho_i = \tilde{\rho}_i$. For example if white vertex i is connected to vertex j by going color 2 then color 3 and is connected to vertex l by going colors 1 then 3 then the labels of j and l should be exchanged in $\tilde{X}_{(N,k)}$. Since the monodromies of g and \tilde{g} are the same and $(B_N, \tilde{\beta})$ and $(\tilde{B}_N, \tilde{\beta})$ are equivalent, the result follows.

In particular, there exists a pullback $(1, 2)$, g such that $\tilde{\sigma}_q = g^{-1}\sigma_q g$. As an example, note that γ in the proof of Theorem 1 is a pullback of $(1, 2)$. It might be hard to see this at first, but note that $(1, 2) = (1, 2)(3) \cdots (N)$. (3) for example can lift to $(mN + 3, (m + 1)N + 3)$, as is the case here. \square

Now that we have shown R -symmetric Adinkra chromotopologies give equivalent Belyi pairs, we can extend the exterior tensor product on Adinkras to an operation on the corresponding Riemann surfaces.

3.3. The Exterior Tensor Product. The tensor product of 2 Adinkras is defined in [27]. If $A_{(N_i, k_i)}$ is an Adinkra chromotopology obtained by quotienting an N_i -cube by a k_i dimensional doubly even code, then

$$A_{(N_1, k_1)} \otimes A_{(N_2, k_2)}$$

is an Adinkra chromotopology obtained by quotienting an $(N_1 + N_2)$ -cube by a $(k_1 + k_2)$ -dimensional code. We can denote it by $A_{(N, k)}$ where $N = N_1 + N_2$ and $k = k_1 + k_2$. It follows immediately that the exterior product extends to a well defined operation on the associated Riemann surfaces.

Proposition 7. *The exterior tensor product on Adinkras extends to a well defined operation on the associated Belyi curves.*

Proof. Since a Belyi curve is equivalent to a ribbon graph, we need to show that the tensor product extends to a well defined operation on the ribbon structure, or rainbow, of the Adinkra chromotopology. The chromotopology of $A_{(N, k)}$ is defined

by the tensor product. The rainbow is a cyclic order of the $N = N_1 + N_2$ colors, which needs to be determined from the rainbows of $A_{(N_i, k_i)}$, $i = 1, 2$, which are cyclic orders on the colors 1 through N_1 and $N_1 + 1$ through $N_1 + N_2$. If r_1 and r_2 are rainbows for $A_{(N, k)}$ obtained by combining the rainbows of $A_{(N_1, k_1)}$ and $A_{(N_2, k_2)}$ in different ways, then $(A_{(N, k)}, r_1)$ and $(A_{(N, k)}, r_2)$ are related by an R -symmetry. Therefore $(A_{(N, k)}, r_1)$ and $(A_{(N, k)}, r_2)$ are equivalent Belyi curves by proposition 6. This means that anyway we choose to define how to combine the rainbows of $A_{(N_1, k_1)}$ and $A_{(N_2, k_2)}$ to obtain the rainbow for $A_{(N, k)}$ will give equivalent Belyi curves. Therefore the tensor product on Adinkras trivially extends to the associated Belyi pairs by just assigning any cyclic order of the N colors to the product as a rainbow. \square

For concreteness, if the rainbow of $A_{(N_1, k_1)}$ is $(1, \dots, N_1)$ and the rainbow for $A_{(N_2, k_2)}$ is $(N_1 + 1, \dots, N_1 + N_2)$ then we choose to use the rainbow $(1, \dots, N_1, N_1 + 1, \dots, N_1 + N_2) = (1, \dots, N)$.

Let us now look at what this operation looks like on the corresponding Riemann surfaces, $X_{(N_1, k_1)}$ and $X_{(N_2, k_2)}$. It is useful to first look at the operation on the monodromies of $X_{(N_i, k_i)}$ over B_{N_i} .

Theorem 5. *Let $\rho_{c,1}$ be the generators of the monodromy group of $X_{(N_1, k_1)}$ over B_{N_1} and $\rho_{c,2}$ be the generators of the monodromy group of $X_{(N_2, k_2)}$ over B_{N_2} . We can label the vertices so that the monodromy group of $X_{(N, k)} = X_{(N_1, k_1)} \otimes X_{(N_2, k_2)}$ over B_N is generated by ρ_c where:*

for $1 \leq c \leq N_1 - 1$

$$(43) \quad \rho_c = \rho_c^{(1)} \rho_c^{(2)} \cdots \rho_c^{(2^{N_2 - k_2})}$$

where $\rho_c^{(j)}$ is given by $\rho_{c,1}$ with $(j - 1)2^{N_1 - k_1 - 1}$ added to each entry i , with $N_1 + 1 \leq i \leq N_1 + N_2 - 1$

$$(44) \quad \rho_c = \rho_c^{(1)} \rho_c^{(2)} \cdots \rho_c^{(2^{N_1 - k_1})}$$

where $\rho_c^{(i)}$ is given by $\rho_{c,2}$ with entry j replaced by $(j - 1)2^{N_1 - k_1} + i$, and

$$(45) \quad \rho_{N_1} = \rho_{N_1} = \prod_{J=1}^{2^{N_2 - k_2}} \rho_{N_1}^{(J)},$$

where $\rho_{N_1}^{(J)}$ is obtained from $\rho_{N_1,1}$ by equation 47. Furthermore, $\rho_{N_1 + N_2} = \rho_1 \rho_2 \cdots \rho_{N_1 + N_2 - 1}$ which describes the $N/1$ 2-colored faces in $X_{(N, k)}$ is given by

$$(46) \quad \rho_N = \prod_{I=1}^{2^{N_1 - k_1}} \rho_N^{(I)},$$

where $\rho_N^{(I)}$ is obtained from $\rho_{N_2,2}$ by equation 49.

Proof. Since the only structure of the Adinkra that we are presently using is the chromotopology and rainbow, we can consider all of the chromotopologies as being in the valise. A *valise Adinkra* is when all of the black vertices have the same height, say 1, and all of the white vertices have the same height, say 0. Label all of the white vertices in $A_{(N_1, k_1)}$ $1_w, \dots, (2^{N_1 - k_1 - 1})_w$. Label the black vertex connected to vertex i_w by color 1 i_b . Similarly, label the vertices of $A_{(N_2, k_2)}$ $1'_q, \dots, (2^{N_2 - k_2 - 1})'_q$, $q = w, b$.

As described in [27], the first step in constructing $A_{(N, k)}$ is to take $2^{N_2 - k_2}$ copies of $A_{(N_1, k_1)}$, one for each vertex of $A_{(N_2, k_2)}$. The colors of the vertices in the copies of $A_{(N_1, k_1)}$ corresponding to black vertices of $A_{(N_2, k_2)}$ are flipped. The dashedness of the edges is also flipped, but we can ignore that for now since we are only considering chromotopologies.

Within the larger space of $A_{(N, k)}$, consider a vertex in the copy of $A_{(N_1, k_1)}$ corresponding to the vertex j'_q in $A_{(N_2, k_2)}$. This vertex must be equivalent to some vertex i_q in $A_{(N_1, k_1)}$. Label the vertex in $A_{(N, k)}$ $([2(j' - 1) + q']2^{N_1 - k_1 - 1} + i)_{q+q'}$. Here we consider $w = 0, b = 1$, and $q + q'$ is addition modular 2.

In the next step of the construction of $A_{(N, k)}$ in [27] the corresponding points in different copies of $A_{(N_1, k_1)}$ are connected by the colored edges of $A_{(N_2, k_2)}$ if the points they correspond to in $A_{(N_2, k_2)}$ are. If we label color c in $A_{(N_2, k_2)}$ by color $N_1 + c$ in $A_{(N, k)}$ and use the labeling described above this step means that if j'_w is connected by color c to l'_b in $A_{(N_2, k_2)}$, then in $A_{(N, k)}$ $([2(j' - 1)]2^{N_1 - k_1 - 1} + i)_q$ is connected to $([2(l' - 1) + 1]2^{N_1 - k_1 - 1} + i)_{q+1}$ by color $N_1 + c$. Using this labeling of vertices $A_{(N, k)}$ really shows how they come from vertices of the 2 component Adinkras $A_{(N_1, k_1)}$ and $A_{(N_2, k_2)}$. Each vertex in $A_{(N, k)}$ comes from the i_q vertex of the $A_{(N_1, k_1)}$ corresponding to the j'_q vertex of $A_{(N_2, k_2)}$, and is labeled by $([2(j' - 1) + q']2^{N_1 - k_1 - 1} + i)_{q+q'}$.

The $2^{N_2 - k_2}$ disjoint copies of $A_{(N_1, k_1)}$ from the first step contain all of the vertices of $A_{(N, k)}$ and all of the edges of colors 1 through N_1 . $A_{(N, k)}$ is obtained by adding additional edges in to the already existing vertices. In particular, ignoring the edges of colors $N_1, \dots, N_1 + N_2$ gives $2^{N_2 - k_2}$ disjoint copies of $A_{(N_1, k_1)}$. This means that for $1 \leq c \leq N_1 - 1$ all of the $c/(c + 1)$ 2-colored faces in $A_{(N, k)}$ come from the $c/(c + 1)$ 2-colored faces in the different copies of $A_{(N_1, k_1)}$. Therefore, for $1 \leq c \leq N_1 - 1$,

$$\rho_c = \rho_c^{(1'_w)} \rho_c^{(1'_b)} \rho_c \rho_c^{(2'_w)} \rho_c^{(2'_b)} \dots \rho_c^{((2^{N_2 - k_2 - 1})'_w)} \rho_c^{((2^{N_2 - k_2 - 1})'_b)},$$

where $\rho_c^{(j'_q)}$ is $\rho_{c,1}$ for the copy of $A_{(N_1, k_1)}$ corresponding to the vertex j'_q in $A_{(N_2, k_2)}$. Recall that $\rho_{c,1}$ is the product of disjoint 2-cycles. Each 2-cycle exchanges the 2 white vertices incident to each $c/(c + 1)$ 2-colored face. Therefore $\rho_{c,1}$ for each copy of $A_{(N_1, k_1)}$ is the same with just the labels of the vertices changed. Since the vertex i_q in the copy of $A_{(N_1, k_1)}$ corresponding to the vertex j'_q in $A_{(N_2, k_2)}$ is labeled by $([2(j' - 1) + q']2^{N_1 - k_1 - 1} + i)_{q+q'}$, $\rho_c^{(j'_q)}$ is obtained from $\rho_{c,1}$ by replacing

i with $[2(j' - 1) + q]2^{N_1 - k_1 - 1} + i$. Note that we have used the result that if i_b is connected to j_b by color c then $c + 1$ then i_w is connected to j_w by color c then color $c + 1$. This follows from claim 1. If we let $J = 2j'_q - 1 + q$ then $\rho_c^{(J)}$ satisfies the conditions of the Theorem for $1 \leq c \leq N_1 - 1$. $\rho_c^{(J)}$ should be considered $\rho_{c,1}$ for $A_{(N_1, k_1)}^{(J)} \subset A_{(N, k)}$.

Before moving to the other cases, note that for $1 \leq c \leq N_1 - 1$, $\rho_c^{(J)}$ has a 2 cycle for each $c/(c + 1)$ 2 colored face in $X_{(N_1, k_1)}$. There are $2^{N_1 - k_1 - 2}$ such faces. Therefore since there are $2^{N_2 - k_2}$ different $\rho_c^{(J)}$, ρ_c has $2^{N - k - 2}$ disjoint 2-cycles

Now let us consider ρ_c for $N_1 + 1 \leq c \leq N - 1$. Similar to the previous case, if we remove the edges of colors $1, \dots, N_1$ from $A_{(N, k)}$, we are left with $2^{N_1 - k_1}$ disjoint copies of $A_{(N_2, k_2)}$. Using the same vertex labeling, each copy of $A_{(N_2, k_2)}$ has one vertex in each copy of $A_{(N_1, k_1)}$ contained in $A_{(N, k)}$. All of the $c/(c + 1)$ colored loops are now contained in these disjoint copies of $A_{(N_2, k_2)}$. Therefore

$$\rho_c = \rho_c^{(1_w)} \rho_c^{(2_w)} \dots \rho_c^{((2^{N_1 - k_1 - 1})_w)} \rho_c^{(1_b)} \dots \rho_c^{((2^{N_1 - k_1 - 1})_b)},$$

where $\rho_c^{(i_q)}$ is $\rho_{c - N_1, 2}$ for the copy of $A_{(N_2, k_2)}$ containing the vertex i_q for $1 \leq i \leq 2^{N_1 - k_1 - 1}$. Recall that the first $2^{N_1 - k_1 - 1}$ black and white vertices label the “first” copy of $A_{(N_1, k_1)}$, so each of the copies of $A_{(N_2, k_2)}$ contains exactly one of these vertices and it makes sense to index the copies by them.

Each $\rho_c^{(i)}$ will be equivalent to $\rho_{c, 2}$ but with the labels of the vertices changed. If (j', l') is one of the disjoint 2-cycles in $\rho_{c, 2}$ then j'_w is connected to l'_w by going color c then color $c + 1$ in $A_{(N_2, k_2)}$. Using our labeling this means that in $A_{(N, k)}$, $([2(j' - 1) + q']2^{N_1 - k_1 - 1} + i)_{q+q'}$ is connected to $([2(l' - 1) + q']2^{N_1 - k_1 - 1} + i)_{q+q'}$, $1 \leq i \leq 2^{N_1 - k_1 - 1}$. ρ_c only lists the white vertices, so we are interested in the case $q + q' = 0$, or $q = q'$. Therefore, $\rho_c^{(i_q)}$ is obtained from $\rho_{c, 2}$ by changing entry j' to $[2(j' - 1) + q]2^{N_1 - k_1 - 1} + i$. Finally, letting $I = i + q2^{N_1 - k_1 - 1}$, we find that $\rho_c^{(I)}$ satisfies the conditions of the theorem for $N_1 + 1 \leq c \leq N - 1$.

Note that ρ_c is the product of $2^{N_1 - k_1}$ $\rho_c^{(j)}$. Each of which is the product of $2^{N_2 - k_2 - 2}$ disjoint 2-cycles. Therefore ρ_c is the product $2^{N - k - 2}$ disjoint 2-cycles.

Now let us consider ρ_{N_1} . If $i_w^{(1)}$ is connected to $i_b^{(2)}$ by color N_1 in $A_{(N_1, k_1)}$, then in $A_{(N, k)}$, $([2(j' - 1) + q]2^{N_1 - k_1 - 1} + i^{(1)})_w$ is connected to $([2(j' - 1) + q]2^{N_1 - k_1 - 1} + i^{(2)})_w$ by color N_1 . In particular, color N_1 keeps us in the same copy of $A_{(N_1, k_1)}$. Color $N_1 + 1$, however, will connect to a vertex in a different copy of $A_{(N_1, k_1)}$, though the same copy of $A_{(N_2, k_2)}$. In particular, since color $1'$ in $A_{(N_2, k_2)}$ connects j'_w to j'_b , in $A_{(N, k)}$ color $N_1 + 1$ connects $([2(j' - 1) + q]2^{N_1 - k_1 - 1} + i^{(2)})_b$ to $([2(j' - 1) + 1 - q]2^{N_1 - k_1 - 1} + i^{(2)})_w$. Using $J = 2j' - 1 + q$, this is represented in ρ_{N_1} by the 2-cycle $([J - 1]2^{N_1 - k_1 - 1} + i^{(1)}, [J - 1 + (-1)^{J+1}]2^{N_1 - k_1 - 1} + i^{(2)})$.

As already noted, $i_w^{(1)}$ is connected to $i_b^{(2)}$ in $A_{(N_1, k_1)}$ by color N_1 . By our labeling, $i_b^{(2)}$ is connected to $i_w^{(2)}$ by color 1. This means that if $i_w^{(1)}$ is connected to $i_b^{(2)}$ by

color N_1 in $A_{(N_1, k_1)}$, then $(i^{(1)}, i^{(2)})$ is one of the disjoint 2-cycles in $\rho_{N_1, 1}$. Therefore, for each 2-cycle $(i^{(1)}, i^{(2)})$ in $\rho_{N_1, 1}$ and $1 \leq J \leq 2^{N_2 - k_2}$ there is a unique 2-cycle in ρ_{N_1} , $([J - 1]2^{N_1 - k_1 - 1} + i^{(1)}, [J - 1 + (-1)^{J+1}]2^{N_1 - k_1 - 1} + i^{(2)})$. Therefore, we can write

$$\rho_{N_1} = \prod_{J=1}^{2^{N_2 - k_2}} \rho_{N_1}^{(J)},$$

where $\rho_{N_1}^{(J)}$ is obtained from $\rho_{N_1, 1}$ by the vertex relabeling

$$(47) \quad (i^{(1)}, i^{(2)}) \mapsto ([J - 1]2^{N_1 - k_1 - 1} + i^{(1)}, [J - 1 + (-1)^{J+1}]2^{N_1 - k_1 - 1} + i^{(2)}).$$

At first glance this would seem to depend on a choice of order for $i^{(1)}$ and $i^{(2)}$. However changing the order leaves the overall product, ρ_{N_1} invariant, as long as we use the same order for each $\rho_{N_1}^{(J)}$. It may just change which $\rho_{N_1}^{(J)}$ each of the individual 2-cycles appears in. This labeling choice is needed because the white vertices connected by the $N_1/(N_1 + 1)$ colored faces are in different copies of $A_{(N_1, k_1)} \subset A_{(N, k)}$ and different copies of $A_{(N_2, k_2)} \subset A_{(N, k)}$.

In the 2 previous cases the connected white vertices were either in the same copy of $A_{(N_1, k_1)}$ or the same copy of $A_{(N_2, k_2)}$. Therefore we could normalize the choice of labeling for the ρ_i based on the labeling of the sub-Adinkra's of $A_{(N, k)}$. The labeling ambiguity for ρ_{N_1} can be removed by grouping the 2-cycles in ρ_{N_1} by the 2-cycles of $\rho_{N_1, 1}$ instead of by J . That is, for each 2-cycle (i, l) appearing in $\rho_{N_1, 1}$ there are the $2^{N_2 - k_2}$ 2-cycles

$$(48) \quad \prod_{J=1}^{2^{N_2 - k_2}} ([J - 1]2^{N_1 - k_1 - 1} + i, [J - 1 + (-1)^{J+1}]2^{N_1 - k_1 - 1} + l),$$

which are invariant under exchange of i and l .

Finally, we note that ρ_N can be found by taking the product of the previous ρ_c , but it is perhaps more informative to follow a similar argument as the one for ρ_{N_1} . If $j'^{(1)}$ is connected to $j'^{(2)}$ by color N'_2 in $A_{(N_2, k_2)}$, then in $A_{(N, k)}$ color $N = N_1 + N_2$ connects $([2(j'^{(1)} - 1) + q]2^{N_1 - k_1 - 1} + i)_w$ to $([2(j'^{(2)} - 1) + 1 - q]2^{N_1 - k_1 - 1} + i)_b$, which is connected by color 1 to $([2(j'^{(2)} - 1) + 1 - q]2^{N_1 - k_1 - 1} + i)_w$. Using $I = i + 2^{N_1 - k_1 - 1}$, $((j'^{(1)} - 1)2^{N_1 - k_1} + I)_w$ is connected by going color N then color 1 to $((j'^{(2)} - 1)2^{N_1 - k_1} + I \pm 2^{N_1 - k_1 - 1})_w$ where the " + " is for $I \leq 2^{N_1 - k_1 - 1}$. Therefore we can write

$$\rho_N = \prod_{I=1}^{2^{N_1 - k_1}} \rho_N^{(I)},$$

where $\rho_N^{(I)}$ is obtained from $\rho_{N_2, 2}$ by relabeling each 2-cycle in $\rho_{N_2, 2}$ by

$$(49) \quad (j'^{(1)}, j'^{(2)}) \mapsto ((j'^{(1)} - 1)2^{N_1 - k_1} + I, ((j'^{(2)} - 1)2^{N_1 - k_1} + I \pm 2^{N_1 - k_1 - 1})),$$

where the " + " is for $I \leq 2^{N_1-k_1-1}$. Again we can see that the seeming ambiguity from a choice in order of $j^{(1)}$ and $j^{(2)}$ is in fact not one by writing

$$(50) \quad \rho_N = \prod_{(j,l) \text{ a disjoint cycle in } \rho_{N_2,2}} \prod_{I=1}^{2^{N_1-k_1}} ([j-1]2^{N_1-k_1} + I, [l-1]2^{N_1-k_1} + I \pm 2^{N_1-k_1-1}).$$

□

Remark 1. This shows that ρ_c can be written as a relabeling of $\rho_{c,1}$ for $1 \leq c \leq N_1$, and a relabeling of $\rho_{c-N_1,2}$ for $N_1 + 1 \leq c \leq N_1 + N_2$.

Remark 2. The labeling of A_N in proposition 2 is an example of such a labeling. Note that in the above Theorem the actual labeling of the white vertices in $A(N_i, k_i)$ with $i = 1, 2$ didn't matter. That is why the labeling of the cube in proposition 2 is only one example. The choice of the order of the white vertices was made so that for all $N_1, N_2 < N$ such that $N_1 + N_2 = N$, if we label A_{N_i} as in proposition 2 and then label $A_{N_1} \otimes A_{N_2}$ following the above Theorem, then it is equivalent to labeling A_N by proposition 2.

Remark 3. If $N_2 = 1$ then there doesn't exist c such that $N_1 + 1 \leq c \leq N - 1 = N_1$. Therefore, the generators of the monodromy group for X_N are completely determined by $\rho_{c,1}$ for $1 \leq c \leq N_1$. Similarly, if $N_1 = 1$ then there does not exist c such that $1 \leq c \leq N_1 - 1 = 0$. We can choose $\rho_2, \dots, \rho_{N_2+1}$ as the generators of the monodromy group of $(X_{(N,k_2)}, B_N)$ which only depend on $\rho_{c,2}$. Note that in the 2 above cases ρ_{N_1} ($N_2 = 1$) or ρ_N ($N_1 = 1$) contains the information of which copy of A_{N_i} is connected to which by the new color.

The case of $N_1 = N_2 = 1$ is unique since for both X_1 and X_2 , ρ_c is the identity for all c . We can see this immediately for X_1 since it is the Belyi base, \mathbb{CP}^1 with embedded graph $\Sigma_0 = A_1$. $X_2 = \mathbb{CP}^1$ with embedded graph A_2 . Therefore X_2 has 2 faces, both with boundary A_2 . For ρ_c to make sense, one would need to differentiate between the 1/2 and 2/1 faces.

We can now look at the action of the tensor product on the Riemann surfaces themselves. Let us first look at the cases where one or both of the N_i are 1, since they are unique as mentioned in the remark above. Consider the case of $N_1 = N_2 = 1$.

We can consider the tensor product of Adinkras, $A_1 \otimes A_1 = A_2$, as an operation on Riemann surfaces, $X_2 = X_1^{(a)} \otimes X_1^{(b)}$. This can be viewed as first taking 2 copies of $X_1^{(a)}$ and 2 copies of $X_1^{(b)}$. Then removing the 2-face of each copy of \mathbb{CP}^1 and connecting their 1 skeletons by adding two 2-cells. Each 2-cell is bounded by the 4 copies of A_1 , alternating a and b . They are connected with opposite orientations to create \mathbb{CP}^1 . The 2 copies of A_1 can be thought of as the equator. The fact that the 2-cells are added with opposite orientation can be related to the different

copies of A_1 being associated to white and black vertices as will be made clearer in the general case. Now consider the case $N_1 \neq 1, N_2 = 1$.

Corollary 4. $X_{(N,k)} = X_{(N_1,k_1)} \otimes X_1$ can be viewed as a $2^{N_1-k_1-1}$ -point connected sum of $X_{(N_1,k_1)}$ with itself.

Proof. There are 2 copies of $A_{(N_1,k_1)}$ in $A_{(N,k)}$ corresponding to $j = 1, 2$ from Theorem 5. If we ignore the edges of color $N_1 + 1$ as well as the faces incident to them in $X_{(N,k)}$, we are left with 2 copies of $X_{(N_1,k_1)}$ with the $N_1/1$ faces removed as can be seen from ρ_c . For $1 \leq c \leq N_1 - 1$, $\rho_c^{(1)} = \rho_{c,1}$, showing that the subsurface of $X_{(N,k)}$ corresponding to the first copy of $A_{(N_1,k_1)}$ has all of the same $c/(c+1)$ faces as $X_{(N_1,k_1)}$ for $1 \leq c \leq N_1 - 1$. However, $\rho_{N_1}^{(1)} \neq \rho_1^{(1)} \cdots \rho_{N_1-1}^{(1)}$, which shows us that $X_{(N_1,k_1)}^{(1)}$ does not have $N_1/1$ colored faces like $X_{(N_1,k_1)}$. This could also be seen by the fact that N_1 and 1 are no longer adjacent to each other. Therefore $X_{(N_1,k_1)}^{(1)}$ is given by $X_{(N_1,k_1)}$ with the $N_1/1$ colored faces removed. Similarly for the second copy of $A_{(N_1,k_1)}$, $\rho_c^{(2)} = \rho_{c,1}$ with vertices relabeled by $i \mapsto i + 2^{N_1-k_1-1}$, $\rho_{N_1}^{(2)} \neq \rho_1^{(2)} \cdots \rho_{N_1-1}^{(2)}$. Showing that $X_{(N_1,k_1)}^{(2)}$ is also a copy of $X_{(N_1,k_1)}$ (disjoint from $X_{(N_1,k_1)}^{(1)}$) with the $N_1/1$ colored faces removed.

Ignoring color $N_1 + 1$ and the faces connected to it we are left with 2 copies of $X_{(N_1,k_1)}$ each with $2^{N_1-k_1-2}$ punctures. The boundary of each hole is a $N_1/1$ colored loop. The holes in $X_{(N_1,k_1)}^{(j)}$ are classified by the 2-cycles in $\rho_{N_1,1}$ with change of labeling $i \mapsto i + j2^{N_1-k_1-1}$. For each hole in $X_{(N_1,k_1)}^{(1)}$ represented by some disjoint 2-cycle in $\rho_{N_1,1}^{(j)}$, (i, l) , there are $2 N_1/(N_1 + 1)$ colored faces connecting hole (i, l) in $X_{(N_1,k_1)}^{(1)}$ to hole $(i + 2^{N_1-k_1-1}, l + 2^{N_1-k_1-1})$ of $X_{(N_1,k_1)}^{(2)}$. These are represented by the two 2-cycles in ρ_{N_1} corresponding to (i, l) in $\rho_{N_1,1}$, see equation 48. Similarly, for each hole there are $2 N/1$ colored faces connecting corresponding holes, represented by the two 2-cycles in $\rho_N = \rho_1 \cdots \rho_{N_1}$. Note that these faces also connect hole (i, l) to hole $(i + 2^{N_1-k_1-1}, l + 2^{N_1-k_1-1})$ by the 2 color property of Adinkras.

Therefore we see that each whole of $X_{(N_1,k_1)}^{(1)}$ is connected to the corresponding hole of $X_{(N_1,k_1)}^{(2)}$ by a tube made of $2 N_1/N$ colored faces and $2 N/1$ colored faces. If we just considered a single hole and ignored all the other holes, this would be the connected sum of $X_{(N_1,k_1)}$ with itself. This however is like doing the connected sum at all $2^{N_1-k_1-2}$ $N_1/1$ colored face of $X_{(N_1,k_1)}$ simultaneously. Hence it is a $2^{N_1-k_1-2}$ -point connected sum of $X_{(N_1,k_1)}$ with itself. \square

Note that for a connected sum of oriented manifolds, the orientation on the boundary of the holes that are connected is reversed. This is incorporated by the tensor product structure on the Adinkra. The holes that need to have their orientation reversed correspond to the black vertex of X_1 .

For both $N_i \neq 1$, it ceases to be a connected sum, since there are more than 2 copies of $A_{(N_1, k_1)}$. The $N_1/(N_1 + 1)$ faces and $N/1$ faces connect hole (i, l) to different holes; in fact to the corresponding holes in different copies of $A_{(N_1, k_1)}$. So the holes are not connected by tubes. In particular, the $N_1 + 1$ edge adjacent to an $N_1/(N_1 + 1)$ face bounds a puncture in a copy of $A_{(N_2, k_2)}$, and similarly for the N edge adjacent to an $N/1$ face. For lack of a better work we will refer to this as a multi-point connected sum between $A_{(N_1, k_1)}$ and $A_{(N_2, k_2)}$ in analogy to the previous case being a multi-point connected sum between $A_{(N_1, k_1)}$ and itself.

Corollary 5. $X_{(N, k)} = X_{(N_1, k_1)} \otimes X_{(N_2, k_2)}$, $X_{(N, k)}$ can be viewed as a multi-point connected sum of $2^{N_2 - k_2}$ copies of $A_{(N_1, k_1)}$ and $2^{N_1 - k_1}$ copies of $A_{(N_2, k_2)}$.

Proof. Forgetting colors $N_1 + 1, \dots, N$ and the 2-cells connected to them in $X_{(N, k)}$ leaves $2^{N_2 - k_2}$ copies of $X_{(N_1, k_1)}$ with the $2^{N_1 - k_1 - 2}$ $N_1/1$ faces removed. This can be seen by looking at ρ_c from Theorem 5. For $1 \leq c \leq N_1 - 1$, $\rho_c^{(j)}$ describes the $c/(c + 1)$ colored faces in $A_{(N_1, k_1)}^{(j)}$, showing that $X_{(N_1, k_1)}^{(j)}$ has all the same $c/(c + 1)$ faces as $X_{(N_1, k_1)}$, for $c \leq N_1 - 1$. This accounts for all of the faces that don't have an edge of color greater than N_1 bounding it, so in particular $X_{(N_1, k_1)}^{(j)}$ does not have any $N_1/1$ colored faces.

Similarly, forgetting the edges of colors $1, \dots, N_1$ and the 2-cells connected to them in $X_{(N, k)}$ leaves $2^{N_1 - k_1}$ disjoint copies of $A_{(N_2, k_2)}$ with the $N_2/1'$ ($(N_1 + N_2)/1$) colored faces removed. Note that the copies of $X_{(N_2, k_2)}^{(i)} \subset X_{(N, k)}$ only intersect the copies of $X_{(N_1, k_1)}^{(j)}$ at the vertices. We could separate them at the vertices, so that we can see in the next step how the vertices are forced to be equated.

Each hole in $A_{(N_1, k_1)}^{(j)}$ is classified by a 2-cycle (l, m) in $\rho_{N_1, 1}^{(j)} = \rho_1^{(j)} \cdots \rho_{N_1 - 1}^{(j)}$. Hole (l, m) in $A_{(N_1, k_1)}^{(j)}$ is connected to hole $(l \pm 2^{N_1 - k_1 - 1}, m \pm 2^{N_1 - k_1 - 1})$ in $A_{(N_1, k_1)}^{(j \pm 1)}$, where we use the $+$ sign if j is odd and the $-$ sign if j is even, by $2 N_1/(N_1 + 1)$ colored faces, as described by the two 2-cycles in ρ_{N_1} containing l and m (see equation 47). The edges of color N_1 that bound this face correspond to edges in the boundaries of the copies of $X_{(N_1, k_1)}^{(j)}$ that are being connected. The other 2 edges of these faces have color $N_1 - 1$ and are in the boundaries of $X_{(N_2, k_2)}^{(i)}$. So the $N_1/(N_1 + 1)$ faces connect 2 copies of $X_{(N_1, k_1)}$ along part of the boundary of corresponding holes and connects 2 copies of $X_{(N_2, k_2)}$ in the other direction. This identifies the vertices along the holes of $X_{(N_1, k_1)}^{(j)}$ to the vertices along the attached holes of $X_{(N_2, k_2)}^{(i)}$.

After the $N_1/(N_1 + 1)$ colored faces are added the resulting manifold still has boundary. We must finally add $N/1$ colored faces along that boundary according to ρ_N . Note that the $N/1$ faces connect holes of $X_{(N_1, k_1)}^{(j)}$ in one direction and holes of $X_{(N_2, k_2)}^{(i)}$ in the other, but will in general connect different holes than the $N_1/(N_1 + 1)$ faces. By this we mean if the hole (l, m) in $X_{(N_1, k_1)}^{(j)}$ is connected to

the hole (l', m') in $X_{(N_1, k_1)}^{(j')}$ then $N/1$ colored faces will in general (except if $N_i = 1$) connect (l, m) to hole in a copy of $X_{(N_1, k_1)}$ other than $X_{(N_1, k_1)}^{(j')}$. \square

Theorem 5 and its corollaries provide a new approach to the question of whether or not an Adinkra is factorizable, i.e. can an Adinkra $A_{(N, k)}$ be written as the tensor product of 2 other Adinkras $A_{(N_1, k_1)} \otimes A_{(N_2, k_2)}$.

4. FROM ODD DASHINGS TO SPIN STRUCTURES

So far we have only considered the underlying chromotopology of an Adinkra. But an Adinkra has much more structure than just its chromotopology. It also has a dashing, and the edges have an orientation. In the next section we will look at the additional geometric structures gained by considering the edge orientations. In this section we will see that including the extra data of a dashing provides the additional structure necessary to describe the Belyi curve associated to the chromotopology as a super Riemann surface (SRS).

Consider a Riemann surface with embedded graph. In [8] it is shown that there is an isomorphism between Kasteleyn orientations (defined below) of the graph and spin structures of the surface given a fixed dimer configuration. We will first review what a Kasteleyn orientation is and show that an odd dashing on an Adinkra defines a Kasteleyn orientation. We will then review how a Kasteleyn orientation defines a spin structure on the surface in the context of Adinkras and their associated Belyi curves. This requires a choice of a dimer configuration on the embedded Adinkra. We will show that there is a canonical choice of a dimer for every Adinkra. This shows that to every Adinkra chromotopology with an odd dashing is associated a spin curve. This provides a way to confirm the counting of dashings from [11], by counting possible spin structures.

A spin curve is an SRS. In section 4.3 we will explicitly describe the superconformal structure on the spin curve associated to an Adinkra. We will do this by using the set of charts from [33] for a Riemann surface with embedded graph and attaching an odd variable to make the transition functions superconformal. We will see that adding an odd variable is natural from the viewpoint of Kasteleyn orientations and their relation to dimers.

4.1. From Odd Dashings to Kasteleyn Orientations. The purpose of this section is to describe how a Kasteleyn orientation is obtained from an odd dashing. Before defining a Kasteleyn orientation it is natural to first consider dimer configurations. This is natural because dimer models on a surface are discretizations of free fermions [9]. In fact, it was the proposal that dimer models and free fermions on Riemann surfaces were equivalent that led to the belief (as was proven in [8]) that Kasteleyn orientations were equivalent to spin structures.

For a bipartite graph Σ , a *perfect matching* is a collection of edges such that every vertex in Σ is incident to exactly one edge. In statistical mechanics a perfect

matching is known as a *dimer configuration*. The individual edges in a dimer configuration are known as *dimers*. For two dimer configurations D and D' on a bipartite graph Σ , the (D, D') -*composition cycles* are the connected components of the subgraph of Σ given by the symmetric difference

$$(51) \quad (D \cup D') \setminus (D \cap D').$$

Each composition cycle is a simple closed curve. For dimers on a surface graph $\Sigma \subset X$ let $\Delta(D, D')$ be the homology class of $(D \cup D') \setminus (D \cap D')$ in $H_1(X; \mathbb{Z}_2)$. Two dimer configurations D and D' on a surface graph $\Sigma \subset X$ are equivalent if $\Delta(D, D') = 0 \in H_1(X; \mathbb{Z}_2)$.

A dimer model is a statistical mechanical model of a system of random perfect matchings. The partition function for a dimer model is given in terms of the Pfaffian of $2^{2g} v \times v$ matrices, where g is the genus of a surface the dimer model can be embedded in and v is the number of vertices in the graph. The matrices are called Kasteleyn matrices, which are signed adjacency matrices corresponding to a Kasteleyn orientation.

A *Kasteleyn orientation* for a graph Σ embedded in a surface X is an orientation of the edges so that as you go around the boundary each face of X counterclockwise you go against the orientation of an odd number of edges.⁶

$$(52) \quad \varepsilon_f^K(e) = \begin{cases} -1, & \text{if } e \text{ is traversed opposite its orientation given by } K \\ 1, & \text{if } e \text{ is traversed in the same direction as } K \end{cases}$$

The orientation K is Kasteleyn if for every face $f \in X$

$$(53) \quad \prod_{e \in \partial f} \varepsilon_f^K(e) = -1.$$

A vertex switch is when the orientations of all of the edges incident to a vertex are reversed. Two Kasteleyn orientations are equivalent if they can be related by a series of vertex switches. The set of equivalence classes of Kasteleyn orientations on $\Sigma \subset X$, $\tilde{\mathcal{K}}$, is shown to be an affine $H^1(X; \mathbb{Z}_2)$ -space in [8], via the map

$$(54) \quad \tilde{\mathcal{K}} \times \tilde{\mathcal{K}} \rightarrow H^1(X; \mathbb{Z}_2), \quad ([K], [K']) \mapsto [K] - [K'] \equiv [\vartheta_{K, K'}],$$

where for an edge $e \in \Sigma$, $\vartheta_{K, K'}(e)$ is 0 if K and K' agree on e and 1 if they disagree. This shows that for a bipartite graph embedded in a Riemann surface of genus g there are 2^{2g} equivalence classes of Kasteleyn orientations.

Recall that the partition function of a dimer model was determined by 2^{2g} Kasteleyn matrices. Each matrix corresponds to an equivalence class of Kasteleyn orientations. The partition function for free fermions on a Riemann surface is also determined from the Pfaffians of 2^{2g} operators. The operators appearing on the

⁶A Kasteleyn orientation relative to going around each face counterclockwise will also be a Kasteleyn orientation relative to going clockwise around each face in our current application. This is because for a Riemann surface associated to an Adinkra, all of the faces are quadrilaterals.

partition function are Dirac operators and correspond to the 2^{2g} spin structures of the genus g Riemann surface. It was the belief that dimer models were discretizations of the free fermion on a Riemann surface that led to the belief that equivalence classes of Kasteleyn orientations are equivalent to spin structures and Kasteleyn operators are equivalent to Dirac operators. We will discuss this more in the next subsection, but now we can describe how to construct a Kasteleyn orientation from an odd dashing.

Proposition 8. *Every odd dashing, D of an Adinkra chromotopology $A_{(N,k)}$ defines a Kasteleyn orientation for $A_{(N,k)}$ embedded in $X_{(N,k)}$.*

Proof. Give the edges of $A_{(N,k)}$ the bipartite orientation B , let's say white to black. Note that this is not a Kasteleyn orientation. As we go around any face, we will go from a white vertex to a black vertex twice and we will go from a black vertex to a white vertex twice. This means we will traverse 2 edges in the direction of B and 2 edges in the opposite direction. Therefore for every face $f \in X_{(N,k)}$

$$\prod_{e \in \partial f} \varepsilon_f^B(e) = 1.$$

Define a new orientation, K , on $A_{(N,k)}$ so that if e is dashed it has the opposite orientation as in B , and if e is solid it has the same orientation as B . This is a Kasteleyn orientation. To see this, consider any face $f \in X_{(N,k)}$. By construction, the faces of $X_{(N,k)}$ are quadrilaterals with boundary given by 2-colored loops in $A_{(N,k)}$. By definition of an odd dashing, either 1 or 3 of the 4 edges bordering f will be dashed. If the edge is solid then $\varepsilon_f^K(e) = \varepsilon_f^B(e)$, but if the edge is dashed then $\varepsilon_f^K(e) = -\varepsilon_f^B(e)$. So ε_f^K has opposite sign as ε_f^B for 1 or 3 edges around each face and is the same for the other edges. Either way we find

$$(55) \quad \prod_{e \in \partial f} \varepsilon_f^K(e) = - \prod_{e \in \partial f} \varepsilon_f^B(e) = -1.$$

Therefore, we see that K is a Kasteleyn orientation by definition. \square

Note that not every Kasteleyn orientation can be obtained from an odd dashing. A Kasteleyn orientation is defined relative to a surface, while an odd dashing is defined on an Adinkra without any dependence on an embedding in a surface. Recall that if $X_{(N,k)}$ and $\tilde{X}_{(N,k)}$ are related by an R -symmetry then they have the same chromotopology, $A_{(N,k)}$, but with different rainbows. This means that different 2 colored loops in $A_{(N,k)}$ have 2-cells attached to them to create $X_{(N,k)}$ and $\tilde{X}_{(N,k)}$. The orientation K given to $A_{(N,k)}$ by proposition 8 is Kasteleyn regardless of whether we consider $A_{(N,k)}$ as embedded in $X_{(N,k)}$ or $\tilde{X}_{(N,k)}$ since the proof that K is Kasteleyn did not depend on which 2-colored faces were filled in. A general Kasteleyn orientation on $A_{(N,k)}$ embedded in $X_{(N,k)}$ will not still be a Kasteleyn orientation when we consider $A_{(N,k)}$ as embedded in $\tilde{X}_{(N,k)}$. This makes the Kasteleyn orientations constructed in proposition 8 very special Kasteleyn

orientations. After describing the relationship to spin structures we will return to the question of which Kasteleyn orientations come from odd dashings. But first we must ensure that the construction of Kasteleyn orientations from odd dashings is compatible with the the notion of equivalence, since spin structures are equivalent to equivalence classes of Kasteleyn orientations.

Proposition 9. *The map from odd dashings to Kasteleyn orientations defined by proposition 8 is well defined and injective as a map from the set of equivalence classes of odd dashings to the set of equivalence classes of Kasteleyn orientations.*

Proof. Given a chromotopology $A_{(N,k)}$, let \mathcal{D} be the set of possible odd dashings on $A_{(N,k)}$ and \mathcal{K} be the set of Kasteleyn orientations. Let $\varphi : \mathcal{D} \rightarrow \mathcal{K}$ be the map from odd dashings to Kasteleyn orientaions described in proposition 8.

Let D_1 and D_2 be equivalent dashings of $A_{(N,k)}$. Then D_1 and D_2 can be related by a series of vertex changes, where the dashedness of each edge incident to a given vertex is changed. The Kasteleyn orientation $K = \varphi(D)$ is defined so that e is oriented from white to black if it is solid and oriented from black to white if it is dashed. Therefore changing the dashedness of an edge in D is equivalent to changing the orientation of the edge in $\varphi(D)$. If D_2 is obtained from D_1 by performing vertex changes at v_1, \dots, v_m , then $K_2 = \varphi(D_2)$ is obtained from $K_1 = \varphi(D_1)$ by changing the orientation of the edges incident to v_1, \dots, v_m . (Note that if an edge is incident to 2 vertices where changes occur then the orientation is changed twice leaving it alone). Therefore K_1 and K_2 are equivalent as Kasteleyn orientations by definition.

Now assume $K_1 = \varphi(D_1)$ and $K_2 = \varphi(D_2)$ are equivalent as Kasteleyn orientations, meaning they can be related by a series of vertex switches, say at v_1, \dots, v_m . First note that φ is injective. K_i gives each edge e an orientation from white vertex to black vertex if it is solid and from black vertex to white vertex if it is dashed by D_i . Therefore if an edge has the same orientation in K_1 and K_2 it must have the same dashedness in D_1 and D_2 . Therefore changing the orientation of an edge in K_i is equivalent to changing the dashedness of the edge in D_i . So D_1 and D_2 can be related by changing the dashedness of edges incident to vertices v_1, \dots, v_m . D_1 and D_2 are equivalent by definition. \square

We have shown that the set of equivalence classes of odd dashings, $\tilde{\mathcal{D}} = \mathcal{D} / \sim$, can be thought of as a subset of the set of equivalence classes of Kasteleyn orientations, $\tilde{\mathcal{K}} = \mathcal{K} / \sim$, under φ . Note that this does not depend on are choice of representing the bipartite orientation as pointing from white to black instead of the other way around. Changing B to point from black to white would give an equivalent Kasteleyn orientation.

For the N -cube there is one equivalence class of odd dashings [11, 37]. Let K be its image under φ . Then K contains all of the Kasteleyn orientations of $A_N \subset X_N$ that have enough symmetry to be Kasteleyn orientations for $A_N \subset \tilde{X}_N$ too, where \tilde{X}_N is related to X_N by an R -symmetry. This means that the orientation

is Kasteleyn for every 2-colored loop in A_N regardless of whether or not a 2-cell is attached, or they are all of the Kasteleyn orientations that give rise to odd dashings. There are 2^{2^N-1} odd dashings in the single equivalence class for the cube [37].

For an Adinkra $A_{(N,k)}$, some of the symmetry is broken and there are 2^k equivalence classes of odd dashings [11, 37]. In the language of [37] the equivalence class of an odd dashing is called labeled switch classes (LSCs). Each LSC contains $2^{2^{n-k}-1}$ odd dashings. We see that 2^k of the 2^{2^g} (here g is given by proposition 1) equivalence classes of Kasteleyn orientations can be obtained by odd dashings. We will see an alternate description of these counts from those given in [37] and [11] after we have described the odd dashings as spin structures.

4.2. From Kasteleyn Orientation to Spin Curve. In this section we will show that an odd dashing on an Adinkra chromotopology $A_{(N,k)}$ defines a spin structure on the associated Belyi curve. First let us review what a spin structure is.

Recall that $\mathrm{SO}(n)$ has a canonical 2-fold cover $\mathrm{Spin}(n) \rightarrow \mathrm{SO}(n)$. For an oriented n -dimensional Riemannian manifold X , let $P_{\mathrm{SO}} \rightarrow X$ be the principal $\mathrm{SO}(n)$ -bundle corresponding to the tangent bundle of X . A spin structure on X is a principal $\mathrm{Spin}(n)$ -bundle $P_{\mathrm{Spin}} \rightarrow X$ with a 2-fold covering map $P_{\mathrm{Spin}} \rightarrow P_{\mathrm{SO}}$ that restricts to the 2-fold covering $\mathrm{Spin}(n) \rightarrow \mathrm{SO}(n)$ on the fibers. A spin structure exists if and only if the second Stiefel-Whitney class $w_2(X) \in H^2(X; \mathbb{Z}_2)$ vanishes.

The set of isomorphism classes of spin structures, $\mathcal{S}(X)$ is an affine $H^1(X; \mathbb{Z}_2)$ -space. Therefore we can think of a spin structure as a choice of whether to lift the SO -bundle trivially or not. That is, for every non-trivial cycle in X , a spin structure is a choice of whether or not a section of the SO -bundle changes sheets as the cycle is traversed. This choice can be extended to the 2-skeleton if and only if $w_2(X) = 0$ (once extended to the 2-skeleton it can be extended to all of X).

For an oriented Riemann surface $H^2(X; \mathbb{Z}_2) = 0$, so a spin structure always exists. If X has genus g then $H_1(X)$ has $2g$ generators. A spin structure can be thought of as a choice of sign for each of the generators, i.e. a homomorphism $H_1(X) \rightarrow \mathbb{Z}_2$. Therefore an oriented genus g Riemann surface has 2^{2g} inequivalent spin structures. As noted earlier, the fact that there are the same number of equivalence classes of Kasteleyn orientations and isomorphism classes of spin structures combined with the relationship between the dimer and free fermion models led to the belief that there should be an isomorphism between Kasteleyn orientations and spin structures. This was proven to be true in [8].

Theorem 6 (D. Cimasoni and N. Reshetikhin). *A dimer configuration D on a graph Σ embedded in a surface X induces an isomorphism*

$$(56) \quad \psi_D : \tilde{\mathcal{K}}(\Sigma) \rightarrow \mathcal{S}(X)$$

from the set of equivalence classes of Kasteleyn orientations on $\Sigma \subset X$ to the set of isomorphism classes of spin structures on X . $\psi_D = \psi_{D'}$ if and only if D and D' are equivalent dimer configurations.

In this way we see that Kasteleyn orientations can be viewed as discretizations of spin structures. We will briefly review the proof of Theorem 6. Cimasoni and Reshetikhin first show that a Kasteleyn orientation, K , and a dimer configuration, D , on a surface graph, $\Sigma \subset X$, define a quadratic form $q_D^K : H^1(X; \mathbb{Z}_2) \rightarrow \mathbb{Z}_2$ on $(H_1(X; \mathbb{Z}_2), \cdot)$, where \cdot is the intersection form. For an oriented simple closed curve $\gamma \in \Sigma$ let

$$\varepsilon^K(\gamma) = \prod_{e \in \gamma} \varepsilon_\gamma^K(e).$$

Here $\varepsilon_\gamma^K(e)$ is given by 1 if the orientation of e given by γ agrees with the orientation from K , and is given by -1 if the 2 orientations disagree. Also let $\ell_D(\gamma)$ be the number of vertices in γ whose adjacent dimer sticks out to the left of $\gamma \subset X$. Represent any class $\alpha \in H^1(X; \mathbb{Z}_2)$ by oriented simple closed curves $\gamma_1, \dots, \gamma_m$, then the quadratic form $q_D^K : H^1(X; \mathbb{Z}_2) \rightarrow \mathbb{Z}_2$ is given by

$$(57) \quad (-1)^{q_D^K(\alpha)} = (-1)^{\sum_{i < j} \gamma_i \cdot \gamma_j} \prod_{i=1}^m (-\varepsilon^K(\gamma_i)) (-1)^{\ell_D(\gamma_i)}.$$

They then prove that for a fixed dimer configuration D on $\Sigma \subset X$, $q_D^K - q_D^{K'} \in \text{Hom}(H_1(X; \mathbb{Z}_2), \mathbb{Z}_2)$ maps to $[K] - [K'] \in H^1(X; \mathbb{Z}_2)$ by the canonical isomorphism $\text{Hom}(H_1(\Sigma; \mathbb{Z}_2), \mathbb{Z}_2) \cong H^1(X; \mathbb{Z}_2)$. This shows that a dimer configuration on a surface graph determines an isomorphism of affine $H^1(X; \mathbb{Z}_2)$ -spaces,

$$(58) \quad \psi_D : \tilde{\mathcal{K}}(\Sigma) \rightarrow \mathcal{Q}(H_1(X; \mathbb{Z}_2), \cdot), \quad [K] \mapsto q_D^K,$$

from the set of equivalence classes of Kasteleyn orientations to the set of quadratic forms on $(H_1(X; \mathbb{Z}_2), \cdot)$. They further prove that for a fixed Kasteleyn orientation $q_D^K - q_{D'}^K \in \text{Hom}(H_1(X; \mathbb{Z}_2), \mathbb{Z}_2)$ is given by $\alpha \mapsto \alpha \cdot \Delta(D, D')$, showing that $\psi_D = \psi_{D'}$ if and only if D and D' are equivalent dimer configurations. Finally, the result of Johnson from [28] that \mathcal{S} is isomorphic to $\mathcal{Q}(H_1(X; \mathbb{Z}_2), \cdot)$ completes the proof.

We have seen that an Adinkra chromotopology $A_{(N,k)}$ defines a Riemann surface $X_{(N,k)}$ with a projection to $\mathbb{C}\mathbb{P}^1$. And that including an odd dashing determines a Kasteleyn orientation on $A_{(N,k)} \subset X_{(N,k)}$. We will now show that an Adinkra chromotopology admits a canonical choice of a dimer configuration on $A_{(N,k)} \subset X_{(N,k)}$ thus defining a spin structure on $X_{(N,k)}$ by Theorem 6.

For a given color c , the set of edges of color c in $A_{(N,k)}$ is a dimer configuration [18]. This is easily seen since, every vertex in $A_{(N,k)}$ is incident to exactly one edge of color c . Adinkra's however have additional structure that constrain the dimer configurations corresponding to different colors.

Proposition 10. *The dimer configurations corresponding to different colors in $A_{(N,k)}$ are equivalent as dimer configurations on the surface graph $A_{(N,k)} \subset X_{(N,k)}$.*

Proof. Let D_i be the dimer configuration corresponding to color c_i in $A_{(N,k)} \subset X_{(N,k)}$. Fix a color c_i and let color c_{i+1} be the next color in the rainbow. The (D_i, D_{i+1}) -composition cycles are the c_i/c_{i+1} colored loops in $A_{(N,k)}$. $X_{(N,k)}$ has 2-cells attached to the c_i/c_{i+1} colored loops, so all of the (D_i, D_{i+1}) -composition cycles are contractible in $X_{(N,k)}$. Therefore $\Delta(D_i, D_{i+1}) = 0 \in H_1(X_{(N,k)}; \mathbb{Z}_2)$, and $D_i \sim D_{i+1}$ by definition. We have shown

$$D_1 \sim D_2 \sim \dots \sim D_N.$$

□

Remark 4. We only explicitly showed that the dimer configurations corresponding adjacent colors are equivalent, but by transitivity the dimer configurations corresponding to all colors must be equivalent. Let c_i and c_j be non-adjacent colors. The (D_i, D_j) -composition cycles are the c_i/c_j colored loops in $A_{(N,k)}$, which are non-contractible in $X_{(N,k)}$. However, we know from the above proposition that the collection of all of the c_i/c_j colored loops is 0 in $H_1(X_{(N,k)}; \mathbb{Z}_2)$. This means that the non-trivial loops in $(D_i \cup D_j) \setminus (D_i \cap D_j)$ must come in pairs.

Furthermore, we could perform an R -symmetry so that c_i and c_j are adjacent in the rainbow. This shows that $\Delta(D_i, D_j) = 0 \in H_1(\tilde{X}_{(N,k)}; \mathbb{Z}_2)$ for any surface $\tilde{X}_{(N,k)}$ related to $X_{(N,k)}$ by an R -symmetry.

Corollary 6. *An Adinkra chromotopology, $A_{(N,k)}$, with an odd dashing, D , defines a spin curve, $X_{(N,k)}^D$. Forgetting the spin structure on $X_{(N,k)}^D$ leaves the same underlying Riemann surface $X_{(N,k)}$ for all odd dashings. Furthermore, $X_{(N_1, k_1)}^D \cong X_{(N_2, k_2)}^{D'}$ if and only if $A_{(N_1, k_1)}$ and $A_{(N_2, k_2)}$ are related by an R -symmetry and $D \sim D'$.*

Proof. As seen in section 3 every chromotopology defines a Belyi curve $(X_{(N,k)}, \beta)$, with R -symmetric chromotopologies giving equivalent Belyi pairs. The inclusion of an odd dashing defines a Kasteleyn orientation by proposition 8, with equivalent dashings defining equivalent Kasteleyn orientations. The chromotopology $A_{(N,k)}$ defines an equivalence class of dimer configuration on $A_{(N,k)} \subset X_{(N,k)}$ by taking the dimer configuration corresponding to the edges of any color in $A_{(N,k)}$. This dimer configuration together with the Kasteleyn orientation on $A_{(N,k)}$ defines a spin structure on $X_{(N,k)}$ by Theorem 6. Furthermore, $X_{(N,k)}^D$ and $X_{(N,k)}^{D'}$ have the same spin structure if and only if $A_{(N,k)}^D$ and $A_{(N,k)}^{D'}$ have equivalent Kasteleyn orientations, if and only if D and D' are equivalent dashings. □

This correspondence between odd dashings on $A_{(N,k)}$ and spin structures on $X_{(N,k)}$ allows us to approach the counting of equivalence classes of odd dashings on $A_{(N,k)}$ in terms of counting allowable spin structures on $X_{(N,k)}$. As noted previously, there is one odd dashing for the N -cube, A_N , up to equivalence. This corresponds

to the equivalence class of Kasteleyn orientations with enough symmetry to be a Kasteleyn orientation relative to every 2-colored loop regardless of whether or not it has a 2-face attached. This clearly corresponds to the trivial spin structure.

A general chromotopology $A_{(N,k)}$ is a projection of the N -cube. The projection breaks some of the symmetry making more spin structures possible. As an example consider the A_4 and $A_{(4,1)}$ chromotopologies. X_4 is a square torus (see Figure 2) and there is only one possible spin structure corresponding to an odd dashing. $X_4 \rightarrow X_{(4,1)}$ is a double cover, so $X_{(4,1)}$ is a rectangular torus with half the area. This removes one of the directions of symmetry in which the Kasteleyn orientation is required to be Kasteleyn. Therefore, there are 2 possible spin structures corresponding to odd dashings, giving the chiral and twisted chiral Adinkras. In general, when we mod an N -cube by a code, each generator of the code will reduce a direction of required symmetry doubling the number of allowable spin structures. Therefore, $X_{(N,k)}$ will have 2^k possible spin structures that correspond to odd dashings on $A_{(N,k)}$. This agrees with number of equivalence classes of odd dashings by [37, prop. 5.7].

As noted, it was shown in [18] that every edge of a given color in a regular colored graph corresponds to a dimer configuration. This correspondence was used in [18] to count colorings of a graph, by counting dimer configurations. In our current context this counts the number of distinct chromotopologies for a given quotients of the N -cube. By distinct we mean that they cannot be related by an R -symmetry. Performing an R -symmetry exchanges colors, but by proposition 10 every color of an Adinkra chromotopology gives an equivalent dimer configuration. Therefore counting dimer configurations up to equivalence corresponds to counting chromotopologies up to R -symmetry. The counting in [18] is performed by attaching odd variables to the vertices and edges of the graph and then performing Grassmann integration. This shows that it is natural to consider odd variables attached to an Adinkra, which as we will see in the following subsection gives $X_{(N_1,k_1)}$ a natural SRS structure.

4.3. Description as a Super Riemann Surface. We now describe the Belyi curve associated to an Adinkra chromotopology with an odd dashing as a super Riemann surface. SRS's were originally defined in [21, 6, 30]. The literature on SRS's is much too extensive to list here. We will mainly be following [36] and [10]. A super Riemann surface, X , is a $1|1$ dimensional complex supermanifold, whose tangent bundle TX has a completely nonintegrable rank $0|1$ subbundle, \mathcal{D} . Here nonintegrable means that if D is a nonzero section of \mathcal{D} then $D^2 = \frac{1}{2}\{D, D\}$ is nowhere proportional to D . X is locally isomorphic to $\mathbb{C}^{1|1}$. We can always choose holomorphic local bosonic and fermionic coordinates $z|\theta$ so that D takes the form

$$(59) \quad D_\theta = \frac{\partial}{\partial \theta} + \theta \frac{\partial}{\partial z}.$$

These are called the superconformal coordinates. A superconformal change of coordinates is given by

$$(60) \quad \begin{aligned} \tilde{z} &= u(z) + \theta \eta(z) \sqrt{u'(z)} \\ \tilde{\theta} &= \eta(z) + \theta \sqrt{u'(z) + \eta(z)\eta'(z)}, \end{aligned}$$

so the transition functions between local coordinates must take this form.

As noted in [36], every SRS can be constructed by gluing together open sets $U \subset \mathbb{C}^{1|1}$ by superconformal transformations. Furthermore, a spin curve can naturally be viewed as an SRS by attaching an odd variable via equation 60 with $\eta = 0$. In this case, $u(z)$ is given by the transition functions for the underlying manifold. We then attach an odd variable with transition functions given by $\tilde{\theta} = \theta \sqrt{u'(z)}$. It remains to determine the sign of the root. This is determined by the spin structure.

Consider local coordinates on the open set U_α and U_β :

$$(61) \quad \begin{aligned} z_\alpha &= u_{\alpha\beta}(z_\beta) \\ \theta_\alpha &= [u'_{\alpha\beta}(z_\beta)]^{1/2} \theta_\beta. \end{aligned}$$

Note that the gluing law for the differential dz_α is $u'_{\alpha\beta}(z_\beta) dz_\beta$. Comparing this with equation 61, we see that θ_α transforms as $(dz_\alpha)^{1/2}$. dz is a section of the canonical bundle. A choice of sign for $\sqrt{u'(z)}$ corresponds to a choice of a root of the canonical bundle, i.e. to a spin structure. This immediately gives the following result by corollary 6.

Corollary 7. *An Adinkra chromotopology with an odd dashing defines a super Riemann surface.*

Before giving explicit charts and transition functions defining the SRS's associated to an Adinkra, let us recall some important features of coverings of SRS's since our spin curves are also Belyi curves.

For a branched cover $p : \tilde{X} \rightarrow X$ where X is an SRS, \tilde{X} does not inherit an SRS structure. \tilde{X} is what is known as a super Riemann surface with a parabolic structure. If $\tilde{x} \in \tilde{X}$ is a degree k ramification point, then \tilde{X} has an order $1 - k$ parabolic structure there. This means that the section $D = \frac{\partial}{\partial \theta} + \theta \frac{\partial}{\partial z}$ in X lifts to $\tilde{D} = \frac{\partial}{\partial \theta} + w^{1-k} \theta \frac{\partial}{\partial w}$ where w is a local coordinate near $\tilde{x} \in \tilde{X}$ such that $w^k = z$. The order of the parabolic structure can be changed by any even number using a blowup operation described in [10]. This means that the parabolic structure due to any odd degree ramification can be removed, whereas the parabolic structure due to any even degree ramification can cannot be removed. The order of the parabolic structure corresponding to an even degree ramification point can always be increased so that the section takes the form

$$(62) \quad \tilde{D}_\theta^* = \frac{\partial}{\partial \theta} + y \theta \frac{\partial}{\partial y}.$$

This shows that there is what is known as a Ramond puncture at \tilde{x} .

There are 2 different types of punctures that can be given to an SRS; Neveu-Schwarz (NS) punctures and Ramond (R) punctures. Bosonic vertex operators can be inserted at NS punctures and fermionic vertex operators can be inserted at R punctures. An NS puncture is what is normally thought of as a puncture where a point from the underlying surface is removed. For an R puncture, no points are removed from the surface, but the nonintegrability of the subbundle fails. In particular, at an R puncture local coordinates can be chosen so that D is given by equation 62.

The Belyi curves corresponding to an Adinkra have even degree ramification at the center of each face (over ∞ in the Belyi base) and degree N ramification at the vertices. This means that there must be R punctures at the centers of each face and at each vertex if N is even in order for the super Riemann structure to be compatible with the Belyi map. If we instead consider $X_{(N,k)} \rightarrow B_N$, then all of the ramification is at the center of the faces and we do not have to consider N being odd or even separately. Recall that B_N is \mathbb{CP}^1 with an embedded graph consisting of N edges and 2 vertices. If we give B_N a super Riemann structure, then $X_{(N,k)}$, the pullback of B_N will have a super Riemann structure with Ramond punctures at the center of each face. Now let us look at charts and transition functions for the SRS's associated to an Adinkra.

For a genus g Riemann surface X with $n \geq 1$ marked points, p_i such that $2 - 2g - n < 0$, and the choice of n positive real numbers a_i there is a unique meromorphic quadratic differential q on X known as a Strebel differential [35]. A Strebel differential q is holomorphic on X minus the n marked points and has a double pole at each marked point.

Recall that a holomorphic quadratic differential q on a Riemann surface X is an element of $H^0(X; K^2)$ where K^2 is the symmetric tensor product of the canonical sheaf. In local coordinates z , q is given by

$$q(z) = f(z)(dz)^2,$$

where $f(z)$ is a locally defined holomorphic function. For a local change of coordinates $w = w(z)$, $q = f(z)(dz)^2 = g(w)(dw)^2$, where

$$(63) \quad f(z) = g(w(z)) \left(\frac{dw(z)}{dz} \right)^2.$$

A meromorphic quadratic differential is a holomorphic quadratic differential except at a finite set of points p_1, \dots, p_n where $q = f_i(z)(dz)^2$ with f_i a meromorphic function with a pole at $z = p_i$. A horizontal leaf of a meromorphic quadratic differential $q = f(z)(dz)^2$ is a real parametric curve $\gamma : (0, 1) \rightarrow X$ such that

$$(64) \quad f(\gamma(t)) \left(\frac{d\gamma(t)}{dt} \right)^2 > 0$$

for all $t \in (0, 1)$. Every compact horizontal leaf α of a Strebel differential is a simple closed curve encircling one of the poles, p_i , and satisfying

$$a_i = \oint_{\alpha} \sqrt{q}.$$

Here the square root is chosen so that the integral is positive when the integral is performed in the positive direction relative to the orientation of X . The length of a noncompact horizontal leaf bounded by 2 zeros $z_0 = \gamma(t_0)$ and $z_1 = \gamma(t_1)$ is

$$L(\gamma) = \int_{z_0}^{z_1} \sqrt{q} = \int_{t_0}^{t_1} \sqrt{f(\gamma(t))} \frac{d\gamma(t)}{dt} dt.$$

It is shown in [33] that for every ribbon graph Σ there is a unique Strebel differential q for the associated dessin d'enfant such that q has zeros at the vertices of Σ . The poles of q are the centers of the faces and the edges of Σ are horizontal leaves.

Example 4.4 of [33] describes the Strebel differential for the Belyi base, \mathbb{CP}^1 with embedded graph Σ_0 consisting of the line segment $[0, 1]$. First they note that the meromorphic quadratic differential

$$q_0 = \frac{1}{4\pi^2} \frac{(d\zeta)^2}{\zeta(1-\zeta)}$$

on \mathbb{CP}^1 has simple poles at 0 and 1 and a double pole at ∞ . $[0, 1]$ is a horizontal leaf of length $\frac{1}{2}$ and $\mathbb{CP}^1 \setminus ([0, 1] \cup \{\infty\})$ is covered by compact horizontal leaves given by

$$(65) \quad \zeta = a \cos \theta + \frac{1}{2} + ib \sin \theta,$$

with

$$a^2 = b^2 + \frac{1}{4}.$$

This change of coordinates gives

$$q_0 = \frac{1}{4\pi^2} (d\theta)^2.$$

The length of each compact leaf is 1. We could scale the length of the edge to be anything we'd like.

They further show in [33] that the unique Strebel differential associated to a ribbon graph defines local coordinates on the corresponding dessin d'enfant or Belyi curve. This means that a Belyi curve coming from an Adinkra, $X_{(N,k)} \supset A_{(N,k)}$ has a unique Strebel differential with zeros at the vertices of $A_{(N,k)}$ and poles at the centers of the faces which defines a canonical choice of local coordinates. We can then attach an odd variable by equation 61 with $\eta = 0$ to define the super Riemann structure. Note that when $X_{(N,k)}$ is viewed as an SRS covering B_N there must be R punctures precisely at the poles of q .

The edges of $A_{(N,k)}$ are noncompact horizontal leaves of q . The lines from the zeros of q to the poles of q are vertical leaves. A vertical leaf is a real parametric curve $\gamma : (0, 1) \rightarrow X_{(N,k)}$ such that

$$(66) \quad f(\gamma(t)) \left(\frac{d\gamma(t)}{dt} \right)^2 < 0$$

for all $t \in (0, 1)$. Since the zeros of q are the vertices of $A_{(N,k)}$ and the poles are the centers of the faces, the vertical leaves connecting the poles and zeros of q together with the noncompact horizontal leaves (the edges of $A_{(N,k)}$) form a canonical triangulation of $X_{(N,k)}$. Each edge of $A_{(N,k)}$ is bounded by 2 triangles in $X_{(N,k)}$. Both triangles share the edge, and the pre-images of ∞ in the 2 faces adjacent to the edge define the other vertices of the 2 triangles. The union of the 2 triangles in $X_{(N,k)}$ adjacent to a given edge E in $A_{(N,k)}$ form a diamond which is the set of all vertical leaves of q that intersect E . Consider E with the bipartite orientation. Therefore labeling the 2 vertices bounding E by v_w and v_b , means E points from v_w to v_b . [33] defines canonical coordinates z so that for a point P in the diamond

$$(67) \quad z = z(P) = \int_{v_w}^P \sqrt{q}.$$

This maps the diamond shape to

$$(68) \quad U_E = \{z \in \mathbb{C} \mid 0 < \operatorname{Re}(z) < 1\},$$

an infinite strip of width 1. Here the width of the strip is given by the length of the edge, and we have set the lengths of all edges in $A_{(N,k)}$ to be 1. To this strip we attach a Grassmann variable θ , making U_E into a patch of $\mathbb{C}^{1|1}$. The local representation for q on U_E is

$$q = (dz)^2.$$

Now consider any vertex V of $A_{(N,k)}$. It has degree N which means that q has a degree $N - 2$ zero there. Therefore there exists a neighborhood U_V centered at V with local coordinates w on which q is given by

$$(69) \quad q = \frac{N^2}{4} w^{N-2} (dw)^2$$

and V corresponds to $w = 0$. On $U_E \cap U_V$

$$q = (dz)^2 = \frac{N^2}{4} w^{N-2} (dw)^2,$$

with $w = 0$ and $z = 0$ corresponding to the same point V . Solving this initial value problem gives transition functions

$$(70) \quad w = w(z) = cz^{2/N},$$

where c is an N th root of unity. In particular edges of adjacent colors must map to adjacent roots of unity, so we may choose $c = e^{\frac{2\pi ji}{N}}$ for edge color j . We also

attach a Grassmann variable ϕ to U_V . By equation 61, the transition function for the odd variables on $U_E \cap U_V$ is given by

$$(71) \quad \phi = \left[\frac{2c}{N} z^{\frac{2}{N}-1} \right]^{1/2} \theta.$$

The sign of the square root is determined by the spin structure which is determined by the odd dashing on the Adinkra.

Finally consider the open disk U_i centered at each pole p_i of q , i.e. at the center of each face F_i of $X_{(N,k)}$. U_i is the collection of all compact horizontal leaves homotopic to p_i . We can choose local coordinates so that on U_i

$$q = -\frac{a_i^2}{4\pi^2} \frac{(du)^2}{u^2},$$

since $\oint \sqrt{q} = a_i$. Furthermore, the boundary of U_i is the 4 edges of $A_{(N,k)}$ that define the face. Each edge has length 1. Therefore

$$a_i = 1 + 1 + 1 + 1 = 4$$

for all i . Solving the differential equation gives the transition functions of $U_i \cap U_E$

$$(72) \quad u = \gamma e^{\frac{\pi iz}{2}},$$

where γ is a constant of integration. If we number the edges 1 through 4 as we go around the face with respect to the orientation of the surface and E is the k th edge, then

$$\gamma = e^{\frac{k\pi i}{2}}.$$

We attach a Grassmann variable χ to U_i . By equation 61, on $U_i \cap U_E$ the transition function for the odd variables is given by

$$(73) \quad \chi = \left[\frac{\pi i \gamma}{2} e^{\frac{\pi iz}{2}} \right]^{1/2} \theta.$$

This explicitly defines charts and transition functions for $X_{(N,k)}$ as an SRS. There is a chart for each vertex, edge and 2-face of $X_{(N,k)}$. Therefore we introduced a local Grassmann coordinate for each vertex, edge and face and the transition functions were obtained by equation 61 to make the transitions superconformal. Again note that if we want to view $X_{(N,k)}$ as covering B_N we must have Ramond punctures at the poles of q .

5. FROM ENGINEERING DIMENSION TO MORSE DIVISOR

We saw in section 3 that the chromotopology of an Adinkra defines a Belyi curve, and in section 4 we saw that including the dashing on the Adinkra defines a spin structure on the Belyi curve. This spin structure allowed us to define the Belyi curve as a super Riemann surface. An Adinkra has one more additional structure we have not yet considered, the orientation of its edges. As noted in section 2 the edge orientation is equivalent to a height function on the vertices where the height

corresponds to twice the engineering dimension of the component fields the vertex represents. Here the white vertices have even rank while the black vertices have odd rank.

In this section we will show that the Adinkra height function, h , defines a discrete Morse function on the SRS in the sense of Banchoff [5]. When the Adinkra doesn't contain any saddle points with multiplicity greater than 1, we will see that h when viewed as a discrete Morse function in terms of Banchoff corresponds (in the sense of [7]) to a discrete Morse function in the sense of Forman [19, 20] on the Morse complex of the SRS. While the Banchoff discrete Morse function can handle saddle points with higher multiplicity, the Forman discrete Morse function cannot. We will briefly discuss how a Forman discrete Morse function can be defined on the "extended" Morse complex discussed in [34] to handle higher multiplicity saddle points.

Finally we will discuss how the height of the vertices of the Adinkra naturally defines a divisor on the SRS. Since the Adinkra height function is both a discrete Morse function and a divisor we call it a *Morse divisor*. Every Adinkra is given by a chromotopology with an orientation and a dashing. Therefore, we will see that taking all of the structure of an Adinkra into account defines an SRS with a Morse divisor.

5.1. From Engineering Dimension to Discrete Morse Function. Morse theory usually pertains to smooth functions on smooth manifolds. There have been many different approaches to discretizing it. Two of the most widely used approaches are those of Banchoff in [5] and Forman in [19, 20]. Since we will mainly be using Banchoff's construction, we will briefly review the relevant features here. We will later discuss how this depiction is related to a Forman discrete Morse function on the induced Morse complex. We will briefly define a Forman discrete Morse function then, but we refer the reader to [7] for a review of the necessary features as well as a discussion of the relationship between the 2 approaches to discretization.

Banchoff's approach to discretizing Morse theory assigns an index to the vertices of finite polyhedra embedded in Euclidean space. In particular he discusses the case of a triangular mesh embedded in Euclidean space. Here we will follow the review of Banchoff's discrete Morse theory for triangle meshes in [34]. Consider a 2-dimensional oriented triangular mesh, M , and a function f defined on the vertices of M such that if v and w are vertices connected by an edge in M then $f(v) \neq f(w)$. We extend f to a piecewise-linear function on M by linear interpolation across the edges and faces of M . Since F takes different values at the 2 endpoints of every edge in M , the gradient of f will be a non-zero constant across all of the edges and faces of M .

The *link* of a vertex v is the set of all vertices v_1, \dots, v_m that are connected to v by an edge together with the edges that connect v_i and v_{i+1} , $1 \leq i \leq m$, where we consider $m + 1 \sim 1$. Here the order of the vertices is determined by

the orientation of the mesh, i.e. we order them as we go around a loop enclosing v counter-clockwise relative to the orientation of M . We denote the link of v by $\text{Lk}(v)$, and the edge connecting vertices v and w by $\langle v, w \rangle$. The *upper link* of v is given by

$$(74) \quad \text{Lk}^+(v) = \{v_i \in \text{Lk}(v) | f(v_i) > f(v)\} \cup \{\langle v_i, v_j \rangle \in \text{Lk}(v) | f(v_i), f(v_j) > f(v)\}.$$

Similarly, the *lower link* is given by

$$(75) \quad \text{Lk}^-(v) = \{v_i \in \text{Lk}(v) | f(v_i) < f(v)\} \cup \{\langle v_i, v_j \rangle \in \text{Lk}(v) | f(v_i), f(v_j) < f(v)\}.$$

Finally, the set of *mixed edges* is defined by

$$(76) \quad \text{Lk}^\pm(v) = \{\langle v^+, v^- \rangle \in \text{Lk}(v) | f(v^+) > f(v) > f(v^-)\}.$$

The link of v decomposes as

$$(77) \quad \text{Lk}(v) = \text{Lk}^+(v) \cup \text{Lk}^-(v) \cup \text{Lk}^\pm(v).$$

The number of mixed edges, $|\text{Lk}^\pm(v)|$, is always even, so we may classify the vertices of M as follows:

Classification of v	Condition
v is a minimum with index 0	$\text{Lk}^-(v) = \emptyset$
v is a maximum with index 2	$\text{Lk}^+(v) = \emptyset$
v is a regular point	$ \text{Lk}^\pm(v) = 2$
v is a saddle point with index 1 and multiplicity $m \geq 1$	$ \text{Lk}^\pm(v) = 2 + 2m$

Banchoff proved in [5] that the Euler characteristic of the mesh can be obtained from the critical vertices by the formula

$$(78) \quad \chi(M) = \sum_{v \in \text{Crit}M} (-m)^{\text{ind } v},$$

where the multiplicity of maxima and minima is $m = 1$.

For this to apply to the SRS associated to an Adinkra we need to define a triangular mesh on the surface. Here we cannot use the canonical triangulation defined by the Strbel differential in the previous section since it has edges of constant height. In fact the super Riemann structure will not play a role here, so it is enough to consider only the Riemann surface $X_{(N,k)}$ associated to an Adinkra chromotopology $A_{(N,k)}$ as described in section 3. The Adinkra embedding in $X_{(N,k)}$ defines a mesh on $X_{(N,k)}$ with quadrilateral faces. The triangulation of $X_{(N,k)}$ is constructed by adding some edges and vertices to $A_{(N,k)}$ so that the faces become triangular. The edges and vertices we need to add depend on the topology of the quadrilateral face we are dividing into triangles.

Each 2-face of $X_{(N,k)}$ can have one of 2 possible topologies. Both topologies are pictured in Figure 1; we refer to them as the *diamond* and *bow-tie*. Note that

the topology does not depend on the dashing or bipartition, so in particular the topologies in Figure 1 are invariant under exchange of white and black vertices. If the topology of the face is the diamond, then we add an edge of a new color, let's say gray, that connects the 2 vertices in the diamond that are the same color but have different heights, see Figure 5.

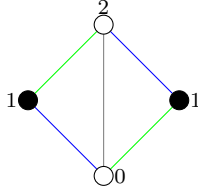


FIGURE 5. The triangulation of faces with the diamond topology. All arrows point up and we have ignored the dashing.

If a face has the bow-tie topology, then we add a vertex to the pre-image of ∞ along the Belyi map β in the face being considered. We can choose this point to be the barycenter of the face, as will be convenient for comparison to a Forman discrete Morse function later. We then connect this new vertex to each of the other 4 vertices in the faces by 4 new edges, each of the same new gray color, see Figure 6. In general many vertices will be incident to multiple gray edges. The key point is that everything that wasn't in the original Adinkra will be colored gray.

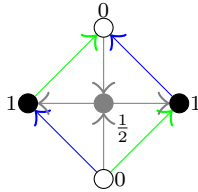


FIGURE 6. The triangulation of faces with the bow-tie topology. Note that we have “unfolded” the bow-tie; the 2 white vertices have the same rank.

The discrete Morse function we are considering here is the height, h , of the vertices. We define the height of the new vertices added to the centers of faces with the bow-tie topology to be the average of the heights of the other 4 vertices incident to the face. Note that while all of the original vertices of the Adinkra have integral height, the new vertices will have half-integral height.

Let us refer to this triangulation of $X_{(N,k)}$ by M . Now note that h satisfies Banchoff's only condition that if $\langle v, w \rangle \in M$, then $h(v) \neq h(w)$. Let $\langle v, w \rangle$ be an edge in M . If it is an edge of the original Adinkra $A_{(N,k)}$ then it must connect a white and black vertex. The white vertex will have even height while the black vertex will have odd height so $h(v) \neq h(w)$. If it is one of the new gray edges we

have added there are 2 possibilities. One possibility is that it was an edge added to a face with the diamond topology. Then it connects 2 vertices of the original Adinkra that have the same color but differ in height by 2, so again $h(v) \neq h(w)$. The other possibility is that it is an edge that was added to a face with the bow-tie topology. In that case the edge connects a vertex from the original Adinkra which has integral height to the new vertex at the center of the bow-tie which has half-integral height, so $h(v) \neq h(w)$. The reason only one edge was added to faces with the diamond topology while 4 edges and a vertex were added to faces with the bow-tie topology to create M was to ensure there were no edges of constant height. If one tried to apply the triangulation for faces of one topology to faces of the other topology there would be edges of constant height.

More importantly, vertices need to be placed at the center of faces with the bow-tie topology because there are critical points there.

Proposition 11. *The vertices at the center of every face with the bow-tie topology are Morse saddle points.*

Proof. Consider the gray point, v , at the center of a bow-tie pictured in Figure 6. It is incident to 4 edges connected to the 4 vertices of the bow-tie. As you go around a loop enclosing v the edges will alternate between entering and leaving v . This corresponds to going around the boundary of the face (which is $\text{Lk}(v)$) and the vertices alternating between having height more and less than the height of v . Therefore every edge in the boundary of the bow-tie is in the set of mixed edges of v and $|\text{Lk}^\pm(v)| = 4$. Therefore v is a saddle point with multiplicity 1 by definition. This is called a Morse saddle, since in classical Morse theory only multiplicity 1 saddle points are allowed. \square

All other critical points must occur at the vertices of the original Adinkra, $A_{(N,k)} \subset M$. This immediately gives the following result.

Corollary 8. *All of the maxima and minima (there must be at least one of each since $A_{(N,k)}$ is finite and $X_{(N,k)}$ compact) must occur at vertices of the embedded Adinkra.*

The vertices of the Adinkra can also be regular points or saddle points.

Proposition 12. *To determine the critical behavior of the vertices of the Adinkra, it is enough to consider the rainbow and the Adinkra orientation. In particular, the new vertices and edges can be ignored.*

Proof. The order of the edges as you go around a loop enclosing a vertex $v \in X_{(N,k)}$ is determined by the rainbow as described in section 3. Therefore the vertices connected to the other end of those edges are ordered by the rainbow. This means that the rainbow determines the order of the vertices in $\text{Lk}(v)$ for all $v \in A_{(N,k)}$. The Adinkra orientation determines the relative height of the vertices in $\text{Lk}(v)$ to the height of v . It remains only to show that the additional gray edges and vertices

in M , which give additional vertices in $\text{Lk}(v)$, can be ignored for determining the critical behavior of v .

Consider a face incident to vertex v . The 2 edges of the face incident to v will have colors i and $i + 1$. Label the other vertices incident to those edges v_i and v_{i+1} . Let us first consider the case where the face has the bow-tie topology. Then $h(v_i) = h(v_{i+1}) = h(v) \pm 1$, so either both v_i and v_{i+1} will be above v or both will be below v . The additional grey vertex that comes between v_i and v_{i+1} in $\text{Lk}(v)$ will have the same relative height to v as v_i and v_{i+1} . Therefore including or not including this point will not effect $|\text{Lk}^\pm(v)|$, or whether or not $\text{Lk}^+(v)$ and $\text{Lk}^-(v)$ are empty.

If the face has the diamond topology and v is not the max or min of the face then there is no additional grey edges between the edge of color i and the one of color $i + 1$. If v is the minimum (maximum) of the diamond then $h(v_i) = h(v_{i+1}) > h(v)$ ($< h(v)$). There is an additional edge in between edges of colors i and $i + 1$ connecting v to the maximum (minimum) of the diamond. Therefore the rank of this point w is $h(w) > h(v)$ ($< h(v)$), and it has the same relative height to v as v_i and v_{i+1} . Therefore following the same argument as before the critical behavior of v does not depend on whether or not we consider w . \square

Together, propositions 11 and 12 show that the Adinkra chromotopology together with the Adinkra orientation determine all of the critical behavior. The additional gray edges and vertices were not used to determine where the critical points were.

A Morse complex for a smooth manifold with a Morse function is a CW-complex with a 0-cell at each minimum, a 1 cell that passes through each saddle and a 2-cell containing exactly one of each of the maxima. It is shown in [16] that if h is Morse-Smale (as is the case when all of the saddle points are Morse saddles) then the Morse complex can be embedded in M . To describe this construction we first need to define a flow path which is the analogue of an integral curve on a mesh.

For a graph Γ with discrete morse function h let $\text{argmin}(\Gamma) = v^-$ where $f(v^-) = \min_{v \in \Gamma} f(v)$. If more than 1 vertex in Γ share the same minimum value, then we pick one of them and argmin always returns that vertex. $\text{argmin}(\text{Lk}(v))$ behaves as a discretization of $-\nabla f(v)$ since it gives the direction of deepest descent. With the idea that things flow down, the *flow path* for a vertex v_0 , $\text{flow}(v_0)$, is defined to be the set of vertices v_0, \dots, v_r , where $v_j = \text{argmin}(\text{Lk}(v_{j-1}))$ and v_r is a minimum, together with the edges $\langle v_j, v_{j+1} \rangle$. Flow paths never cross but can merge. If two flows merge then they will never separate. A flow cannot not cross a saddle point.⁷ This means that if the flow reaches a vertex v_j in the link of a saddle point v_s , then v_s is not considered in computing $\text{argmin}(v_j)$.

⁷A flow can originate at a saddle point, so v_0 is the only point in a flow that can be a saddle point.

In [16] it is shown how flows can be used to define a Morse complex embedded in M . Let us first consider the case where there do not exist saddle points of multiplicity greater than 1. Define a 0-cell at each minimum of M . Consider a Morse saddle v_s . $\text{Lk}^-(v_s)$ has 2 connected components, label them A and B . Let $v_A = \text{argmin}(A)$ and define v_B similarly. For each Morse saddle in M we define a 1-cell by the collection of edges $\{\text{flow}(v_A), \langle v_A, v \rangle, \langle v, v_B \rangle, \text{flow}(v_B)\}$. The ends of the 1-cell are the end vertices of the flows $\text{flow}(v_A)$ and $\text{flow}(v_B)$, which are minima. So the boundary of the 1-cell is attached to the corresponding 0-cells. This defines the 1-skeleton Y^1 of the Morse complex $Y \subset M$. The 2-cells of Y are the connected components of $M - Y^1$. Each one will contain exactly one maximum since it is compact and does not contain any saddle points by construction. In [16] saddle points of higher multiplicity are dealt with by showing a saddle point at height h_s with multiplicity $m > 1$ can split into m Morse saddle points at height h_s . We will not follow this approach since we do not want to introduce additional critical points that don't correspond to $\beta^{-1}(\{0, 1, \infty\})$. Instead we will follow [34] where they define an extension of the Morse complex. Before describing this extension, let us look a little closer at the case when there are no saddle points of multiplicity greater than 1, as this is the case for an important "base" example.

When all of the saddle points are Morse saddles, there is a simple relationship between the Adinkra height function as a Banchoff discrete Morse function and the standard ranking on the face poset of the Morse complex as a Forman discrete Morse function. In what follows we assume familiarity with posets. Let P be a poset and consider the function $f : P \rightarrow \mathbb{R}$. f is a *Forman discrete Morse function* (FDMF) if for every $b \in P$ there exists at most one $a \in P$ such that $a \prec b$ and $f(a) \geq f(b)$, and there is at most $c \in P$ such that $b \prec c$ and $f(b) \geq f(c)$. For a FDMF function f , an element $b \in P$ is *Forman critical* if there does not exist $a \in P$ such that $a \prec b$ and $f(a) \geq f(b)$, and there does not exist a $c \in P$ such that $b \prec c$ and $f(b) \geq f(c)$. If an element is not critical it is *ordinary*.

For a CW-complex Y , the face poset $P(Y)$ is the poset consisting of an element for each cell of Y with the order relation $\sigma < \tau$ if σ is in the boundary of τ . $P(Y)$ has a natural rank where the rank of each cell is its dimension. This rank function on $P(Y)$ is a FDMF where every element is critical.

Consider the face poset $P(Y)$ for the Morse complex, Y , constructed from the mesh M , and the standard rank function f . Every cell in Y corresponds to a Banchoff critical point in M . Therefore every Forman critical element in $P(Y)$ corresponds to a Banchoff critical point in M . The Forman critical 0-cells correspond to Banchoff minima, the critical 1-cells correspond to Banchoff Morse saddles, and the critical 2-cells correspond to Banchoff maxima. This is the mapping from the critical points of a FDMF on a finite regular CW-complex to the Banchoff critical points of a barycentric subdivision of the CW-complex found in [7].

Example 4 (The Valise Adinkra). Consider a valise Adinkra where all of the white vertices have height 0 and all of the black vertices have height 1. Then every white vertex is a minimum and every black vertex is a maximum. Furthermore every quadrilateral face has the bow-tie topology since all of the white vertices have the same height and all of the black vertices have the same height. Therefore there is a Morse saddle at the center of each face. Since there are 2^{N-k-1} vertices of each color and $N2^{N-k-2}$ faces, we see that $X_{(N,k)}$ has 2^{N-k-1} maxima, 2^{N-k-1} minima, and $N2^{N-k-2}$ Morse saddles. Therefore by equation 78

$$(79) \quad \chi(X_{(N,k)}) = 2^{N-k-1} + 2^{N-k-1} - N2^{N-k-2}.$$

Solving $\chi(X_{(N,k)}) = 2 - 2g$ for g shows that $X_{(N,k)}$ has genus

$$(80) \quad g = 1 + 2^{N-k-3}(N - 4),$$

for $N \geq 2$. Note that this agrees with the genus found in proposition 1 even though it only depends on the number of vertices and faces and not on the number of edges. In general it is much easier to find maxima and minima of Adinkras than saddle points, so after finding the genus of $X_{(N,k)}$ by proposition 1 equation 78 constrains the number of saddle points there can be. We will discuss this more after describing higher multiplicity saddle points.

The Morse complex CW-decomposition of $X_{(N,k)}$, Y defined by the mesh contains a 0-cell at each white vertex. For each pair of white vertices that bound a face there is a 1-cell connecting them. This is the vertical line connecting the white vertices in Figure 6. The 2-cells are the complements of the 1-cells. The 2 triangular regions left in Figure 6 after removing the gray vertical line are regions of two disjoint 2-cells. Each one contains a single maximum occurring at the black vertex. Therefore $P(Y)$ has a critical 0 cell corresponding to every minimum of $X_{(N,k)}$, a critical 1-cell corresponding to the Morse saddles of $X_{(N,k)}$, and a critical 2-cell corresponding to each maxima of $X_{(N,k)}$.

In general, Adinkras can have saddle points with higher multiplicity as we will see in an explicit example later. Banchoff discrete Morse theory has no problem handling such critical points, but trouble arises when trying to construct the Morse complex. As noted earlier, these difficulties were avoided in [16] by showing that higher multiplicity saddle points can be split into multiple Morse saddle points. We would prefer not to introduce new vertices, so we will use the extended Morse complex defined in [34]. To construct the *extended Morse complex* we begin by placing a 0-cell at each minimum just like for the Morse complex, but now we additionally place a 0-cell at each saddle point. Consider a saddle point v_s with multiplicity m . $\text{Lk}^-(v_s)$ has $m + 1$ components A_i . For each connected component let $v_i = \text{argmin}(A_i)$ and define a 1-cell by the collection of edges $\{< v, v_i >, \text{flow}(v_i)\}$. So one end of each 1-cell is a 0-cell corresponding to the saddle point while the other end is a 0-cell corresponding to a minimum. Each saddle point of multiplicity m is incident to $m + 1$ 1-cells. Note that if there are only Morse

saddles, the extended Morse complex replaces each 1-cell in the Morse complex by 1 0-cell and 2 1-cells, so it does not change the genus formulation. It is possible for 2 flow paths to merge before reaching a minimum. If this occurs we place a 0-cell at the vertex where the flows merge and we replace the remaining part of the 2 merged flows by a single 1-cell. Since we have added a 0-cell and a 1-cell, this does not affect the genus. Now in addition to 1-cells that connect minima to saddle points we can have 1-cells that connect merge points to minima or saddle points.

Let Y_e be the extended Morse complex and $P(Y_e)$ be its face poset. If we took the standard ranking everything would be critical including the merge vertices which do not correspond to Banchoff critical points. To overcome this, we define the following ranking on $P(Y_e)$. Let f be the function that assigns 3 to each 2-cell, 0 to each 0-cell corresponding to a minimum or saddle point, 2 to any 1-cell incident to a saddle point, 1 to all other 1-cells, and 1 to the 0-cells corresponding to merge points. As can be easily checked, f is a FDMF with all of the 0-cells corresponding to minima and saddle points critical and all of the 0-cells corresponding to merge points ordinary. Additionally all of the 2-cells are critical and the 1-cells incident to a saddle point are critical. The 1-cells corresponding to merged flows, i.e. the ones connecting a merge point and a minimum, are all ordinary.

As before the critical 2-cells correspond to maxima, but now the critical 0-cells can correspond to minima or saddle points and there is no longer a single critical 1-cell for each saddle point. If there is a non-critical 1-cell incident to a critical 0-cell then the 0-cell must correspond to a minimum following the discussion of the critical cells. Similarly, if a critical 0-cell is connected to non-critical 0-cell by a critical 1-cell then the critical 0-cell must be a saddle point. Furthermore if there are l critical 1-cells incident to it, then it must have multiplicity $l - 1$. There may not always be merge points, hence non-critical cells, however. Therefore we need a better way to determine if a critical 0-cell corresponds to a minimum or saddle point. If the critical point has the largest Adinkra height out of both endpoints of any 1-cell it is adjacent to then it is a saddle point and if it is the smallest then it is a minimum. The 1 cells allows us to determine the critical behavior of 2 vertices by comparing their heights to only each other.

Example 5 (The (6,0) Fully Extended Adinkra). Consider the fully extended (6,0) Adinkra pictured in Figure 7 with the rainbow (purple, green, light blue, orange, blue, red). There is clearly a single maximum and a single minimum. There are no bow-ties, so all of the saddle points must occur at vertices of the Adinkra. By proposition 12 we can determine all of the saddle points from just the Adinkra and the rainbow.

A vertex will be regular if and only if all of the edges the point in the same direction relative to the vertex (in or out of the vertex) are adjacent to each other. All of the vertices in the second row are trivially regular since they only have one edge pointing in to them. The first vertex on the left in the 3rd row from the

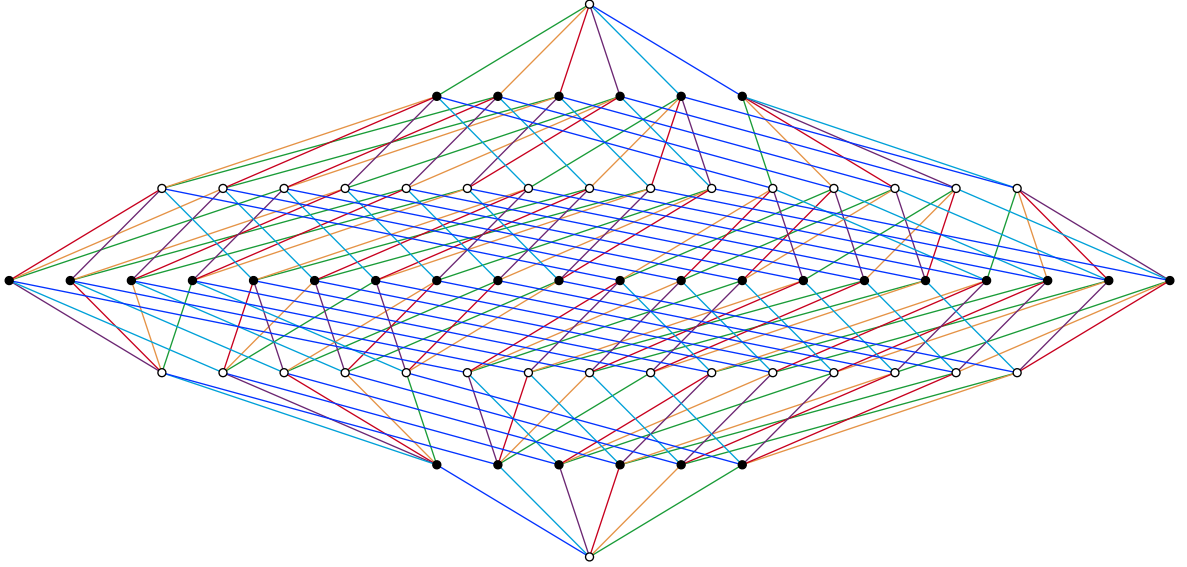


FIGURE 7. The fully extended $(6,0)$ Adinkra. All edges point up and the edge dashing is ignored.

bottom is not regular since the only edges pointing into it are blue and light blue which are not adjacent in the rainbow. The fourth vertex in from the left on that same row is regular however since the 2 incoming edges are blue and orange which are adjacent. The outgoing edges are red, purple, green, and light blue which form a chain of adjacent colors.

Returning to the first vertex on the left in the third row that was not regular; it turns out to be a Morse saddle. Since the incoming edges (which are light blue and blue) are not adjacent their adjacent edges must go in the opposite direction and there must be 2 sign flips for each edge corresponding to the 2 sides of adjacency. This gives a total of 4 sign flips, which is exactly what $|\text{Lk}^\pm(v)|$ counts. Showing that the point is indeed a Morse saddle.

To be a saddle point with multiplicity 2, also called a monkey saddle, there need to be 6 sign flips. This means that there must be 3 edges going in the same direction with none of them adjacent to each other. There is only 2 ways this can happen; the 2 ways purple, light blue, and blue can go one way while green orange, and red go the other. Both possibilities occur. They are at the first and last vertices in the middle row. In all, there turn out to be 2 monkey saddles and 30 Morse saddles. To understand this count consider the third row. There are 15 ways we can have 2 of 6 colors point down corresponding to all 15 vertices in the row. There are 6 ways that the 2 colors will be adjacent and 9 ways they will not. Therefore, that row contains 6 regular points and 9 Morse saddles. By

equation 78

$$(81) \quad \chi(X_6) = 1 + 1 - 30(1) - 2(2) = -32.$$

This shows that X_6 has genus 17 which agrees with proposition 1. Note that this also agrees with the genus computed for the valise Adinkra found in example 4.

Every Adinkra can be obtained from the valise Adinkra by raising and lowering vertices. As we “unfold” the valise Adinkra, bow-ties are undone and become diamonds. The Morse saddle points in the valise Adinkra are forced to move to the vertices of the Adinkra as the bow-ties become undone. Eventually, as can be seen by the previous example, it is possible for Morse saddles to merge and create saddle points of higher multiplicity. The number of saddle points that can occur at vertices of the embedded Adinkra is constrained by the genus of $X_{(N,k)}$ found by proposition 1.

5.2. Description as a Divisor. In the previous section we provided a *topological* interpretation of the combinatorial notion of an orientation/height assignment/ranked poset for an Adinkra. In this section, by focusing on the underlying Riemann surface structure coming from the chromotopology, we shift the attention to *geometric* interpretations for this same structure. The key notion is that of a *divisor* on a Riemann surface, i.e., an assignment of integer values to a finite set of points on the Riemann surface. In our case, the height assignment assigns an integer (possibly zero) height to each white and black vertex.

Now these are very special divisors in that the only points with nonzero coefficients assigned are (a subset of) those corresponding to the imbedded graph vertices. There are discrete variants of the definition of a divisor on a Riemann surface which are particularly natural to consider in our setting. One involves extending the set of points to include the entire graph, not necessarily just vertices [3, 4, 2]. This is especially important when one considers metrized graphs and their associated tropical curves [31, 24]. In the case of Adinkras, where the ribbon graph structure is already specified, studying divisors on the (compact) tropical curve is the next step before the general case of divisors on an arbitrary Riemann surface.

Whichever variant we choose to consider, there are some common features that stand out.

Firstly, the valise Adinkra now appears completely naturally, since the Belyi map factors through a map from the Riemann surface to the “beach ball”, B_N , with a single boson (at 0) a single fermion (at ∞) and N colored lines connecting them. This is a function f in the function field of our Riemann surface, and the associated principal divisor $\text{div}(f)$ corresponds to the height assignment with each fermion at height 1 (i.e., simple zeros of f) and each boson at height -1 (i.e., simple poles of f). This also suggests that, rather than scaling the engineering dimension by two, we may want to use the convention that the heights of adjacent bosons/fermions are odd integers which differ by two (i.e., scale by four).

There is also a partial ordering on all divisors on a Riemann surface given by $D_1 \leq D_2$ if and only if $D_2 - D_1$ is effective (i.e., each integer coefficient appearing is nonzero). Note that when Adinkras associated with D_1 and D_2 are related by an overall shift in heights, this means that the “higher” one is \geq the “lower” one. We could normalize this shift by making the lowest height assigned always zero (the “minimal effective representative”), but another very natural normalization of the shift would be to consider the lowest such that $\deg(D) \geq 0$ (which would be compatible with the valise Adinkra above).

Finally, there are several variants of the Riemann-Roch theorem which apply to graphs [3, 4], tropical curves [31, 24], metrized complexes of curves [1], Riemann surfaces, and even super Riemann surfaces. The Riemann-Roch theorem in the case of Riemann surfaces provides a link between the canonical bundle K_X (the square-root of which is our spin structure/odd dashing), the genus of the Riemann surface X (itself determined by the (N, k)), the dimension of the linear series associated with the divisor D , and the total degree (sum of heights) $\deg(D)$. We expect that each of the geometric variants of this formula will provide a meaningful constraint on the physics of N -extended one-dimensional supersymmetry algebras.

APPENDIX A. COMPLETION OF PROOF OF THEOREM 1

Here we complete the proof of Theorem 1 which requires proving claim 2. Before we can do that we need some facts about S_o and S_e and how they partition the $a_k^{(i)}$. First we need a result about modding sums of powers of 2 by a power of 2.

Claim 3. If i is the sum of distinct powers of 2 with all powers greater than or equal to 1 then $(i + 1) \pmod{2^{k-1}} \in [1, 2^{k-2}]$ if and only if i does not contain $k - 2$ as a power.

Proof. If $x \geq k - 1$ then $2^x \pmod{2^{k-1}} = 0$. Therefore $i \pmod{2^{k-1}}$ is a sum of distinct powers of 2 with powers less than or equal to $k - 2$. The sum of distinct powers of 2 with all powers strictly less than $k - 2$ will be less than 2^{k-2} . Therefore, $(i + 1) \pmod{2^{k-1}} \in [1, 2^{k-2}]$ if and only if i doesn't contain 2^{k-2} as a term. \square

Now let us turn our attention to the effect of our partitioning on the edge labels. For convenience we repeat the definition of the edge labeling $a_k^{(i)}$ (equation 12) here

$$(82) \quad a_k^{(i)} = \begin{cases} (2^{k-2} + i - 1)N + k, & \text{if } i \pmod{2^{k-1}} \in [1, 2^{k-2}], \\ (i - 1 - 2^{k-2})N + k, & \text{otherwise.} \end{cases}$$

Define $m_k^{(i)}$ so that $a_k^{(i)} = m_k^{(i)}N + k$. The first result we will need is

Claim 4. If $i \in S_o \cup S_e$ and $i \pmod{2^{k-1}} \in [1, 2^{k-2}]$ then $(i + 1) \pmod{2^{k-1}} \in [1, 2^{k-2}]$. Similarly, if $i \in S_o \cup S_e$ and $i \pmod{2^{k-1}} \notin [1, 2^{k-2}]$ then $(i + 1) \pmod{2^{k-1}} \notin [1, 2^{k-2}]$.

Proof. Let us denote the interval $[1, 2^{k-2}]$ by I_k . Let us assume $i \pmod{2^{k-1}} \in I_k$, but $i+1 \pmod{2^{k-1}} \notin I_k$. This is only possible if $i \pmod{2^{k-1}} = 2^{k-2}$, but all $i \in S_o \cup S_e$ are odd. Similarly, if $i \pmod{2^{k-1}} \notin I_k$, but $i+1 \pmod{2^{k-1}} \in I_k$, then $i \pmod{2^{k-1}} = 2^{k-1}$. Therefore neither case is possible for $i \in S_e \cup S_o$. \square

The above claim shows us that for $i \in S_o \cup S_e$, $m_k^{(i+1)} = m_k^{(i)} + 1$. Also note that for i odd $m_1^{(i)} = m_2^{(i+1)}$. We need two more results about how our partition of the odd indices splits up the $m_k^{(i)}$ before proving claim 2.

Claim 5. For all $i \in S_e$ and distinct $k, k' \geq 3$ there exists $i' \in S_e$ such that $m_{k'}^{(i')} = m_k^{(i)}$.

Proof. $i-1$ is the sum of an even number of distinct powers of 2. Let $i' = i \pm 2^{k-2} \pm 2^{k'-2}$. Here we add the copy of 2^x if i doesn't already contain it, and subtract it if i does. This clearly makes $i' \in S_e$, since we are either adding/subtracting 2 powers of 2 that are distinct from the others, or adding in one and subtracting another.

If $i-1$ doesn't contain powers $k-2$ or $k'-2$ then by claim 3 $i \pmod{2^{k-1}} \in [1, 2^{k-2}]$ and $m_k^{(i)} = i-1+2^{k-2}$. For $i' = i+2^{k-2}+2^{k'-2}$, $i' \pmod{2^{k'-1}} \notin [1, 2^{k'-2}]$ and $m_{k'}^{(i')} = i' - 1 - 2^{k'-2} = i - 1 + 2^{k-2}$.

If $i-1$ contains both $k-2$ and $k'-2$ as powers then $i \pmod{2^{k-2}} \notin [1, 2^{k-2}]$. Therefore $m_k^{(i)} = i-1-2^{k-2}$. Letting $i' = i-2^{k-2}-2^{k'-2}$, $i' \pmod{2^{k'-1}} \in [1, 2^{k'-2}]$, and $m_{k'}^{(i')} = i' - 1 + 2^{k'-2} = i - 1 - 2^{k-2}$.

If $i-1$ doesn't contain $k-2$ as a power but does contain $k'-2$ as a power then by claim 3, $i \pmod{2^{k-1}} \in [1, 2^{k-2}]$ and $m_k^{(i)} = i-1+2^{k-2}$. For $i' = i+2^{k-2}-2^{k'-2}$, $i' \pmod{2^{k'-1}} \in [1, 2^{k'-2}]$ and $m_{k'}^{(i')} = i' - 1 + 2^{k'-2} = i - 1 + 2^{k-2}$.

If $i-1$ doesn't contain $k'-2$ as a power but does contain $k-2$ as a power then by claim 3, $i \pmod{2^{k-1}} \notin [1, 2^{k-2}]$ and $m_k^{(i)} = i-1-2^{k-2}$. For $i' = i-2^{k-2}+2^{k'-2}$, $i' \pmod{2^{k'-1}} \notin [1, 2^{k'-2}]$ and $m_{k'}^{(i')} = i' - 1 - 2^{k'-2} = i - 1 - 2^{k-2}$. \square

There is one final result that we need before proving claim 2.

Claim 6. For any $k \geq 3$ $\{m_1^{(i)} | i \in S_o\} = \{m_k^{(i)} | i \in S_e\}$.

Proof. Choose $k \geq 3$ and let $i_1 \in S_o$. $m_1^{(i_1)} = i_1 - 1$ is a sum of an odd number of distinct powers of 2. If one of the powers is $k-2$ then let $i_2 = i_1 - 2^{k-2}$. If it doesn't contain $k-2$ as a power then let $i_2 = i_1 + 2^{k-2}$. Clearly i_2 is in S_e in both cases, since $i_2 - 1$ is the sum of an even number of distinct powers. Now note that $m_k^{(i_2)} = m_1^{(i_1)}$.

If $i_1 - 1$ contains $k-2$ as a power then $(i_1) \pmod{2^{k-1}} \notin [1, 2^{k-2}]$ by claim 3. Therefore $(i_1 - 2^{k-2}) \pmod{2^{k-1}} \in [1, 2^{k-2}]$, so $m_k^{(i_2)} = i_2 - 1 + 2^{k-2} = i_1 - 1$.

If $i_1 - 1$ doesn't contain 2^{k-2} as a term then $i_1 \pmod{2^{k-2}} \in [1, 2^{k-2}]$. Therefore for $i_2 = i_1 + 2^{k-2}$, $m_k^{(i_2)} = i_2 - 1 - 2^{k-2} = i_1 - 1$.

Now consider $k \geq 3$ and $i_2 \in S_e$. By claim 3, $i_2 \pmod{2^{k-1}} \in [1, 2^{k-2}]$ if and only if i_2 doesn't contain $k-2$ as a power. Therefore $m_k^{(i_2)} = i_2 - 1 \pm 2^{k-2}$, where the plus sign occurs when i_2 doesn't contain the power $k-2$ and the minus sign is for when it does. Let $i_1 = i_2 \pm 2^{k-2}$, where we add 2^{k-2} if i_2 does not contain it in its sum of distinct powers of 2 and subtract it if it does. $i_1 - 1$ is the sum of an odd number of distinct powers of 2, so $i_1 \in S_o$. Furthermore, $m_1^{(i_1)} = i_1 - 1 = m_k^{(i_2)}$. \square

We can now prove claim 2 completing the proof of Theorem 1. For convenience we relist the definition of γ here. Let

$$(83) \quad \alpha = \prod_{\substack{i=1 \\ \text{odd}}}^{2^{N-1}} (a_1^{(i)}, a_2^{(i+1)})(a_1^{(i+1)}, a_2^{(i)}),$$

$$(84) \quad \beta_o = \prod_{i \in S_o} (a_1^{(i)}, a_1^{(i+1)})(a_2^{(i)}, a_2^{(i+1)}),$$

and

$$(85) \quad \beta_e = \prod_{i \in S_e} \prod_{k=3}^N (a_k^{(i)}, a_k^{(i+1)}).$$

Then

$$(86) \quad \gamma = \alpha \beta_o \beta_e.$$

proof of claim 2. As noted, for i odd $m_2^{(i+1)} = m_1^{(i)}$, and $m_2^{(i)} = m_1^{(i+1)}$. Therefore, α is given by

$$(87) \quad \alpha = \prod_{m=1}^{2^{N-1}} ((m-1)N+1, (m-1)N+2).$$

Conjugation by α clearly sends σ_0 to $\tilde{\sigma}_0$ since α exchanges the edges of colors 1 and 2 appearing in the same disjoint N -cycle (i.e. that are incident to the same white vertex). Now note that by claims 4,5, and 6 $\beta = \beta_o \beta_e$ can be written as the product of disjoint elements of $S_{N2^{N-1}}$ of the form

$$(88) \quad \beta_m = \prod_{k=1}^N (mN+k, (m+1)N+k).$$

Now we will show that β_m commutes with $\tilde{\sigma}_0 = \alpha^{-1} \sigma_0 \alpha$ for all m to show $\tilde{\sigma}_0 = \beta^{-1} \alpha^{-1} \sigma_0 \alpha \beta$. Consider an edge e . If it isn't given by $mN+k$ or $(m+1)N+k$ then β_m leaves it invariant. So let's assume e is given by $(m+q)N+k$ where $q = 0$

or 1. Then

$$\begin{aligned}
\beta_m^{-1}\tilde{\sigma}_0\beta_m((m+q)N+k) &= \beta_m^{-1}\tilde{\sigma}_0((m+1-q)N+k) \\
&= \beta_m^{-1}((m+1-q)N+k') \\
&= (m+q)N+k' \\
&= \tilde{\sigma}_0((m+q)N+k)
\end{aligned}$$

This shows $\tilde{\sigma}_0 = \gamma^{-1}\sigma_0\gamma$.

Now we will show $\tilde{\sigma}_1 = \gamma^{-1}\sigma_1\gamma$ by direct computation. For $k \neq 1, 2, 3$ and $i \in S_o$

$$\begin{aligned}
\beta^{-1}\alpha^{-1}\sigma_1\alpha\beta(a_k^{(i)}) &= \beta^{-1}\alpha^{-1}\sigma_1\alpha(a_k^{(i)}) \\
&= \beta^{-1}\alpha^{-1}\sigma_1(a_k^{(i)}) \\
&= \beta^{-1}\alpha^{-1}(a_{k-1}^{(i)}) \\
&= \beta^{-1}(a_{k-1}^{(i)}) \\
&= a_{k-1}^{(i)}
\end{aligned}$$

The same holds true for $i-1 \in S_o$.

For $k \neq 1, 2, 3$ and $i \in S_e$

$$\begin{aligned}
\beta^{-1}\alpha^{-1}\sigma_1\alpha\beta(a_k^{(i)}) &= \beta^{-1}\alpha^{-1}\sigma_1\alpha(a_k^{(i+1)}) \\
&= \beta^{-1}\alpha^{-1}\sigma_1(a_k^{(i+1)}) \\
&= \beta^{-1}\alpha^{-1}(a_{k-1}^{(i+1)}) \\
&= \beta^{-1}(a_{k-1}^{(i+1)}) \\
&= a_{k-1}^{(i)}
\end{aligned}$$

Similarly for $k \neq 1, 2, 3$ and $i-1 \in S_e$

$$\begin{aligned}
\beta^{-1}\alpha^{-1}\sigma_1\alpha\beta(a_k^{(i)}) &= \beta^{-1}\alpha^{-1}\sigma_1\alpha(a_k^{(i-1)}) \\
&= \beta^{-1}\alpha^{-1}\sigma_1(a_k^{(i-1)}) \\
&= \beta^{-1}\alpha^{-1}(a_{k-1}^{(i-1)}) \\
&= \beta^{-1}(a_{k-1}^{(i-1)}) \\
&= a_{k-1}^{(i)}
\end{aligned}$$

For $k = 1$ and i or $i - 1 \in S_o$

$$\begin{aligned}
\beta^{-1}\alpha^{-1}\sigma_1\alpha\beta(a_1^{(i)}) &= \beta^{-1}\alpha^{-1}\sigma_1\alpha(a_1^{(i+(-1)^{i+1})}) \\
&= \beta^{-1}\alpha^{-1}\sigma_1(a_2^{(i)}) \\
&= \beta^{-1}\alpha^{-1}(a_1^{(i)}) \\
&= \beta^{-1}(a_2^{(i+(-1)^{i+1})}) \\
&= a_2^{(i)}
\end{aligned}$$

For $k = 1$ and i or $i - 1 \in S_e$

$$\begin{aligned}
\beta^{-1}\alpha^{-1}\sigma_1\alpha\beta(a_1^{(i)}) &= \beta^{-1}\alpha^{-1}\sigma_1\alpha(a_1^{(i+(-1)^{i+1})}) \\
&= \beta^{-1}\alpha^{-1}\sigma_1(a_2^{(i+(-1)^{i+1})}) \\
&= \beta^{-1}\alpha^{-1}(a_1^{(i+(-1)^{i+1})}) \\
&= \beta^{-1}(a_2^{(i)}) \\
&= a_2^{(i)}
\end{aligned}$$

For $k = 2$ and i or $i - 1 \in S_o$

$$\begin{aligned}
\beta^{-1}\alpha^{-1}\sigma_1\alpha\beta(a_2^{(i)}) &= \beta^{-1}\alpha^{-1}\sigma_1\alpha(a_2^{(i+(-1)^{i+1})}) \\
&= \beta^{-1}\alpha^{-1}\sigma_1(a_1^{(i)}) \\
&= \beta^{-1}\alpha^{-1}(a_N^{(i)}) \\
&= \beta^{-1}(a_N^{(i)}) \\
&= a_N^{(i)}
\end{aligned}$$

For $k = 2$ and i or $i - 1 \in S_e$

$$\begin{aligned}
\beta^{-1}\alpha^{-1}\sigma_1\alpha\beta(a_2^{(i)}) &= \beta^{-1}\alpha^{-1}\sigma_1\alpha(a_2^{(i)}) \\
&= \beta^{-1}\alpha^{-1}\sigma_1(a_1^{(i+(-1)^{i+1})}) \\
&= \beta^{-1}\alpha^{-1}(a_N^{(i+(-1)^{i+1})}) \\
&= \beta^{-1}(a_N^{(i+(-1)^{i+1})}) \\
&= a_N^{(i)}
\end{aligned}$$

For $k = 3$ and i or $i - 1 \in S_o$

$$\begin{aligned}
\beta^{-1}\alpha^{-1}\sigma_1\alpha\beta(a_3^{(i)}) &= \beta^{-1}\alpha^{-1}\sigma_1\alpha(a_3^{(i)}) \\
&= \beta^{-1}\alpha^{-1}\sigma_1(a_3^{(i)}) \\
&= \beta^{-1}\alpha^{-1}(a_2^{(i)}) \\
&= \beta^{-1}(a_1^{(i+(-1)^{i+1})}) \\
&= a_1^{(i)}
\end{aligned}$$

For $k = 3$ and i or $i - 1 \in S_e$

$$\begin{aligned}
\beta^{-1}\alpha^{-1}\sigma_1\alpha\beta(a_3^{(i)}) &= \beta^{-1}\alpha^{-1}\sigma_1\alpha(a_3^{(i+(-1)^{i+1})}) \\
&= \beta^{-1}\alpha^{-1}\sigma_1(a_3^{(i+(-1)^{i+1})}) \\
&= \beta^{-1}\alpha^{-1}(a_2^{(i+(-1)^{i+1})}) \\
&= \beta^{-1}(a_1^{(i)}) \\
&= a_1^{(i)}
\end{aligned}$$

Therefore we have shown $\gamma^{-1}\sigma_q\gamma = \tilde{\sigma}_q$ for $q = 0, 1$.

□

REFERENCES

- [1] O. Amini and M. Baker. Linear series on metrized complexes of algebraic curves. *ArXiv e-prints*, April 2012, 1204.3508.
- [2] Y. An, M. Baker, G. Kuperberg, and F. Shokrieh. Canonical representatives for divisor classes on tropical curves and the Matrix-Tree Theorem. *ArXiv e-prints*, April 2013, 1304.4259.
- [3] M. Baker and S. Norine. Riemann-Roch and Abel-Jacobi theory on a finite graph. *ArXiv Mathematics e-prints*, August 2006, math/0608360.
- [4] M. Baker and S. Norine. Harmonic morphisms and hyperelliptic graphs. *ArXiv e-prints*, July 2007, 0707.1309.
- [5] T.F. Banchoff. Critical Points and Curvature for Embedded Polyhedral Surfaces. *The American Mathematical Monthly*, 70(5):475–485, May 1970.
- [6] M.A. Baranov and Albert S. Schwarz. On the Multiloop Contribution to the String Theory. *Int.J.Mod.Phys.*, A2:1773, 1987.
- [7] E. D. Bloch. Polyhedral Representation of Discrete Morse Functions on Regular CW Complexes and Posets. *ArXiv e-prints*, August 2010, 1008.3724.
- [8] D. Cimasoni and N. Reshetikhin. Dimers on Surface Graphs and Spin Structures. I. *Communications in Mathematical Physics*, 275:187–208, October 2007, arXiv:math-ph/0608070.
- [9] R. Dijkgraaf, D. Orlando, and S. Reffert. Dimer models, free fermions and super quantum mechanics. *Adv.Theor.Math.Phys.*, 13, 2009, 0705.1645.
- [10] Ron Donagi and Edward Witten. Supermoduli Space Is Not Projected. 2013, 1304.7798.
- [11] C. Doran, K. Iga, and G. Landweber. An application of Cubical Cohomology to Adinkras and Supersymmetry Representations. *ArXiv e-prints*, July 2012, 1207.6806.

- [12] C. F. Doran, M. G. Faux, S. J. Gates, T. Hübsch, K. M. Iga, and G. D. Landweber. On Graph-Theoretic Identifications of Adinkras, Supersymmetry Representations and Superfields. *International Journal of Modern Physics A*, 22:869–930, 2007, arXiv:math-ph/0512016.
- [13] C. F. Doran, T. Hübsch, K. M. Iga, and G. D. Landweber. On General Off-Shell Representations of Worldline (1D) Supersymmetry. *ArXiv e-prints*, October 2013, 1310.3258.
- [14] C.F. Doran, M.G. Faux, Jr. Gates, S.J., T. Hübsch, K.M. Iga, et al. Adinkras for Clifford Algebras, and Worldline Supermultiplets. 2008, 0811.3410.
- [15] C.F. Doran, M.G. Faux, Jr. Gates, S.J., T. Hübsch, K.M. Iga, et al. Codes and Supersymmetry in One Dimension. *Adv.Theor.Math.Phys.*, 15:1909–1970, 2011, 1108.4124.
- [16] Herbert Edelsbrunner, John Harer, and Afra Zomorodian. Hierarchical morse complexes for piecewise linear 2-manifolds. In *Proceedings of the seventeenth annual symposium on Computational geometry*, SCG '01, pages 70–79, New York, NY, USA, 2001. ACM.
- [17] Michael Faux and Jr. Gates, S.J. Adinkras: A Graphical technology for supersymmetric representation theory. *Phys.Rev.*, D71:065002, 2005, hep-th/0408004.
- [18] J. O. Fjærestad. Dimer and fermionic formulations of a class of colouring problems. *Journal of Physics A Mathematical General*, 45(7):075001, February 2012, 1109.0157.
- [19] Robin Forman. Morse Theory for Cell Complexes. *Advances in Mathematics*, 134:90–145, 1998.
- [20] Robin Forman. Witten-Morse Theory For Cell Complexes. *Topology*, 37(5):945979, 1998.
- [21] Daniel Friedan. Notes On String Theory and 2-Dimensional Conformal Field Theory. 1986.
- [22] S. J. Gates and L. Rana. Ultra-multiplets: a new representation of rigid 2D, $N = 8$ supersymmetry. *Physics Letters B*, 342:132–137, February 1995, hep-th/9410150.
- [23] S. J. Gates, Jr. and T. Hübsch. On Dimensional Extension of Supersymmetry: From Worldlines to Worldsheets. *ArXiv e-prints*, April 2011, 1104.0722.
- [24] Andreas Gathmann and Michael Kerber. A riemannroch theorem in tropical geometry. *Mathematische Zeitschrift*, 259(1):217–230, 2008.
- [25] Frank Herrlich and Gabriela Schmithüsen. Dessins d’enfants and origami curves. In *Handbook of Teichmüller theory. Vol. II*, volume 13 of *IRMA Lect. Math. Theor. Phys.*, pages 767–809. Eur. Math. Soc., Zürich, 2009.
- [26] T. Hübsch and G. A. Katona. A Q-Continuum of Off-Shell Supermultiplets. *ArXiv e-prints*, October 2013, 1310.3256.
- [27] Tristan Hübsch. Weaving Worldsheet Supermultiplets from the Worldlines Within. 2011, 1104.3135.
- [28] Dennis Johnson. Spin structures and quadratic forms on surfaces. *J. London Math. Soc. (2)*, 22(2):365–373, 1980.
- [29] Gareth A. Jones. Maps on surfaces and Galois groups. *Math. Slovaca*, 47(1):1–33, 1997. Graph theory (Donovaly, 1994).
- [30] I. Manin. Critical Dimensions of String Theories and the Dualizing Sheaf on the Moduli Space of (Super) Curves. *Funct.Anal.Appl.*, 20:244–245, 1987.
- [31] G. Mikhalkin and I. Zharkov. Tropical curves, their Jacobians and Theta functions. *ArXiv Mathematics e-prints*, December 2006, math/0612267.
- [32] Robert Miller. Doubly-even codes. http://www.rlmliller.org/de_codes/.
- [33] M. Mulase and M. Penkava. Ribbon Graphs, Quadratic Differentials on Riemann Surfaces, and Algebraic Curves Defined Over $\bar{\mathbb{Q}}$. *ArXiv Mathematical Physics e-prints*, November 1998, arXiv:math-ph/9811024.
- [34] Xinlai Ni, Michael Garland, and John C. Hart. Fair morse functions for extracting the topological structure of a surface mesh. *ACM Trans. Graph.*, 23(3):613–622, August 2004.
- [35] Kurt Strebel. *Quadratic Differentials*. Springer, 1984.

- [36] Edward Witten. Notes On Super Riemann Surfaces And Their Moduli. 2012, 1209.2459.
[37] Y. X Zhang. Adinkras for Mathematicians. *ArXiv e-prints*, November 2011, 1111.6055.

(Charles Doran and Stefan Mendez-Diez) DEPARTMENT OF MATHEMATICAL AND STATISTICAL SCIENCES, UNIVERSITY OF ALBERTA, EDMONTON, AB T6G 2G1, CANADA
E-mail address, Charles Doran: doran@math.ualberta.ca

(Kevin Iga) NATURAL SCIENCE DIVISION, PEPPERDINE UNIVERSITY, MALIBU, CA 90263, USA
E-mail address, Kevin Iga: kiga@pepperdine.edu

(Greg Landweber) MATHEMATICS PROGRAM, BARD COLLEGE, ANNANDALE-ON-HUDSON, NY 12504-5000, USA
E-mail address, Greg Landweber: gregland@bard.edu

E-mail address, Stefan Mendez-Diez: sdiez@math.ualberta.ca